

This electronic thesis or dissertation has been downloaded from the King's Research Portal at <https://kclpure.kcl.ac.uk/portal/>



Live-cell FTIR spectroscopy as a novel bioanalytical tool for anti-diabetic drugs research

Poonprasartporn, Anchisa

Awarding institution:
King's College London

The copyright of this thesis rests with the author and no quotation from it or information derived from it may be published without proper acknowledgement.

END USER LICENCE AGREEMENT



Unless another licence is stated on the immediately following page this work is licensed

under a Creative Commons Attribution-NonCommercial-NoDerivatives 4.0 International

licence. <https://creativecommons.org/licenses/by-nc-nd/4.0/>

You are free to copy, distribute and transmit the work

Under the following conditions:

- Attribution: You must attribute the work in the manner specified by the author (but not in any way that suggests that they endorse you or your use of the work).
- Non Commercial: You may not use this work for commercial purposes.
- No Derivative Works - You may not alter, transform, or build upon this work.

Any of these conditions can be waived if you receive permission from the author. Your fair dealings and other rights are in no way affected by the above.

Take down policy

If you believe that this document breaches copyright please contact librarypure@kcl.ac.uk providing details, and we will remove access to the work immediately and investigate your claim.

**LIVE-CELL FTIR SPECTROSCOPY AS A NOVEL
BIOANALYTICAL TOOL FOR
ANTI-DIABETIC DRUGS RESEARCH**

ANCHISA POONPRASARTPORN

1782617

Doctor of Philosophy

Abstract

The incidence and mortality rate of diabetes is increasing globally against the variety of currently available anti-diabetic drugs in clinical practice. Unfortunately, current pre-clinical approaches in drug discovery of novel anti-diabetic compounds have not met the increasing demand associated with a high cost and time-consuming research. Therefore, a cost-effective, reliable, and high throughput method that provides critically essential mechanistic information on the drug-cell interaction is urgently needed in the pre-clinical selection of new anti-diabetes drug candidates. This thesis aims to develop a new screening approach based on live-cell FTIR spectroscopy. And the purpose is that this low-cost technique provides information regarding the biomarker alteration between cell and anti-diabetic drugs comparable to the conventional method.

We developed the measurement approach in the first result chapter (chapter 3). We illustrated that multi-reflection ATR FTIR spectroscopy could acquire high-quality spectra of live cells in their aqueous culture medium containing different glucose concentrations for the first time. The results were compared with the reference chemical spectra and confirmed with results from the literature. Hepatoma cancer cell line, namely HepG2, was investigated with a medium of high and low glucose concentration. The difference spectra showed significant spectral changes in the IR absorbance bands between low and high glucose treatment. Glycogen and ADP: ATP spectra are the cellular changes from high glucose treated cells that can be evidence of metabolism alteration according to increasing high cellular glucose uptake.

In contrast, low glucose treated cells have shown the rising of phosphate, and nucleic acid, which refers to normal cell growth.

In chapter 4, we applied this approach to study the cellular changes of insulin sensitivity and insulin-resistance HepG2 cells when exposed to a high glucose environment. The experiment was categorized into four sections: normal glucose with/without insulin and high glucose with/without insulin-containing culture medium. The spectral changes between insulin and normal glucose-treated cells have shown significant differences with a broad feature of carbohydrate and phosphate regions in the loadings plot. This refers to the sensitivity of HepG2 cells in normal glucose conditions after insulin addition. However, the high glucose treated insulin has shown different spectral changes compared to the normal glucose treatment indicating that the response from insulin resistance HepG2 to insulin can be distinguished by the live-cell FTIR method. The insulin resistance HepG2 model has been set up and tested against two insulin sensitizers, metformin, and resveratrol. The significantly increasing glycogen absorbance peaks after adding insulin sensitizers indicate an increasing hepatic glucose uptake compared to the control. Moreover, the FTIR results are also comparable with the conventional glycogen assay.

In chapter 5, we applied the developed method to study a new anti-diabetic drug with a different mechanism of action. PF—04991532, a novel glucokinase activator compound, has been tested to study the mechanism of the glucose-lowering effect in diabetic HepG2 cells. However, the spectral change between high glucose and PF-04995132 with high glucose treated cell were insignificant for all treatment time. This is because the HepG2 cell line lacks

gene expression regarding this compound's mechanism of action. This insignificant result confirms that the live-cell approach is a specific method that can show negative results when the drug is ineffective because the mechanism of action is not activated.

In conclusion, the work presented in this thesis has successfully shown that live-cell FTIR spectroscopy combined with PCA can discriminate biochemical alteration in cells under treatment of different glucose levels, insulin, and drugs. Therefore, this technique can be an alternative low-cost screening tool for studying the anti-diabetic drug *in vitro*. Furthermore, further study of this label-free technique can provide information regarding other diabetes cells, e.g., pancreas or kidney, combined with automated measurement and machine learning to establish the tool for diabetes drug screening.

Table of Contents

Abstract.....	2
Table of figures	9
Table of tables.....	11
Acknowledgement	12
Abbreviations.....	13
Chapter 1 Introduction	14
2.1 Diabetes classification.....	21
2.2 Diagnosis of diabetes	22
2.3 Diabetes complications	23
2.4 Diabetes medication management.....	24
3.Diabetes Drug Development Process	33
3.1 Pre-clinical development	35
3.2 Pre-clinical screening assays	35
3.2.1 Analytical technologies	35
3.2.1.1 Colorimetry	35
3.2.1.2 Chromatography	36
3.2.1.3.1 Mass spectroscopy.....	36
3.2.1.3.2 Nuclear magnetic resonance (NMR) spectroscopy.....	37
3.2.1.3.3 Near-infrared and Raman spectroscopy	38
3.2.1.3.4 Infrared spectroscopy	39

3.2.1.3.5 Fourier Transform Infrared Spectroscopy (FTIR)	43
3.2.1.3.6 FTIR live cells Spectroscopy	44
3.2.1.3.8 FTIR approach and diabetes research.....	48
4.The principle of Multi-reflection (Multi Bounce) ATR	51
5.Multivariate analysis	53
6. Principal component analysis (PCA).....	53
7. Aims.....	54
Chapter 2 Method Development and Experimental Design.....	55
2.1 Introduction	55
2.2 Cancer Cell Lines	55
2.2.2 Cell culture	57
2.2.2.1 Cell counting and viability testing.....	57
2.2.2.2 Live-cell FTIR measurement preparation.....	58
2.2.2.3 Growth rate of HepG2 cells in DMEM high glucose and DMEM CO ₂ independent medium	59
2.2.2.4 Density and Attachment of HepG2 cells on the ATR plate	60
2.3 ATR FTIR Measurement	61
2.3.1 Multi-Reflection ATR Accessory.....	61
2.3.2 Live Cell FTIR measurement.....	61
2.3.2.1 Obtaining Reproducible of Live Cells ATR FTIR Spectra	63
2.3.3 Cell Viability assay	64
2.3.4 Solutions/drugs treatment preparation	64

2.3.4.1 FTIR Spectra of Compounds/Drugs	65
2.3.4.2 Considering using 2% FBS in HepG2 compound treatment.....	65
2.3.5 FTIR data analysis.....	66
2.3.6.1 Water Vapour Correction.....	67
2.3.6.2 Spectra truncation	68
2.3.6.3 Baseline correction	69
2.3.6.5 Vector normalization	70
2.3.7 PCA analysis of Live-cell FTIR spectra.....	70
 Chapter 3 Live cell ATR-FTIR spectroscopy as a novel bioanalytical tool for cell glucose metabolism research	 71
3.1 Abstract.....	71
3.2 Introduction	72
3.4 Results.....	76
3.5 Discussion.....	82
 Chapter 4 Label-free study of intracellular glycogen level in Metformin and Resveratrol-treated insulin-resistant HepG2 by live-cell FTIR spectroscopy	 89
4.1 Introduction	89
4.2 Materials and Methods.....	91
4.3 Results.....	94
4.4 Discussion.....	103
 Chapter 5 Live-cell FTIR approach to investigate the mechanism of action from liver selective glucokinase activator	 107

5.1 Introduction	107
5.2 Material and methods	115
5.3 Results and Discussions	116
Chapter 6 Conclusions and Future work.....	123
6.1 Conclusions	123
6.2 Future Work.....	126

Table of figures

Figure 1. Glucose metabolism in 4 different stages: 1A fasting, 1B feeding stage in the non-diabetic model. 1C fasting, 1B feeding stage in the diabetic model	16
Figure 2. Summary of human hepatic glucose metabolism.....	21
Figure 3. Summary of diabetes drug development process	34
Figure 4 . Schematic diagram of FTIR spectrometer	43
Figure 5. Schematic diagram of the multi-reflections ATR element [45] Schematic diagram of the mulreflections ATR elemen.....	52
Figure 6. Typan blue exclusion test for HepG2 cell using Countess® Automated Cell Counter	58
Figure 7. Image of HepG2 cells at 24 hours of seeding on the ATR element (A) and T25 flask (B) ...	60
Figure 8. A schematic diagram showing the live-cell ATR-FTIR experiment set up	61
Figure 9. Photo of Bruker spectrometer modified to a temperature-controlled ATR plate for the live-cell FTIR measurement.....	62
Figure 10. HepG2 FTIR live-cell spectra every 2hr of seeding time (A) and the error bars of 24th hour (B).....	63
Figure 11. The FTIR spectra of PF-04991532 (blue), metformin (orange), and Resveratrol (grey)....	65
Figure 12. The absorbance value of HepG2 cell in 10% FBS (Red color) and 2% FBS DMEM CO ₂ independent medium (blue color) after 6 hours of refreshing medium.....	66
Figure 13. An ATR FTIR different spectrum o HepG2 cells (blue) and after (green) water vapor compensation.....	67
Figure 14. An ATR FTIR different spectrum of HepG2 cells before (A) and after truncation (B)	68
Figure 15. The FTIR spectrum before baseline correction (A) and B represents the spectrum after baseline correction.....	69
Figure 16. Image of HepG2 cells at different time of seeding on the ATR element and T25 flask, respectively; 24 hour A and B, 48 hour C and D, 72 hour E and F	77
Figure 17. HepG2 live-cell FTIR spectra every 2 hr. of seeding time (A) and the error bar of 24th hour (B).....	78
Figure 18. HepG2 cell viability compared to control (3.8mM) for 24, 48 and 72 hours with error bars representing the standard deviation between the three independent repeated experiments	79
Figure 19. Spectra of HepG2 treated with 25mM glucose in 3 different time points (24, 48 and 72 hour) with spectra range between 3800-800 cm ⁻¹ (A) and spectra range between 1780-900 cm ⁻¹ (B)	80
Figure 20. The spectral changes as a function of time (left panel) between HepG2 treated in high (Red) and normal (Blue) glucose solution and the corresponding PCA1 score and loading plots (right panel) at (A) 24th, (B) 48th and (C) 72nd hour.....	81
Figure 21. Comparison of normal glucose treated HepG2 FTIR spectra for time 24th 48th and 72nd hour.....	84
Figure 22. Comparison of high glucose treated HepG2 normalized FTIR spectra for time 24th 48th and 72nd hour	85
Figure 23. Comparison between ATP-ADP FTIR spectrum and high glucose treated HepG2 at time 24 th	87
Figure 24. HepG2 cell viability in high (25mM) and normal glucose (4 mM) medium with 100nM insulin (brick plot) and without insulin (plain plot) of 24 h seeding with the error bar represents standard deviation	95
Figure 25. HepG2 morphology in diabetic model or control (high glucose 25 mM and 100 nM insulin) in different time points	96

Figure 26. HepG2 morphology in diabetic hepG2 model and 2mM metformin treatment in different time points	96
Figure 27. HepG2 morphology in diabetic hepG2 model and 50 μ M Resveratrol treatment in different time points	97
Figure 28. The comparison of three replicate HepG2 FTIR spectra between high glucose (blue) and high glucose + insulin (red) with PCA score at time 1 h(A) and 18 h (B) and the comparison of three replicate HepG2 FTIR spectra between normal glucose (light green) and normal glucose + insulin (magenta) with PCA score and loadings at time 1 h(C), and 18 h (D) with error bars representing the standard deviation.....	100
Figure 29. The comparison of three replicate HepG2 FTIR spectra between high glucose+ insulin: control (green) and high glucose+ insulin + 2mM metformin; treatment (purple) with PCA score at time 1 h(A) and 18 h (B) and the comparison of three replicate HepG2 FTIR spectra between high glucose+ insulin: control (green) and high glucose+ insulin + 50 μ M Resveratrol; treatment (orange) with PCA score and loadings at time 1 h(C), and 18 h (D) with error bars representing the standard deviation	101
Figure 30. The comparison of the integrated absorbance of glycogen peak by FTIR approach among metformin (purple), Resveratrol(orange), and control(green) over 24 hours treatment (A) and the comparison of glycogen amount in diabetic HepG2 model by glycogen assay among diabetic HepG2 (control) with metformin or resveratrol treatment at time 1, and 18 h (B) with error bars representing the standard deviation.....	102
Figure 31. A characteristic of glycogen peak from 4 mg/mL (pink), 2mg/mL(blue) glycogen solution and at 6th h of resveratrol treatment	106
Figure 32. A glucokinase network containing tissue throughout the body	108
Figure 33. The role of Glucokinase activators in pancreatic and hepatic cells	109
Figure 34. Glucokinase activity in hepatocyte[105]	110
Figure 35. The viability of HepG2 cells after PF-04991532 for the 24-hour treatment with error bars representing the standard deviation between the three independent repeated experiments	116
Figure 36. The comparison of live-cell FTIR spectra between control (green color) and PF-04991532 (pink color) and box plot for time 10 (A), 10 min(B), 1h (C), 2 h(D),3 h (E) 4h(F), 6(G), 12(H), and 24 h (I) with error bars representing the standard deviation between the three independent repeated experiments.....	119

Table of tables

Table 1 The diagnosis criteria of diabetes	22
Table 2. Doubling time of HepG2 cells in DMEM high glucose, DMEM CO ₂ independent	45
Table 3. Summary of general information and characteristic of HepG2 cell lines.....	56
Table 4. Doubling time of HepG2 cells in DMEM high glucose, DMEM CO ₂ independent.....	59

Acknowledgment

I would like to thank you for the enormous support from my supervisor, Andrew Chan. He is always patient, understands, has many soft skills, and helps me in all the Ph.D. aspects. I have learned a lot of skills while being a student under his supervision in KCL, and so many times, I think I am so lucky to have him as my supervisor. He will be my role model for self-improvement and my future career. And also, thanks Cristina Legido Quigley, my second supervisor, for accepting me into her research group, for great advice, and for the general support.

Secondly, I greatly appreciate my family (Poonprasartporn and Kitwithee), who always 'be there' when I needed them, never gave up on me when I failed, and always trusted me when my confidence was unsteady. And I would like to thank all Thai and UK friends for their support, especially Revadee Liam-Or, Jongkol Promjan, Ralph Green, Orapan Apirakkan, Makiko Kawashita, Chutinan Chai-yo, Chaiwat Siangsirisak, Trin Sappakhun, Chayma Machuma, Fetime, Cicy, Yuan, and many more.

Big thanks to the Thai royal government and the Thai Scholar team for providing the scholarship; it is the most incredible opportunity I have ever had. This grant made my life change forever; my perspective is broader; my abilities have been discovered and improved for the better. My colleagues from Sirindhorn College of Public Health Chonburi and Praboromrajchanok Institute also greatly support me. I so much appreciated all your help and kindness.

Thank you for the friendship and help from my colleagues, staff in IPS, and my research group, especially Ali Altharawi, for teaching me in the lab during my 1st year Ph.D. student, and for all of the general support. I also thank Abdulrahman Aloumi, Mohammed Alsalhi, Ohood Alshareef, and Sirawut Tubtim from Chan's research group. A special thanks to Dominic (Shiu Butt), MSc Pharmaceutical Science, IPS, who taught me the Pychem analysis when I was 2nd year Ph.D. made me generate lots of research for the public and made the world a better place.

Lastly, I did not terminate my study thanks to myself, although I almost did it many times. All afford in every day, including the weekend and holidays when I came to the lab, has been paid off and made me be me today. Ph.D. overseas is challenging, with a different language and culture, far away from family, particularly during the pandemic. However, I have proved that I did it great in the most challenging academic journey. I cannot say that this is my success; everyone who always supports my achievement is our success. Lastly, I would like to thank Peerasilp Wiwattananon, who is always a great supporter, a great listener, and always beside me and made it an incredible academic journey.

Abbreviations

Abbreviations	Meaning
HIV	human immunodeficiency virus
AIDS	acquired immunodeficiency syndrome
LDL	low-density lipoprotein
NADPH	nicotinamide adenine dinucleotide phosphate
DNA	deoxyribonucleic acid
RNA	ribonucleic acid
FBS	foetal bovine serum
ADP	Adenosine diphosphate
ATP	Adenosine triphosphate
GIP	glucose-dependent insulintropic polypeptides
GLP	glucagon-like peptide

Chapter 1 Introduction

Diabetes remains one of the leading causes of death globally, with 4 million deaths reported in 2019, and it is predicted that it will be the 7th leading cause of death worldwide in 2030. It was estimated that more than 400 million are living with diabetes to date, which could rise to 700 million in 2045. Around 20% of the elderly (>65 years old) have diabetes, and 374 million people are at increased risk of developing type 2 diabetes. Moreover, it was estimated that half of the people with diabetes are underdiagnosed [1-3]. Diabetes is a major cause of micro and macrovascular complications such as retinopathy, nephropathy, atherosclerosis, and peripheral artery disease, which can worsen the patients' quality of life. The global annual cost of treatment and the disease and the management of its complications was 825 billion dollars in 2014, with the highest cost to individual countries being in China (\$170 billion), the USA (\$105 billion), and India (\$73 billion), respectively [4].

Diabetes occurs when blood glucose, also called blood sugar, reaches the upper limit without control. Blood glucose is the primary source of energy and comes from the diet. Insulin, a hormone made by β -cells from the pancreas, helps absorb the glucose from the diet into the cell. When carbohydrate food is digested into glucose, which enters the bloodstream, insulin moves glucose out of the blood and into cells, where glucose molecules are metabolized to generate energy or stored. However, having diabetes or long-term high blood sugar, the body cannot break down glucose into energy because there is either insufficient insulin to enable cells to absorb glucose, or the cells are not responding to the insulin produced. Besides, having an excessive amount of blood glucose can cause subsequent health problems.

1. Diabetes cell metabolism

Studying cell metabolism is the basis for establishing good quality diabetes research and anti-diabetes drug development. This section includes the fundamental of normal glucose metabolism and diabetes pathophysiology.

The review of cell glucose metabolism and its regulations [32] and the diabetes pathophysiology [33, 34] has been described below.

1.1 Normal physiology

Blood glucose is related to and changed by the glucose input and output rate in the circulations. The glucose input source is obtained in three ways: glucose absorption from the gut during feeding, glycogen breaking down to glucose (glycogenolysis), glucose production, or gluconeogenesis in the liver.

Glycogenolysis and gluconeogenesis are controlled by the pancreatic hormone glucagon produced by α -cells. This mechanism is the primary glucose production process during the fasting period's first 8-12 hours. If fasting is continued, the liver is the organ that regulates glucose homeostasis.

Glucoregulatory hormones involve insulin, glucagon, amylin, GLP-1, glucose-dependent insulintropic peptide (GIP), epinephrine, cortisol, and growth hormone. Insulin and amylin arrive from the β -cells, glucagon from the α -cells of the pancreas, and GLP-1 and GIP from the L-cells of the intestine.

The glucoregulatory hormones are developed to balance blood glucose concentration in a limited range. During the fasting state, glucose remains in circulation at a stable rate. To keep consistence with glucose utilizing rate, endogenic glucose production is

essential. Practically, the source of endogenous glucose production comes from the liver. Renal glucose production considerably improves the systemic glucose reserve, but only during extreme starving conditions (figure 1).

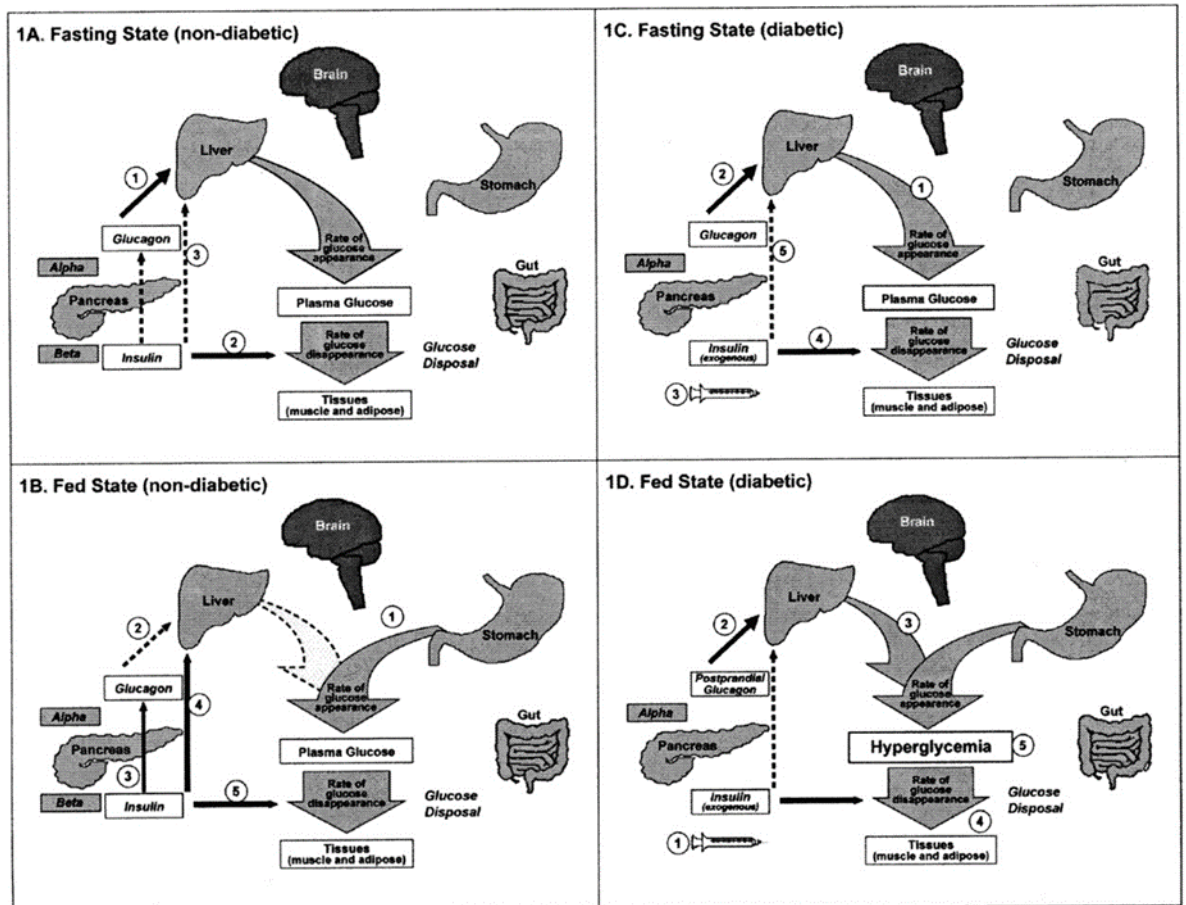


Figure 1. Glucose metabolism in 4 different stages: 1A fasting, 1B feeding stage in the non-diabetic model. 1C fasting, 1B feeding stage in the diabetic model [32]

1.1 β -cell Hormones

1.1.1 Insulin

Insulin, a small protein, consists of 2 peptides and 51 amino acids. It is the only known pancreatic β -cell hormone that lowers blood glucose concentration immediately after meals. Insulin is secreted and bound to the receptors in fat, liver, and muscle cells to stimulate glucose utilization.

Insulin reduces blood glucose in three ways: first, insulin activates peripheral cells, e.g., primarily muscle, to uptake glucose. Second, it promotes hepatic glucose production (gluconeogenesis) during fasting. Lastly, insulin concomitantly glucagon secretion from the pancreas during the feeding stage. As a result, it stops hepatic glycogenolysis and gluconeogenesis to reduce blood glucose. Other insulin actions that can lower blood glucose include fat synthesis, protein synthesis in muscle, and cell growth proliferation stimulations.

Insulin is sensitively secreted in response to blood glucose concentration. It usually is not secreted if the blood glucose level is below 3.3 mmole/l. After a regular meal, insulin is secreted in two phases; first, a rapid release of pre-insulin, then increased insulin production and released in response to the rising blood glucose concentration. Glucose is the most potent stimulator of insulin. Other stimuli include amino acids, arginine, leucine, and lysine, GLP-1 and GIP (gut hormone during the feeding stage), and parasympathetic stimulation via the vagus nerve.

1.1.2 Amylin

Amylin is a neuroendocrine hormone-containing 37–amino acid peptide expressed and released with insulin via pancreatic β -cells in response to nutrient consumption. Clinical studies have determined that the plasma concentration of insulin and amylin excretion is similar [32]. They are at relatively low concentrations in blood during the fasting stage but increase in the feeding stage. Amylin deficiency is observed in type 1 and impaired in type 2 diabetes patients.

Pre-clinical studies [33] demonstrated that amylin co-ordinately works with insulin in the rate of glucose appearance and disappearance in the circulation for controlling abnormal glucose concentration increases.

1.3 α -cell hormone: Glucagon

Glucagon, consisting of 29 amino acids, is an essential pancreatic α -cells hormone in the catabolism pathway. Roger Unger discovered it in the 1950s[34]; glucagon was categorized as having opposing insulin effects. Glucagon plays a significant role in maintaining plasma glucose concentration during fasting by encouraging hepatic glucose production.

Glucagon was the first to be described with the term “bi-hormonal” in the a a diabetic disease characterized by insulin insufficiency and glucagon surplus [34, 35]. Hepatic glucose production is predominantly regulated by glucagon to maintain blood glucose levels within a normal limit during fasting. When plasma glucose concentration drops below the normal level, glucagon secretion rises, producing hepatic glucose and restoring plasma glucose level to the normal range. Glucagon secretion is suppressed during the feeding stage.

In diabetic status, there is insufficient repression of glucagon secretion after-meal (hyperglucagonemia). Glucose from hepatic glucose production is released into the bloodstream. Essentially, insulin produced from Beta cells cannot reinstate the normal insulin concentrations and suppress glucagon secretion. Thus, an abnormally high glucagon-to-insulin ratio stimulates hepatic glucose production.

1.4 Incretin hormone: GLP and GIP

Perley et al. [36]. Illustrated that food consumption increased insulin release more potently than intravenous glucose injection. This effect is called the “incretin” that food signaling from the gut to the bloodstream is a vital hormone when food appears in the digestive system. Besides, these gut hormones help regulate gastric emptying and bowel movement.

Many incretin hormones have been identified [37]; GIP and GLP-1 are some of the essential hormones for glucose metabolism. GIP activates insulin secretion and controls fat metabolism but does not suppress glucagon secretion or gastric emptying. GLP-1 is a more potent incretin hormone than GIP. It is secreted in a more significant amount and is more crucial to human's health.

GLP-1 also increases insulin secretion in a glucose-dependent manner but is rapidly reduced after a meal in type 2 diabetes or impaired glucose tolerance patients. GLP-1 has a half-life of about 2 minutes in plasma, and its utilization is controlled predominantly by the enzyme dipeptidyl peptidase-IV (DPP-IV), which rapidly inactivates GLP-1.

1.5 Diabetes pathophysiology

Type 1 diabetes has been classified as autoimmune-mediated pancreatic β -cells disruption disease. The resulting insulin deficiency also affects the secretion of amylin. As a result, the post-meal glucose concentration is sustainably increased due to a lack of insulin-responding glucose control, inadequate hepatic glucose production control, and abnormal gastric emptying.

In the early stage of type 2 diabetes, the post-meal β -cell function becomes abnormal, characterized by lacking a rapid response to insulin after a meal. Insulin resistance, concomitant with ongoing β -cell disruption, and decreased availability of insulin, amylin, and GLP-1 can cause hyperglycemia complications.

Gastric emptying abnormality is frequent in both type 1 and types 2 diabetes. If gastric emptying is increased, meal-derived glucose presentation to the blood circulation is inadequately timed with insulin delivery. Furthermore, an absence or delayed insulin

response promotes postprandial hyperglycemia. Amylin and GLP-1 control gastric emptying by slowing the gut's nutrient delivery.

1.6 Hepatic glucose metabolism

The liver plays an essential role in glucose homeostasis. Understanding normal hepatic glucose metabolism can help better understand the pathophysiology of obesity and diabetes mellitus. Liver glucose metabolism includes glycosylation and is also related to fatty acid metabolism.

The liver utilizes glucose from ingested carbohydrates from the gut via the hepatic portal vein. The phosphorylation of glucose follows this to glucose-6 phosphate (G6P) via the glucokinase enzyme. G6P is then continued to be metabolized through several pathways. Most G6P is used to produce glycogen through glucose 1-phosphate and UDP-glucose during the feeding stage. The remaining UDP-glucose is used to form UDP-glucuronate and UDP-galactose, the intermediate substrates in the glycosylation process.

The second pathway of glucose 6-phosphate metabolism is fructose 6 phosphate generation allowed the initiation of the hexosamine pathway to process UDP-N-acetylglucosamine or enter the glycolytic pathway to produce pyruvate and then acetyl-CoA. Acetyl-CoA can enter the tricarboxylic acid (TCA) cycle to be oxidized or delivered to the cytosol to integrate fatty acids when glucose overloads in the hepatocyte.

Finally, G6P can be converted into NADPH and ribose 5-phosphate via the pentose phosphate pathway. Glucose metabolism produces intermediate metabolites for glycosylation. In addition, to metabolize carbohydrates, the liver breakdown glycogen to produce glucose in other tissues, primarily lactate and alanine (gluconeogenesis), as summarised in [figure 2](#) [38].

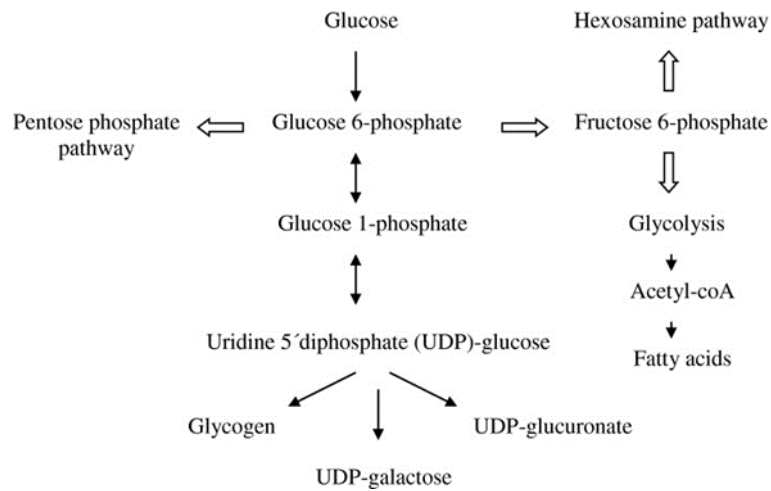


Figure 2. Summary of human hepatic glucose metabolism [9]

2.1 Diabetes classification

Generally, diabetes can be classified into the following general categories: type 1, type 2, gestational, and miscellaneous [5, 6].

2.1.1 Type 1 diabetes can emerge at any age but most commonly occurs in children and young adults. Due to β -cell destruction, the body produces little or no insulin, so patients need daily insulin injections to keep blood glucose levels under control.

2.1.2 Type 2 diabetes is the major type in adults accounting for around 90% of all diabetes cases. When type 2 diabetes develops, the body does not use the insulin it produces effectively, and it is referred to as “insulin resistance”. An active physical lifestyle and a healthy diet may positively help to improve the symptoms. However, most type 2 diabetes patients require oral medications and insulin injections to control their blood glucose levels.

2.1.3 Gestational diabetes (GDM) is diabetes that comprises high blood glucose during the second or third trimester of pregnancy and is associated with subsequent health problems for both mother and child. GDM often disappears after pregnancy, but the mothers and their children would have an increased risk of type 2 diabetes later in life.

2.1.4 The individual types of diabetes due to other causes include, e.g., monogenic diabetes syndromes (such as neonatal diabetes and maturity-onset diabetes of the young [MODY]), pancreas-related diabetes (such as cystic fibrosis), and drug-induced diabetes (such as in the treatment of HIV/AIDS or after organ transplantation).

2.2 Diagnosis of diabetes

2.2.1 Diagnostic Tests for Diabetes

Diabetes can be diagnosed based on HbA1C percentage (average blood glucose, or blood sugar, level over the past three months) or plasma glucose criteria, using either the fasting plasma glucose (FPG)/ fasting blood sugar (FBS) or the 2-hour plasma glucose (2-h PG) value after a 75-g oral glucose tolerance test (OGTT).

Table 1. The diagnosis criteria of diabetes

A1C \geq 6.5%
OR
FPG \geq 7.0 mmol/L
Fasting is determined as no calories intake for at least 8 hours.*
OR
2-h PG \geq 11.1 mmol/L
during an OGTT. The test should be performed as described by the WHO, using a glucose load containing equal to 75 g of anhydrous glucose dissolved in water.*
OR
In a patient with typical symptoms of hyperglycemia or hyperglycaemic crisis, random plasma glucose \geq 11.1 mmol/L

** In the absence of unequivocal hyperglycemia, results should be confirmed by repeat testing.*

2.3 Diabetes complications

Diabetes increases the risk of many serious health problems. The complications consist of 2 types: acute type, which can develop at any time, and chronic type, which builds up over time. Both complications can be delayed and preventable. However, once long-term complications have developed, they can cause severe damage if unchecked and untreated.

2.3.1 Acute complications

- Hypoglycemia or low blood sugar
- Hyperglycemia or high blood sugar
- Hyperosmolar Hyperglycaemic State (HHS) is a lethal emergency event found only in type 2 diabetes patients. It's caused by severe dehydration and very high blood sugar level.

2.3.2 Chronic complications

- Skin complications, e.g., bacterial infection, fungal infection, and other diabetes-related skin conditions.
- Eye complications, e.g., glaucoma, cataracts, retinopathy
- Neuropathy involves **peripheral neuropathy**. This type can cause tingling, pain, numbness, or weakness in your feet and hands. **Autonomic neuropathy** affects the nerves in the body that control body systems.
- Nephropathy (kidney disease)
- High blood pressure, also called hypertension-increase the risks of heart attack, stroke, eyes and kidney problems

The American Diabetes Association (ADA) has recommended integrating specific targets for several physiological parameters in type-2 diabetes[7]. Targets include controlling HbA1c levels <7%, blood pressure <130/80, reducing the risk of hypoglycemia events, and neutralizing, or losing weight, if obese. To answer the multiple desired outcomes, composite endpoints (CEPs) increase the usage in clinical trials as primary or secondary outcomes. [8-10]. These endpoints have been applied in various clinical, especially in cardiovascular disease (CVD). The following topic will describe the current anti-diabetic medication and some clinical studies that included the composite endpoint in diabetic and cardiovascular outcomes.

2.4 Diabetes medication management[11]

2.4.1 Oral medication therapy

There are different types of medicines that work in various pathways to lower blood sugar level.

2.4.1.1 Alpha-glucosidase inhibitors e.g., Acarbose (Precose) and Miglitol (Glyset). These medications lower blood sugar levels by blocking the breakdown of starch-absorbing enzymes in the intestine. This mechanism also slows the rise in blood sugar levels after a meal. These drugs should take with the first bite of each main meal. These drugs may have side effects, including bloating and diarrhea.

2.4.1.2 Biguanides, e.g., Metformin (Glucophage), is a potent antihyperglycemic agent and recommended as the first-line oral therapy for type 2 diabetes (T2D). Biguanides lower blood sugar levels by decreasing liver glucose production. They also lower blood sugar levels by making liver and muscle tissue more sensitive to insulin (insulin sensitizer) to absorb glucose. Generally, metformin is safe to use, the side effect

of metformin is relatively mild such as diarrhea, but this is improved when the drug is taken with food.

An updated meta-analysis in 2019[12] of metformin effect on all-cause and cardiovascular mortality in patients with coronary artery diseases revealed that metformin reduces all-cause mortality and cardiovascular events in coronary artery disease (CAD) patients. However, for myocardial infarction patients and CAD patients without T2DM, metformin has no significant effect on reducing the incidence of cardiovascular events. Moreover, metformin has a better outcome of reducing the incidence of cardiovascular events than sulfonylureas. Furthermore, an update in 2020[13], in the T2DM patients with underlying chronic Kidney Disease(CKD), Metformin has a good profile in reducing risks of all-cause mortality and cardiovascular events in patients with T2DM and mild-to-moderate CKD.

2.4.1.3 Sulfonylureas

Sulfonylureas stimulate insulin release from beta cells in the pancreas. Chlorpropamide (Diabinese) is the only first-generation sulfonylurea currently in use. Second-generation sulfonylureas are more potent than first-generation drugs. The third-generation drugs, including glimepiride (Amaryl), glipizide (Glucotrol and Glucotrol XL), and glyburide (Micronase, Glynase, and Diabeta) are generally taken one to two times a day due to the short duration of action, to mimic physiological insulin. All sulfonylurea drugs have similar effects on blood sugar levels but can lead to hypoglycemia, weight gain side effects, and interaction with other medications.

In 2007, a systematic review and meta-analysis studied about hypoglycemia and cardiovascular event of sulfonylurea (Glyburide)[14] compared with similar drug mechanisms, e.g., insulin secretagogues or insulin injection. Glyburide caused more hypoglycemia than other insulin secretagogues and other sulfonylureas. There was no

evidence that Glyburide was associated with an increased risk of cardiovascular events, mortality, or weight gain. However, in 2014, a systematic review and meta-analysis showed that gliclazide and glimepiride were associated with a lower risk of all-cause and cardiovascular-related mortality than glibenclamide [15]. It is suggested that selecting sulfonylurea should be carefully considered regarding increasing mortality risk.

2.4.1.4 Dipeptidyl peptidase-4 (DPP-4) inhibitors

This drug class can improve the HbA1C level without the hypoglycemia side effect. The mechanism of action is to prevent the disintegration of GLP-1. GLP-1 can lower blood glucose levels in the body but is broken down quickly after it is released into the system, so it is inadequate when injected as a single drug. By interfering with the breakdown of GLP-1, DPP-4 inhibitors extend the active half-life of GLP-1 in the body and lower blood glucose levels only when activated. DPP-4 inhibitors do not increase patients' weight and positively affect cholesterol levels. *Sitagliptin (Januvia)*, *Saxagliptin (Onglyza)*, *Vildagliptin (Galvus)*, *Linagliptin (Trajenta®)*, and *Alogliptin (Vipidia)* are currently the five gliptins available in the UK.

DPP4-I significantly lowers the glycemic level (HbA1c, FPG), especially vildagliptin and linagliptin, compared to placebo. Additionally, linagliptin has the most significant probability of reducing BMI. Besides, DPP4-I was associated with not increasing the incidence of adverse events. Among the DPP4-I group, vildagliptin and sitagliptin have the lowest possibility of reducing hypoglycemia and urinary tract infection [16].

There is no significant difference in major adverse cardiovascular events risk between DPP-4 inhibitors and placebo groups. DPP-4 inhibitors show a significantly reduced risk of major adverse cardiovascular events compared to sulfonylureas. While SGLT2 inhibitors might have a lower risk than DPP-4 inhibitors[17].

2.4.1.5 SGLT2 Inhibitors

SGLT2 inhibitors (SGLT2i) are the latest class of oral anti-hyperglycemic agents that have been FDA approved for diabetes mellitus treatment[18]. The kidney is one of the major organs involved in glucose metabolism; blood glucose passes through it can either be excreted or reabsorbed. Sodium-glucose transporter 2 (SGLT2) is located in the tubular kidney to reabsorb glucose. A current class of diabetes medication, SGLT2 inhibitors, was introduced into the market in 2013[18], blocking this mechanism, and causing excess glucose to be urinated. Canagliflozin (Invokana), dapagliflozin (Farxiga), and empagliflozin (Jardiance) are some of the FDA-approved SGLT2 inhibitors that are available to treat type 2 diabetes.

Tentolouris et al.[19] have reviewed the SGLT2i inhibitors class on antidiabetic and cardioprotective properties. SGLT2i reduce Hb1Ac by 0.5%–1.0% and have shown beneficial effects on body weight, blood pressure, lipid profile, and improved endothelial function. Importantly, SGLT2i have shown a cardio and renoprotective effect related to improved cardiac cell metabolism and reduced cardiac fibrosis. The significant adverse effect of SGLT2i includes urinary tract and genital infections and diabetic ketoacidosis. Moreover, the association of SGLT2i with lower limb amputations, Fournier gangrene, risk of bone fractures, female breast cancer, male bladder cancer, orthostatic hypotension, and acute kidney injury also have been raised.

Although SGLT2i has shown a favorable profile in cardiovascular morbidity and mortality, other metabolic disorders that often coexist with DM, such as excess body weight and arterial hypertension, would substitute metformin as the first-line single treatment. However, it is suggested that head-to-head RCTs comparing SGLT2i with

metformin are needed to explain whether SGLT2i can safely substitute metformin as first-line therapy in DM management[19].

2.4.1.6 Thiazolidinediones (TZDs)

Thiazolidinediones including Rosiglitazone (Avandia) and pioglitazone (ACTOS) improve insulin function in the muscle and fat cells and reduce liver glucose production. Due to the serious liver problem side effect, the first generation of a drug in this group, troglitazone (Rezulin), was removed from the market. Rosiglitazone and pioglitazone do not show this liver problem side effect, but users are still closely monitored for liver function as a precaution. Both drugs appear to elevate the risk of heart failure in some patients, and it is controversial whether rosiglitazone may contribute to an increased risk of heart attacks.

A meta-analysis study of Rosiglitazone in 2007[20, 21], years after its launch, was related to severe cardiovascular events in diabetic patients. As a result, the drug was taken off the market due to safety concerns from FDA and The European Medicines Agency (EMA) but reintroduced years later in the US after further studies and metanalysis did not confirm the increased risk.

The controversy regarding the effects of rosiglitazone on cardiovascular events and mortality persists 3 years after a meta-analysis initially raised concerns about the use. In 2010, Steven E et al. [22]. have revisited an updated meta-analysis of risk for myocardial infarction and cardiovascular mortality. The current findings suggest an unfavorable benefit-to-risk ratio for rosiglitazone.

2.4.1.7 Non-sulfonylurea secretagogues

This class of drugs is relatively new compared to the sulfonylureas, with the

the first drug, Meglitinide, was approved by the US Food and Drug Administration in 1997. Meglitinides work similarly to the sulfonylureas but with a few significant differences. It binds to the sulfonylurea receptor in beta cells, but the sulfonylureas bind at a different part of the receptor. The interaction of the meglitinides with the receptor is not as strong as that of the sulfonylureas, translating to a much shorter duration of action, and a higher blood glucose level is needed before the drug induces insulin secretion in the pancreas.

Meglitinides stimulate the beta cells to release insulin.

Nateglinide (Starlix) and repaglinide (Prandin) are two examples of meglitinides. They are taken before each meal to relate to the physiological insulin in the digestive system. Because Meglitinides stimulate insulin release, it is possible to cause hypoglycemia. Moreover, alcohol and some medicines are to be avoided while taking these drugs.

2.4.1.8 Dopamine-2 Agonists

Sympatholytic Dopamine₂ or D₂ receptor agonist group has been approved for type 2 diabetes treatment such as Bromocriptine. According to animal and clinical studies, taking Bromocriptine within 2 hours of awakening stimulates low hypothalamic dopamine levels and suppresses excessive sympathetic tone in the central nervous system (CNS). This results in a reduction in post-meal plasma glucose levels due to the enhanced hepatic glucose production suppression. Adding bromocriptine to poorly controlled type 2 diabetic patients treated with diet alone, metformin, sulfonylureas, or thiazolidinediones produces a 0.5–0.7% decrease in HbA_{1c}. Bromocriptine also declines fasting and post-meal plasma-free fatty acid (FFA) and triglyceride levels. Bromocriptine reduced the major cardiovascular endpoint by 40% from a 52 double-blind, placebo-controlled study in type 2 diabetic patients. The mechanism of the drug's beneficial effect on cardiovascular disease is still underdetermined.

2.4.4.9 Bile Acid Sequestrants (BASs)

The cholesterol-lowering medication, BAS, reduces blood glucose levels in diabetic patients, but the mechanism is not yet well clarified. BASs help remove cholesterol from the body, especially LDL cholesterol, which is often raised in diabetic patients causing cardiovascular problems. This medicine reduces LDL cholesterol by binding with bile acids in the digestive tract; in response, the liver generates more bile acids for replacement, thus consuming and reducing LDL cholesterol in blood circulation. Because BASs are not absorbed into the bloodstream, they are usually safe for use by patients who have liver problems. Due to its mechanism of action, the common side effects of BASs can include flatulence and constipation.

2.4.2 Injection therapy

2.4.2.1 Insulin

2.4.2.1.1 Rapid-acting insulin begins to work immediately after injection reaches the highest blood concentration within 1 hour and continues to work for 2 to 4 hours

2.4.2.1.2 Regular or short-acting insulin reaches the bloodstream typically, within 30 minutes after injection; peaks are around 2 to 3 hours after injection and are adequate for roughly 3 to 6 hours

2.4.2.1.3 Intermediate-acting insulin works within 2 to 4 hours after injection peaks at 4 to 12 hours and is sufficient for around 12 to 18 hours

2.4.2.1.4 Long-acting insulin reaches the bloodstream several hours after injection and is likely to lower glucose levels moderately and evenly over 24 hours

2.4.2.2 GLP-1 agonists or incretin mimetics

This medication class works by elevating the “incretins” hormones. These

hormones help stimulate insulin only after meals and reduce hepatic glucose production by suppressing glucagon release. They reduce the rate at which the stomach digests food and empties and can also reduce appetite.

There are six Incretin mimetic/GLP-1 analogs currently available:

Exenatide (twice-daily injection)	or	Byetta
Exenatide (once-weekly injection)	or	Bydureon
Liraglutide (once-daily injection)	or	Victoza
Lixisenatide (once-daily injection)	or	Lixumia
Dulaglutide (once-weekly injection)	or	Trulicity
Semaglutide (once weekly injection)	or	Ozempic

The study on the reduction of cardiovascular events in some of the GLP-1 analogs has been exemplified below:

In the EXSCEL study[23], among type 2 diabetic patients with or without experience of a cardiovascular disease event, exenatide 2 mg once weekly did not significantly differ between patients who received exenatide and placebo.

In the LEADER trial[24], diabetic patients at high CV risk were randomized to receive liraglutide or placebo as an additive to other glucose-lowering drugs. Type 2 diabetes patients at high risk of CV events treated with liraglutide significantly reduced HbA1c, had a lower risk of hypoglycemia, and less encountered glycaemic worsening than similar patients who received the placebo.

SUSTAIN-6 study[25] showed that in type 2 diabetic patients who have high cardiovascular risk, the rate of cardiovascular death, nonfatal myocardial infarction, or nonfatal stroke was significantly lower among patients receiving semaglutide than patients who received placebo.

2.4.3 Miscellaneous drugs with the potential to control blood glucose

dysregulation

2.4.3.1 Ranolazine

Ranolazine is a medication used to treat heart-related chest pain or chronic angina and has evidence to lower HbA1c and FBG levels in clinical trials[26]. Cardiac infarction results from reduced both ATP fluxes and energy supply to the various critical components for the single cardiac myocyte's contraction–relaxation cycle. These include proteins that control myocyte ion balance. Therefore, intracellular sodium and calcium concentration are interrupted, related to myocardial damage following infarction.

The proposed Ranolazine mechanism inhibits the cardiac late-phase sodium current during cardiac repolarization, improving sodium-calcium homeostasis and reducing myocardial infarction. In patients with coronary artery disease and diabetes, ranolazine has been clinical evidence for decreasing HbA1c levels in 2 trials—the Combination Assessment of Ranolazine in Stable Angina (CARISA) trial [27] and the Metabolic Efficiency with Ranolazine for Less Ischemia in Non-ST-Elevation Acute Coronary Syndromes-Thrombolysis in Myocardial Infarction 36 (MERLIN-TIMI 36) trial[28].

2.4.3.2 Sevelamer

Many diabetic patients have coexisting kidney disease. In patients with chronic kidney disease, sevelamer is used to control hyperphosphatemia. In a single-center, randomized, crossover, open-label, intention-to-treat study, sevelamer was revealed a significantly reduce HbA1c, total cholesterol, and triglycerides than calcium carbonate compared to control[29]. However, the mechanism behind sevelamer's effect on the anti-diabetic effect is still unclear. Sevelamer is also a bile sequestrant, along with receiving a phosphate binder. Therefore, sevelamer's effect on HbA1c has probably been related to bile acid-binding ability.

Colesevelam is a bile sequestrant that is approved by the FDA for diabetes and has been shown to lower HbA1c and FBG.[30] Sevelamer magnifies the delivery of bile acids to the distal colon via its bile sequestration capability. Thus it promotes GLP-1 release and modulates HbA1c[31].

Although many pharmacotherapies are available to treat this disease, there is still a need to develop new medications with better efficacy and tolerability. Side effects such as hypoglycemia, gastrointestinal discomfort, weight gain, and cardiovascular or kidney complications are some of the major issues associated with current medications. These side effects can lower drug adherence in patients, contributing to their uncontrolled blood glucose levels.

3. Diabetes Drug Development Process

The process of new drug development is a complicated, time-consuming and expensive process subjected to substantial regulatory requirements. Before the 1960s, there was no established drug authorizing and regulation process. Clinical trials were not closely regulated, or the license approval managed. Post-trial follow-up was not unexpected. The congenital disabilities associated with thalidomide caused changes in the regulation, involving the productive testing of a drug's safety and efficacy. The Food and Drug Administration (FDA) launched the Drug Amendments Act of 1962 in the United States and the Medicines Act of 1968 in the United Kingdom.

Several drug regulations have been changed due to unfavorable side effects from the notable drugs, which expeditates further evaluation of drug safety. The adverse events in rosiglitazone resulted in the required cardiovascular safety demonstration for drugs proposed for type 2 diabetes treatment. The remarkable difference between

ordinary and diabetes drug development is in the demonstration of cardiovascular safety in the clinical trial[33].

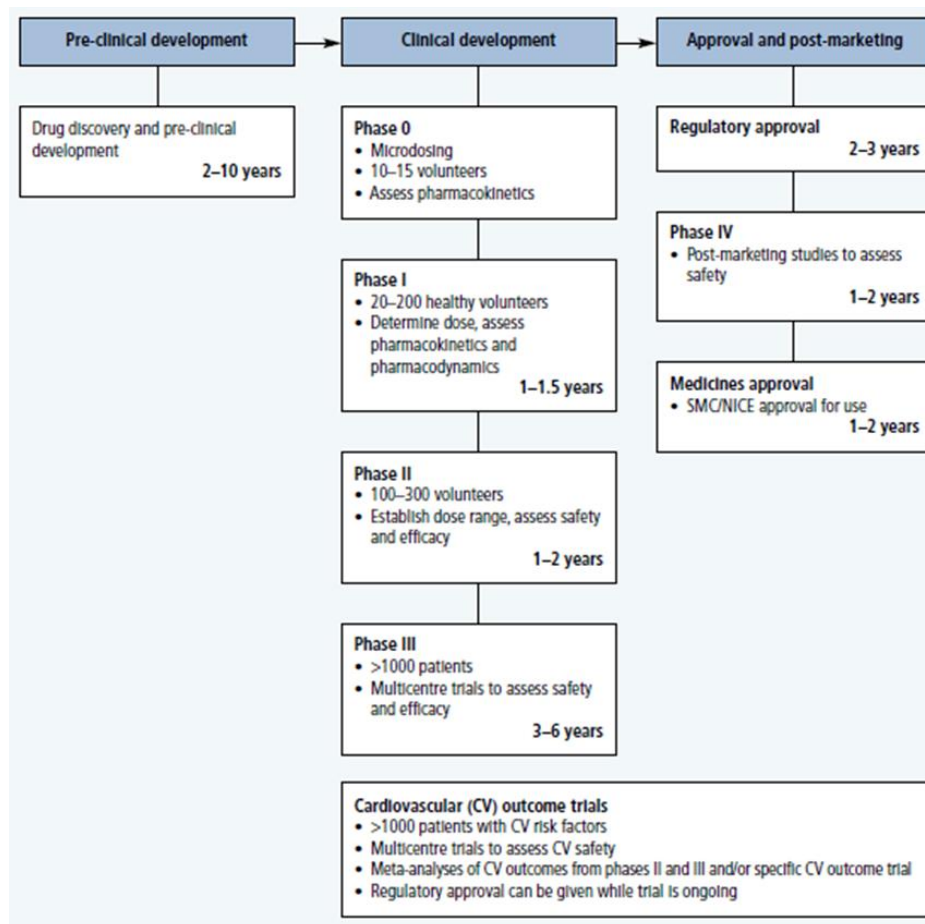


Figure 3. Summary of diabetes drug development process [33]

In the early screening process, *in vitro* assays described below enable the finding of lead compounds to be continued to be developed in the drug development process. The lead compounds can be tested *in vivo* in animal models for their anti-diabetes properties. The efficacy and safety profiles were then carried out before entering clinical trials.

To summarize, a successful anti-diabetic drug depends extensively

on applying satisfactory pre-clinical models[34-36]. Consequently, it is essential to develop an adequate pre-clinical screening assay that promotes precision, high accuracy, and robustness to accelerate the new development of an anti-diabetes drug.

3.1 Pre-clinical development

3.2 Pre-clinical screening assays

3.2.1 Analytical technologies[37]

3.2.1.1 Colorimetry

Colorimetry is close to spectrophotometry, which is one category of electromagnetic spectroscopy that provides the quantitative evaluation of the reflection or transmission properties of a material as a function of wavelength.

Spectrophotometry is a quantitative measurement of light absorption substance by measuring light intensity as light radiation invades to sample solution. Basically, each substance individually absorbs or transmits light over a specific wavelength range.

Photometers is a device of a spectrometer, also called spectrophotometers, that can measure light intensity at various wavelengths. The ultraviolet, visible, and infrared radiation are the most common radiation applied to spectrophotometry.

In addition, the colorimetric method can measure the active component in numerous essential drugs. Moreover, it supports a semi-quantitative technique to provide drug potency; a more intense color change or darker color indicates a more substantial component. The accuracy of the colorimetric method is derived from a spectroscopic device that measures light's absorbance through a substrate. However, colorimetry can provide restricted information and damage the sample under examination.

3.2.1.2 Chromatography

Chromatography distinguishes mixed compounds based on a variety of chemical and physical characteristics. It can take discrete drug additives for further analysis and, when coupled with a suitable detector, produces qualitative and quantitative data about the active compounds and contaminants. Thus, this is the most standard analytical method used in drug assessment. Chromatography varies from the traditional techniques, such as thin-layer chromatography (TLC) with a visual investigation, to more sophisticated laboratory protocol, such as high-performance liquid chromatography (HPLC) used with mass spectrometry in tandem. The limitation of this method is similar to the colorimetric tests; chromatography disrupts the drug sample.

High-performance liquid chromatography or HPLC is an advanced. When concomitant with the subtle detectors, highly sensitive chromatography technique is recognized as the standard drug content analytical technique. However, correlated detection technology can be expensive and require skilled operators. The systems also require steady electrical power, which can be a barrier in some developing countries.

Gas chromatography is the most robust chromatographic approach, produces comparable data as other chromatography methods. However, it can only be used to analyze dissociated vaporous materials, such as the remaining solvents or any vapor impurities, and still requires highly trained people to operate. This technology can only be used when the interested compounds come to be analyzed in the gas from within the analytical temperature limit, and the analyte does not degrade within the operating temperature.

3.2.1.3.1 Mass spectroscopy

Mass spectroscopy is an established analytical technique that is relatively technically demanding. This technique produces rich structural data and accurate molecular

weight of the compound under inspection. In addition, mass spectroscopy can recognize many active compounds and additives and some impurities[38-40]. Mass spectrometry-based assays have been established to screen complex compounds, e.g., natural product extracts, to expand the molecular diversity of drug leads. Mass spectrometry usage in supporting combinative library synthesis and purification is addressed, and screening applications such as frontal affinity chromatography-mass spectrometry, gel permeation chromatography-LC-MS[41]

However, mass spectrometers require a steady electrical power source that can sustain in developing countries. However, this technique is expensive in terms of capital and running costs. The instrument requires skilled personnel to set it up and requires plenty of sample preparation steps. They are also destructive techniques that need a sample to be in solution form and free from particulate matter [42]

3.2.1.3.2 Nuclear magnetic resonance (NMR) spectroscopy

Nuclear magnetic resonance (NMR) spectroscopy evaluates the interaction of nuclei with electromagnetic radiation. It is a technique suitable for nuclei with a non-zero spin, such as the hydrogen and carbon-13, that allows quantitative information with little sample preparation[43]. NMR spectroscopy plays a vital role in the drug discovery and development process. NMR screening procedures are very systematic and variable in discovering high-affinity ligands for biologically related macromolecules, interpreting ligand-binding sites, and recognizing small molecules with various binding affinities. Thus this technique is proven to be a valuable and robust tool in the structure-based drug design.[44].

However, the NMR apparatus is costly and requires sturdy electrical power reserves, well-controlled temperatures, and full-skilled chemists for the operation. Resonance peak integration area can contribute detailed information about structural

composition; the area under each peak relates to the number of nuclei (in protons or carbon-13 atoms) corresponding to that individual signal.[43]

3.2.1.3.3 Near-infrared and Raman spectroscopy

Near-infrared spectroscopy (NIRS) is a spectroscopic method based on the absorption of electromagnetic (EM) radiation at wavelengths 780 to 2,500 nm to excite specific molecular vibrations. NIR spectroscopy is the interaction between light and sample that the NIR detector measures as transmittance and absorbance. The molecular bonds most sensitive to excitation in this spectrum region tend to be polar, with the vibrations changing the bond's dipole moment. Transmittance relates to the light intensity that passes entirely through the sample and is interpreted at the detector. Absorbance is a measurement of light absorption from a sample.

NIR can typically penetrate much further into a sample than mid-infrared radiation that gives two advantages; a more significant amount of material is exposed, declining sampling error and allowing for spectroscopic sampling without removing the material from the original container. Near-infrared spectroscopy can be beneficial in probing bulk material with a bit of sample preparation. The typical applications include medical and physiological diagnostics and research, including blood sugar, pulse oximetry, functional neuroimaging, etc. There are also applications in other areas such as pharmaceutical, quality control, atmospheric chemistry, combustion research, and astronomy. The application in pharmaceutical assays typically applies to qualitative analysis, quantitative analysis, determination of active compounds in pharmaceutical dosage form, and considerations for intact dosage form analysis rather than drug discovery [45].

Raman spectroscopy is a non-destructive tool that provides information on qualitative and quantitative drug ingredients and additives. Raman spectroscopy relies strictly

on the non-elastic scattering of photons from a laser source. When photons from the laser interact with the material, the energy from these photons is partially absorbed, and the remaining energy is re-emitted as scattered light at a different frequency. The scattered light is shifted from the original laser frequency by an amount that depends on the energy absorbed by the molecular bonds. In contrast to NIR, the molecular bonds associated with Raman scattering are non-polar. The spectrum generated by a Raman instrument generally has sharper and better-resolved peaks than NIR, which can provide more chemical information about unknown samples. In contrast, Raman spectroscopy requires more technical expertise than NIR. The Raman excitation laser can penetrate optically clear materials such as glass or plastic, limiting the spectroscopic interference from the sample containers.

This technique also provides information about chemical structure and identity, phase and polymorphism, intrinsic stress/strain, contamination, and impurity[46]. The application of Raman spectroscopy is involved in both drug discovery and development aspects [47, 48]. This can approximate the drug's molecular activity and demonstrate a drug's physicochemical properties, such as its partition coefficient. Raman spectroscopy's immense potential should be further investigated in the future[49].

3.2.1.3.4 Infrared spectroscopy

The infrared region in the electromagnetic field that this thesis will be a focus on the mid-infrared ($4000 - 400 \text{ cm}^{-1}$) due to the most common analytical spectroscopy for bioanalysis because it provides the sharpest band and more information about disease-biological relations. Mid-infrared spectroscopy's fundamental interaction between the sample and the IR beam is absorbed by the sample's functional groups that vibrate in stretching, bending, and distortion movements, causing an excitation to the molecular

vibration. This absorbance and wavelength are correlated specifically to the bonds present in the molecule.

3.2.1.3.4.1 The principle of Infrared Spectroscopy

Electromagnetic radiation (EM radiation or EMR) refers to the waves (of the electromagnetic field) described as synchronized oscillations of electric and magnetic fields that travel through the harmonic space. For a transverse wave, the wavelength λ is determined by the distance between two adjacent crests (or troughs), frequency ν (the number of waves passings at a particular point of a time unit), or energy E . The wavelength λ frequency ν and energy E correlation are described in **Equation 1** and **Equation 2**. It is often to use the wavenumber unit ($\bar{\nu}$) in the vibrational spectroscopy analysis, which is defined as the number of waves in one centimeter (cm^{-1}), as it is proportional directly to E and ν .

Equation 1: Energy of electromagnetic radiation

$$E=hc\bar{\nu}$$

Equation 2: Frequency of electromagnetic radiation

$$\nu=c/\lambda$$

Where;

E is the energy of electromagnetic waves (J)

h is the Plank's constant (6.625×10^{-34} Joule-seconds or J s)

λ is the wavelength (cm)

ν is the frequency (s^{-1})

$\bar{\nu}$ is the wavenumber in cm^{-1}

c is the speed of light (2.998×10^8 m/s)

There must be a change in dipole moment for IR radiation to be absorbed. These vibrational motions cause the dipole moment to change as the bond expands and contracts. Chemical bonds absorb IR radiation if the radiation energy matches the bond's vibrational energy during the molecular vibrations. The absorption level of IR radiation is proportional to the change of dipole moment and causes the vibrational energy to transit to the next higher level. In a simple diatomic molecule performing harmonic oscillation, Hooke's law describes such motion's vibrational frequency in **Equation 3**.

Equation 3: Hooke's Law for vibrational frequency

$$\nu = \frac{1}{2\pi} \sqrt{\frac{f}{u}}$$

Where;

ν is the frequency of harmonic oscillation

f is the bond force constant

u is the reduced mass of a diatomic molecule given by **Equation 4**.

Equation 4: The reduced mass of a diatomic molecule

$$u = \frac{m_1 m_2}{m_1 + m_2}$$

A polyatomic molecule incorporates three types of movement; rotational, translational, and vibrational. The N atoms molecule will have $3N$ degrees of freedom along the Cartesian plane's x , y , and z -axes. The number of vibrations will be $3N$, subtracting 3 translational and 3 rotational movements. Generally, a non-linear molecule with N atoms has $3N - 6$ normal vibration modes, while a linear molecule has $3N - 5$ modes because the molecular axis rotation cannot be observed. A small molecule can generate many distinctive

vibrational modes and produce a complex fingerprint-like absorbance pattern in the mid-infrared region. These vibrations can be categorized merely as stretching or bending vibrations.

Practically, the transmission is a conventional setup for an IR experiment. The IR absorbance spectrum obtained by measuring the intensity of an IR light passing through the sample of interest can be calculated by **Equation 5**.

Equation 5: Absorbance IR light

$$A = -\log I/I_0$$

Where;

A is the absorbance of IR light

I is the intensity of transmitted light

I_0 is the intensity of incident light

The ratio (I/I_0) is termed transmittance, T.

The spectrum consists of various absorbance peaks, which appear at wavenumbers correlated to the molecular vibrational frequencies of the sample. Light absorbance is proportional to the path length and concentration of a sample described in Beer-Lambert law- hence it is a quantitative analysis. **Equation 6**.

Equation 6: Beer's-Lambert Law

$$A = \epsilon c l$$

Where:

A is the absorbance of the species

ϵ is the molar absorptivity coefficient

c is the concentration in mole per liter

l is the pathlength in centimetres

3.2.1.3.5 Fourier Transform Infrared Spectroscopy (FTIR)

A.A. Michelson[50] has been developed the FTIR spectrometer, as shown in figure 4. The interferometer consists of an IR source, fixed and mobile mirrors, beam splitter, and detector. When the beam splitter is split, the light beam into two different pathways to the two mirrors, then the light is reflected and recombined at the beam splitter. The resulting beam intensity is analyzed as a function of the position of the mobile (sliding) mirror. The analyzed IR intensity enables an interferogram to be obtained. Then an IR spectrum can be established by Fourier transform to generate a single beam spectrum with the corresponding wavenumber on the x-axis.

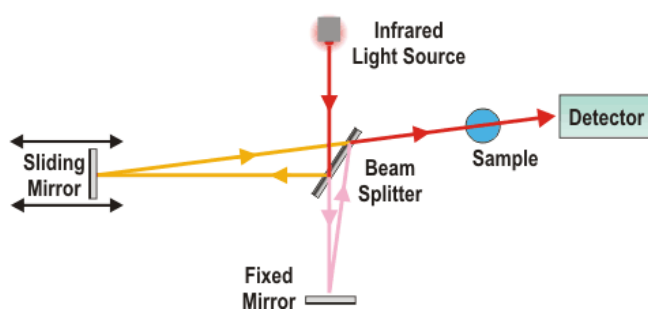


Figure 4 . Schematic diagram of FTIR spectrometer [21]

This developmental technology improves the measurement speed compared to the traditional dispersive instrument. This also enhanced the signal-to-noise ratio because of the higher throughput of light. The benefit of a non-destructive, sensitive, and minimal sample preparation requirement made this suitable for the cellular-based study.

3.2.1.3.6 FTIR live cells Spectroscopy

Many studies have been measuring dried or fixed cells to avoid the the dominance of water absorbance (mainly OH stretching and bending bands at 3500 cm^{-1} and 1640 cm^{-1}). However, studies have shown that the IR spectra of dried cells are different from live cells[51]. In the fixation process, a dehydrated cell affects the DNA conformation and transforms it from B-form to A-form. This resulted in weaker and broader DNA peaks and difficulties differentiating other cellular components like protein, RNA, and carbohydrates. [52] Moreover, adherent cells are sometimes harvested with a proteolytic enzyme known as trypsin. This can cause plasma membrane protein remodeling and apoptotic induction. [53] However, this effect can be diminished when cells are stabilized in the medium for a few hours before FTIR scanning. The dehydration effect can be reduced when cells are rehydrated in an aqueous environment before measurements [53].

FTIR spectroscopy with attenuated total reflection (ATR) sampling method allows a continuous study of live cells in the aqueous environment. [54] According to the water band's dominance in the mid-IR region, water band subtraction and optimizing the FTIR measurement's effective path length can minimize the influence of water. Furthermore, this method is preferable because it allows performing cellular studies in a similar way to the *in vitro* cell studies and minimizes the potential artifacts from the trypsinizing, fixing, and drying process.

Besides, FTIR live cell measurement can be made continuously and frequently

to the same batch of cells with a temporal resolution potentially down to less than a few seconds. It can identify transient cellular events challenging to detect from dry cell samples or using standard biochemical assays[55].

Table 2. IR vibrational bands of the cell components in the 1800-900 cm^{-1} region

IR Absorption Peak (cm^{-1})	Allocation	Cellular Components
960-970	Stretching of C–O, C–C	Deoxyribose in cellular nucleic acids
1000-1150	Phosphodiester stretching	Phosphorylated Proteins
		Polysaccharide
1020-1050	Stretching of C–O, C–C	Reasonably specific of Nuclei acid in the absence of Glycogen
		Glycogen
1050-1070	Stretching of C–O deoxyribose	DNA
1050-1100	Stretching of C–O–C	Nucleic acids, Phospholipids
1050-1100	PO ²⁻ stretching modes	Nucleic Acids
	P–O–C antisymmetric stretching of phosphate	Polysaccharide

	ester C-OH stretching of polysaccharides	
1080-1120	Symmetric phosphate stretching PO^{2-} P-O-C symmetric stretching of phosphodiester	Phosphodiester linkage in DNA and RNA Phospholipids
1100-1150	Symmetric stretching of C-C, C-O, C-O-C and C-OH, and C=O stretching	Carbohydrates Glycogen
1220-1240	Asymmetric PO^{2-} stretching	Phosphodiester linkage in DNA and RNA Phospholipids
1400	Symmetric stretching of COO^-	Fatty acids, Amino acids, Lipids
1415	C-O-H in-plane bending	Carbohydrates, DNA, RNA and proteins
1470-1250	Symmetric and Asymmetric CH_2 and CH_3 bending	Lipids Proteins

1560-1500	C–N–H bending and C–N stretching	Amide II
1600	Asymmetric stretching of COO-	Fatty acids, Amino acids, Lipids
1655-1630	C=O stretching	Amide I
1700-1750	Ester C=O stretching	Fatty acids, Nucleic acids

The major structural components of a eukaryotic cell are proteins, carbohydrates, lipids, and nucleic acids. These are IR-active molecules and can be detected using FTIR spectroscopy. FTIR spectroscopy is increasingly employed in analyzing biological samples such as tissues and cells.[56] For example, FTIR is included to study membrane lipids[57], proteins' secondary structure[58], and the DNA structure.[52] Also, FTIR spectroscopy can detect and distinguish their major components in studies of biological samples[59]. A conclusion of the influential IR bands with cellular components spectral assignments in the 1800-900 cm^{-1} region is represented in Table 2[60-62].

Overall, in the cell's spectral absorbance of the region, 1800-1300 cm^{-1} is correlated with proteins, especially the carbonyl stretching (C=O) of amide I at $\sim 1640 \text{ cm}^{-1}$ and N–H bending and C–N stretching of amide II at $\sim 1540 \text{ cm}^{-1}$. The spectral absorbance of various amino acid side chains and lipids' C–H bending can be discovered at 1450-1400 cm^{-1} . Infrared peaks in the 1300-900 cm^{-1} region indicate the absorption of the amide III ($\sim 1240 \text{ cm}^{-1}$), the symmetric ($\sim 1080 \text{ cm}^{-1}$) and asymmetric ($\sim 1240 \text{ cm}^{-1}$) stretching of the PO_2^- in the DNA, C–O–P stretching of lipids/phospholipids and C–O stretching of carbohydrates. Moreover, FTIR spectroscopic studies have been utilised to discriminate cells in their cell cycle stage[63],

apoptosis[64, 65], distinguish the difference between cancer cell lines[66], and predict the invasiveness of cancer cells. [67]

3.2.1.3.8 FTIR approach and diabetes research

FTIR has been introduced in diabetes and metabolism research since 2007 as a diagnostic tool for analyzing chemical deposition in hair samples with different blood sugar levels. The spectral differences between normal and high blood sugar from human scalp hair samples suggested that the FTIR method may provide a rapid, non-invasive, and effective way for diabetes diagnosis and detecting chemical changes that have evolved from the diseases[68].

In 2013, FTIR was shown to be able to discriminate between healthy and diabetic rats' tissue samples from rat kidney plasma membrane apical sides (brush-border membranes), liver microsomal membranes, and Extensor digitorum longus (EDL) and Soleus (SOL) skeletal muscle tissues. The variety of changes in the spectral features, e.g., frequency and signal intensity/area, was observed in diabetic tissues and membranes compared to the control samples combined using cluster analysis that successfully distinguished between diabetic and control groups [69].

Eikje N.[70] has demonstrated a real-time assessment and continuous monitoring of glucose in skin tissue from blood glucose diffusion using horizontal attenuated total reflectance (HATR) Fourier transform infrared (FTIR) spectroscopy. The capillary glucose levels from the skin detected by HATR were related to the glucose that increased and circulated via blood flow. He also suggested that this technique can be used as the metabolic activity monitor of glucose uptake in the epidermal skin and might have a potential clinical interpretation of glucose metabolism activity.

Attenuated total reflection (ATR) Fourier transform infrared spectroscopy (FTIR) combined with eXtreme Gradient Boosting (XGBoost) ensemble learning algorithm has been established as a rapid diagnosis model of pre-diabetes. The peripheral blood samples were collected and measured for the fasting blood sugar and 2 h blood sugar levels of the oral glucose tolerance test (OGTT). In addition, they determined the control and diabetes groups according to the WHO diagnostic criteria. ATR FTIR with XGBoost model had a specificity of 100.00%, a sensitivity of 85.00%, and an accuracy of 93.33% for the pre-diabetes and healthy subject differentiation. This measurement mode is simple and time-efficient, with no need for sample pre-processing. Moreover, the developed model provides a fast, precise method for pre-diabetes diagnosis[71].

The FTIR technique has been reported to predict, non-invasively, blood hemoglobin A1c (HbA1c) and be able to screen for diabetes. Humans with and without diabetes have been examined, and FTIR spectra were extracted from their lip surfaces. The lip surface spectra correlate significantly to the HbA1c levels and blood glucose samples. Specifically, the peaks at around $1300\text{--}1400\text{ cm}^{-1}$ of the lip surface spectrum distinguished subjects with higher and lower HbA1c levels. Furthermore, the correlation between HbA1c levels from partial least squares (PLS) regression analysis and FTIR spectra of the lip was highly significant for predicting HbA1c levels. Thus, the FTIR technique has been proposed as an effective tool for diabetes screening of patients with higher HbA1c levels[72].

Infrared spectroscopy was employed as a diagnostic tool for diabetic prediction by analyzing the molecular and sub-molecular spectral features in the saliva of non-diabetes and healthy subjects. The different spectral analysis illustrates several major metabolic components - lipid, proteins, glucose, thiocyanate, and carboxylate - can be used to separate healthy and diabetic saliva. This technique's overall diabetes diagnosis accuracy

was 100% on the training and 88.2% on the validation set. To conclude, infrared spectroscopy can be used to establish the complex biochemical profiles in saliva and identify several potential diabetes-associated spectral signatures[73].

ATR-FTIR spectroscopy has been used to evaluate the saliva of non-diabetic (ND), diabetic (D), and insulin-treated diabetic (D+I) rats to identify biomarkers that can be used for glucose monitoring. The spectrum of the saliva of ND, D, and D+I rats revealed several distinct vibrational modes, between 1452 cm^{-1} and 836 cm^{-1} . The two unique vibrational modes were pre-validated by ROC curve analysis with a significant correlation with glycemia. In the comparison between the ND and D+I rat, the classification of D rats was accomplished with a sensitivity of 100%, and an average specificity of 93.33% and 100% using bands 1452 cm^{-1} and 836 cm^{-1} , respectively. Furthermore, the 1452 cm^{-1} and the 836 cm^{-1} spectral bands proved to be robust spectral biomarkers and highly correlated with glycemia (R^2 of 0.801 and 0.788, $P < 0.01$, respectively). Spectral salivary biomarkers derived from FTIR spectroscopy may provide a novel robust alternative for diabetes monitoring using non-invasive technology. [74]

FTIR spectroscopy of hair samples is also able to follow up the diabetes medication; metformin from three months of treatment. Significant spectral differences were observed between pre-and post-treatment from the hair fiber samples. The ATR-FTIR hair spectra of diabetic patients (pre-and post-treatment) and healthy subjects have been studied. The absorbance values of some of the specific bands of biomolecules present in the hair samples, e.g., protein, lipids, and glucose, are observed for both pre-and post-treatment subjects. It was summarized that these biomarkers are remarkably different between pre-and post-treatment hair samples. The results are further statistically validated with the dependent t-test, which reported that the two groups' spectral variations are statistically significant. [75]

FTIR is clearly shown to have the discriminative power to distinguish the biochemical profiles of a diabetic and healthy person. However, metabolism in live cells, which can improve understanding of diabetes and is ideal for diabetes-related research, has not yet been demonstrated. Therefore, IR vibrational bands of the cell components which are detectable by FTIR spectroscopy, especially phosphate components, which are essential in the energy cycle and diabetes metabolism, e.g., carboxylate, are expected to see information that can answer the gap in these research areas by using the Live-cell FTIR approach.

4.The principle of Multi-reflection (Multi Bounce) ATR

An attenuated total reflection accessory works by measuring the attenuation of light from the internal reflection of the infrared beam at the interface of the ATR element and sample (Figure 5). An infrared beam is shone directly onto an optically dense crystal with a high refractive index to produce an internal reflection at a specific angle more significant than the critical angle, and the IR-absorbing sample with a low refractive index is attached on the measurement side. This internal reflectance resulted in an evanescent wave that extended beyond the crystal's surface into the sample. The penetration depth for ZnS ATR crystal with 2.25 refractive index and 45° incidence angle used is in the 1-3 μm calculated using Equation 7. There must be good contact between the sample and the crystal surface. The evanescent wave will be attenuated in infrared spectrum areas where the sample energy is absorbed. The attenuated evanescent wave is traveled back to the IR beam, exiting the opposite end of the crystal, and proceeded to the detector in the IR spectrometer. The system then generates an infrared spectrum[76, 77]. This is advantageous for live-cell measurement. The penetration depth is deep enough to detect the cellular component attached to the

crystal surface but not too deep, so the culturing medium beyond the cell does not contribute significantly to the spectrum.

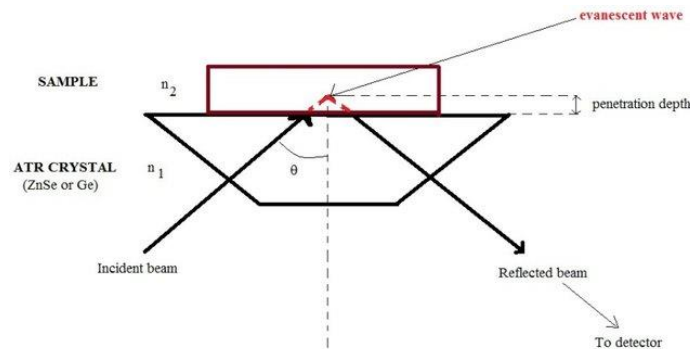


Figure 5. Schematic diagram of the multi-reflections ATR element [45]

Equation 7: Depth of penetration in the multi-reflection ATR element

$$d_p = \frac{\lambda}{2\pi n_1 \sqrt{\sin^2 \theta - \left(\frac{n_1}{n_2}\right)^2}}$$

Where;

d_p is the depth of penetration

λ is the wavelength of the incident light (cm)

n_1 is the refractive index of the ATR element

n_2 is the refractive index of the sample

θ is the angle of the incident light

Multi-reflection ATR application can produce a sufficient path length for measuring live cells attached to the ATR crystal. The internal path length is proportional to the number of reflections; the multi-reflection procedure will allow the effective path length improvement to intensify the signal-to-noise ratio by probing the cellular components of live cells attached to the ATR element. [77] Besides, the small penetration depth in the ATR and

hence the small signal of the medium is resulting in an improvement of the signal-to-noise ratio of the acquired spectra.

5. Multivariate analysis

Multivariate analysis is the statistical and mathematical study of data where multiple measurements are made in each experimental setting. The relationships among multivariate measures and their data structure are significant. According to the FTIR-live cell approach, each obtained spectrum is informative and contains the cellular composition and changes related to the compound or drug exposure. Rather than relying on the study of a single peak, this analysis helps identify the multiple hidden factors that contribute to the spectral changes. Supervised and unsupervised are the two main categories used in the multivariate analysis of FTIR spectral data[78, 79].

6. Principal component analysis (PCA)

PCA is a popular multivariate analysis method. This technique has a non-prior knowledge requirement (unsupervised) about the data to explain samples' relationships under examination. The main benefit of PCA is that it reduces the dimensionality of multivariate data [80]. During the analysis, the original variables from the data matrix (**D**) are converted to calculate the new variables combined linearly with the original variables and called principal components (PC). This conversion produces two new matrixes; a matrix (**V**) of PC, i.e., the eigenvectors, and a matrix (U) of scores, i.e., the eigenvalues. The first PC reveals the most notable variations in the data set, whereas the second PC orthogonal to the first PC reveals the second most variations of the data. Similarly, the other orthogonal components to the first PC generated by the same protocol consecutively categorize it from their PC's subscription. The relation between components and variables was acquired from the loading plot and displayed as a spectrum. The loading plot represents the significant variables that

are related to the spectra. It also shows the parallel and non-parallel between IR peaks. Essentially, it arranges the understanding of the significant changes that are difficult to detect from the raw spectra. The original matrix (D) data is regenerated by the multiplication of V and U plus the reminder (E) as shown in **Equation 8** [81].

$$D = UV^T + E \quad \text{Equation 8}$$

7. Aims

This thesis aims to illustrate that live-cell ATR-FTIR spectroscopy is essential for evaluating live cells, diabetes-related compounds, or anti-diabetes drug interaction. It also aims to develop the technique as a reproducible tool for diabetes studies in the pre-clinical screening process of anti-diabetes drug development.

The aims are described with the following objectives:

1. To develop and improve the live-cell measurement using ATR-FTIR spectroscopy and apply principal component analysis to enhance spectroscopic data's significance.
2. To develop a complementary tool for diabetes-related study due to the effect of live cells and diabetes-related compounds. This is accomplished by studying the interaction among the hepatocyte carcinoma cell line (HepG2), glucose, and insulin. The results are confirmed by comparing the metabolic changes observed from the spectroscopic data and the diabetes metabolism literature.
3. To illustrate, the cellular change measured in FTIR spectra is related to the drug's mechanism of action. Specifically, insulin sensitizer drug metformin, a novel drug PF-04995132, and a natural compound, Resveratrol, are evaluated. PCA is used to discriminate the control (without drug treatment) and drug treatment in a live-cell FTIR study.

Chapter 2 Method Development and Experimental Design

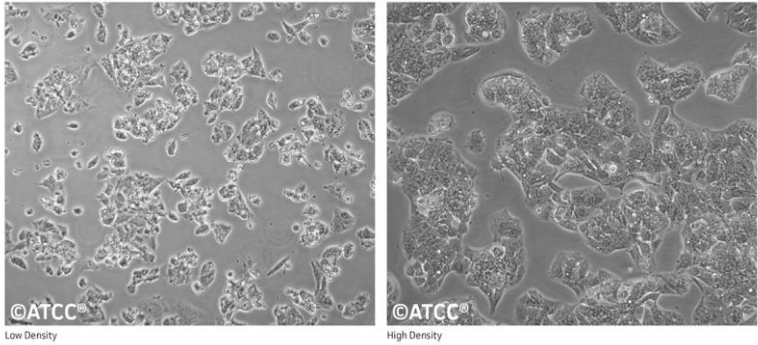
2.1 Introduction

The live-cell FTIR spectroscopy measurement method has been successfully developed before for testing anti-cancer agents[82]. However, the technique has not been applied to study anti-diabetic drugs. To be comparable to the conventional biochemical *in vitro* assays for the study of anti-diabetic drugs and be an alternative tool for analyzing cell metabolism alteration, all cell culture processes, sample preparation, and ATR-FTIR measurements are designed to keep the conditions and cell viability during the FTIR experiment similar to the convention *in vitro* assays.

2.2 Cancer Cell Lines

This work has selected the HepG2 or Hepatocellular Carcinoma (HCC), hepatoma cell line, or hepatoblastoma cell line. Since most diabetic metabolism occurs in the human liver, many studies have commonly used the HepG2 model in diabetes-related cells-metabolism research[83-87]. These adherence cells are compatible with the ATR-FTIR approach, in which the IR beam from the interferometer can probe the attached cells on the ATR plate and produce the spectroscopic results from the cell alterations. The general information and characteristics of the HepG2 cell line are summarized in Table 3 [56].

Table 3. Summary of general information and characteristic of HepG2 cell lines

General information	
Organism	<i>Homo sapiens</i> , human
Tissue	Liver
Morphology	epithelial-like
Culture properties	Adherent
Disease	hepatocellular carcinoma
Age	15 years adolescent
Gender	Male
Ethnicity	Caucasian
Characteristic	
Image	<p>ATCC Number: HB-8065 Designation: Hep G2</p>  <p>©ATCC® Low Density ©ATCC® High Density</p>
Derivation	HepG2 was derived from a hepatocellular liver carcinoma of a 15-year-old Caucasian male.
Clinical data	15 years Caucasian male
Receptor Expression	insulin; insulin-like growth factor II (IGF II)

2.2.2 Cell culture

For both *in vitro* and live cell ATR-FTIR experiments represented in this thesis, HepG2 (ATCC® HB-8065™) (obtained from maintained stock at passage 18) was kindly provided by Professor Khuloud T. Al-Jamal, Insitute of Pharmaceutical Science, King's College London. Cells were cultured in Dulbecco's Modified Eagle Medium (DMEM) (Sigma-Aldrich, D6429) and supplemented with 10% v/v Foetal Bovine Serum(FBS) (Sigma-Aldrich, F7524), 2mM L-glutamine (Sigma-Aldrich, G7513), 1% v/v penicillin-streptomycin (Sigma-Aldrich, P4333), 1% non-essential amino acids (Sigma-Aldrich, M7145). The cells were maintained in a T25 flask in a 5% CO₂ incubator at 37°C. Microbiological decontamination and cleaning procedures have been routinely done every two weeks following the standard protocol. [88]

2.2.2.1 cell counting and viability testing

This step is routinely conducted before each of the live cell FTIR measurements. Cell counting was performed in the early stage of cell culture to comprehend the cell doubling time, calculate the splitting ratio for maintaining cells, and control the harvesting time for the live-cell FTIR experiment. For cell counting, cells were cultured in a T25 flask and harvested at 80% confluence by washing with 1X phosphate Buffered Saline (PBS) three times, then 1mL of 0.25% trypsin (1:250) in Hank's balanced salt solution (HBSS) with 0.1% EDTA-disodium and kept in the CO₂ incubator at 37°C for 5 minutes. Then, around 3 mL of new medium solution was added to the flask and mixed by pipetting to make a cell suspension. After that, a 0.4% trypan blue stain was used to test the viability percentage of cells. The concept behind the trypan blue dye exclusion test is that a damaged cell membrane will be allowed the dye to enter inside and stain the cell, whereas viable cells will have no staining observed. This test protocol is an equal volume of cell suspension, and the trypan blue dye stain (20uL mixed solution) was loaded for 10 uL into the chamber of Countess® Automated Cell Counter (Figure

6). The red dots on the cell counter screen represent the dead cells that the device can detect from the dye exclusion test, while viable cells have shown in green.



Figure 6. Trypan blue exclusion test for HepG2 cell using Countess® Automated Cell Counter

2.2.2.2 Live-cell FTIR measurement preparation

When cultured HepG2 cells reached 80% confluence, they were trypsinized and centrifuged 1,000 x g into a pellet. This is followed by rinsing and resuspending the pellet in DMEM CO₂ independent medium (Gibco,18045054) supplemented with 10% FBS, 2mM L-glutamine, 1% penicillin-streptomycin, and 1% Non-essential amino acids. 2 million of HepG2 suspension (1 million cell/ mL) was seeded and formed a cell monolayer on the ATR plate. DMEM CO₂ independent medium was used to avoid the requirement of 5% CO₂ at the sampling chamber of the spectrometer. The cell suspension was incubated for 24 hours to allow cell attachment. Once cells were attached, which is indicated by slow but steady growth in the amide II band from the FTIR measurement (at around 24 hours after seeding), a DMEM CO₂ independent medium, with the designated treatments, supplemented with 2% FBS was used in the experiment (a lower percentage of FBS was used to avoid interference to spectral changes from cell growth). The first measurement immediately after the treatment was used

as the background. The spectral change was then monitored for 24, 48, or 72 hours with a measure taken every 10 minutes. Each experiment was repeated for 3 times based on 3 independent cultures with cells from a similar passage number (within the 10) and measured on a different day.

2.2.2.3 Growth rate of HepG2 cells in DMEM high glucose and DMEM CO₂ independent medium

This project is the first to use DMEM CO₂-independent medium to avoid carbon dioxide in the FTIR setup. Previous studies used the L-15 medium during the ATR FTIR measurement to cultivate cells in a CO₂-free environment with the same FBS percentage (10%). However, HepG2 was found to have a significant difference in growth rate with L-15 as shown with the lowest doubling time than other media presented in the [table 4](#). Furthermore, the thesis project emphasizes cell diabetes metabolism, where glucose plays an important role. DMEM CO₂ independent medium contains glucose; therefore, it is more suitable for this study than L-15, which includes D-galactose as the energy source.

Table 4. Doubling time of HepG2 cells in DMEM high glucose, DMEM CO₂ independent

Cells	Medium	Initial seeding count (T25 flask)	Cell count after 72 hrs	Viability (%)	Doubling time (hr)
HepG2	DMEM high glucose	4 x 10 ⁴ / cm ²	3.53 x 10 ⁶	87%	40
	DMEM CO ₂ independent medium		2.33 x 10 ⁶	87%	59
	L-15		1.45 x 10 ⁶	92%	70

2.2.2.4 Density and Attachment of HepG2 cells on the ATR plate

A complete attachment of HepG2 cells on the ATR surface is a prerequisite for the ATR sampling method. Therefore, cell confluence used in the live-cell FTIR method was adjusted and tested to confirm that the cell monolayer remained viable during the experiment. The live-cell density required to obtain complete coverage of the 5 cm² area of the ATR element is calculated based on cell counting at 80% confluence in a T25 flask. Cells that reached 80% confluence in the T25 flask were counted, harvested, and seeded on the ATR plate to form a monolayer. A reflective optical microscope with a 5x objective (L2003 microscope fitted with a digital camera) and transmission mode (Hund Willovert S 35550) were used to ensure the adherence and the formation of a monolayer of cells. The images captured 24 h after seeding were compared between cells cultured in the ATR plate and in a T25 flask in a 5% CO₂ environment. The cells have shown a similar healthy morphology with a monolayer of cells wholly adhered to the ZnS ATR plate. (Figure 7)

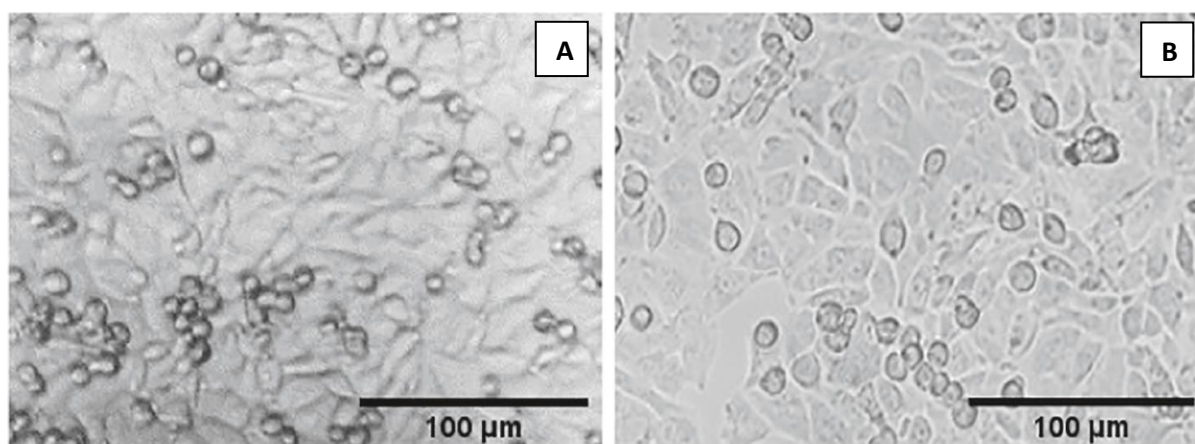


Figure 7. Image of HepG2 cells at 24 hours of seeding on the ATR element (A) and T25 flask (B)

2.3 ATR FTIR Measurement

2.3.1 Multi-Reflection ATR Accessory

A temperature-controlled ZnS attenuated total reflectance (ATR) plate with 10 reflections on the sampling site and 45° ATR element (80 mm X 10 mm X 4 mm) was purchased from Crystran Ltd., UK. The sufficient path length obtained from this accessory is approximately 20-30 μm with a penetration depth of nearly 2-3 μm . The trough plate's measurement surface area is 5 cm^2 , where attached live cells were measured. The capacity of the trough is around 2.5 mL of culturing medium. The container was sealed with a warmed lid to avoid evaporation, as shown in (figure 8)

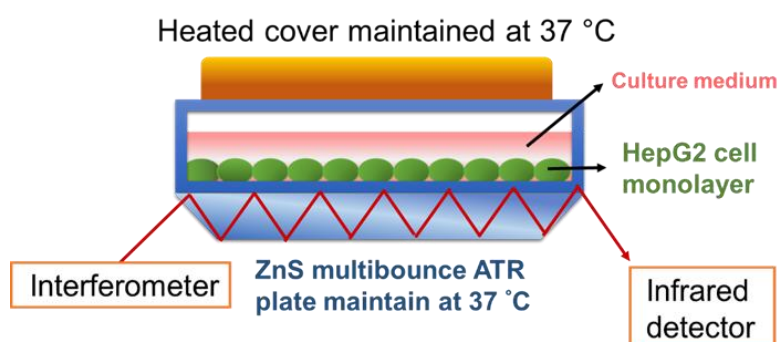


Figure 8. A schematic diagram showing the live-cell ATR-FTIR experiment set up

2.3.2 Live Cell FTIR measurement

An FTIR spectrometer (Tensor II, Bruker Optics) fitted with a room temperature deuterated L-alanine doped triglycine sulfate (RT-DLaTGS) detector was used. It adapted to an ATR accessory described in 2.3.1 to acquire continuous live-cell FTIR spectra (Figure 9). Measurement was taken every 10 minutes with 9 minutes of scanning time (1024 scans so that six spectra were collected hourly). The IR spectrum of cells was measured in the spectral region 4000 to 800 cm^{-1} with a resolution of 8 cm^{-1} and 5 kHz scanning speed. Blackman-Harris 3 Term function with power spectrum correction mode and phase resolution 32 was selected

in an interferogram. OPUS 7.8 software (Tensor II, Bruker) was used for the initial data processing, such as atmospheric vapor removal, baseline correction, 2nd derivative calculations, and vector normalization. The absorbance profile of the cell during cell attachment was monitored continuously and plotted in [Figure 10A](#) from seeding to the moment before adding the experimental culture medium.



Figure 9. Photo of Bruker spectrometer modified to a temperature-controlled ATR plate for the live-cell FTIR measurement

2.3.2.1 Obtaining Reproducible of Live Cells ATR FTIR Spectra

To study compound and cell interaction, acquiring reproducible FTIR live-cell spectra is the first step to its implementation. The average spectra of three independent measurements of live HepG2 cells in the IR region 1800-900 cm^{-1} measured at different time points after seeding has shown all the expected peaks of cellular components (Fig 10A). For the repeated measurements, the standard deviation from 3 measurements at the 24th hour is represented (Fig 10B). The relatively small error bars underlined the reproducibility of the live cell ATR FTIR measurements.

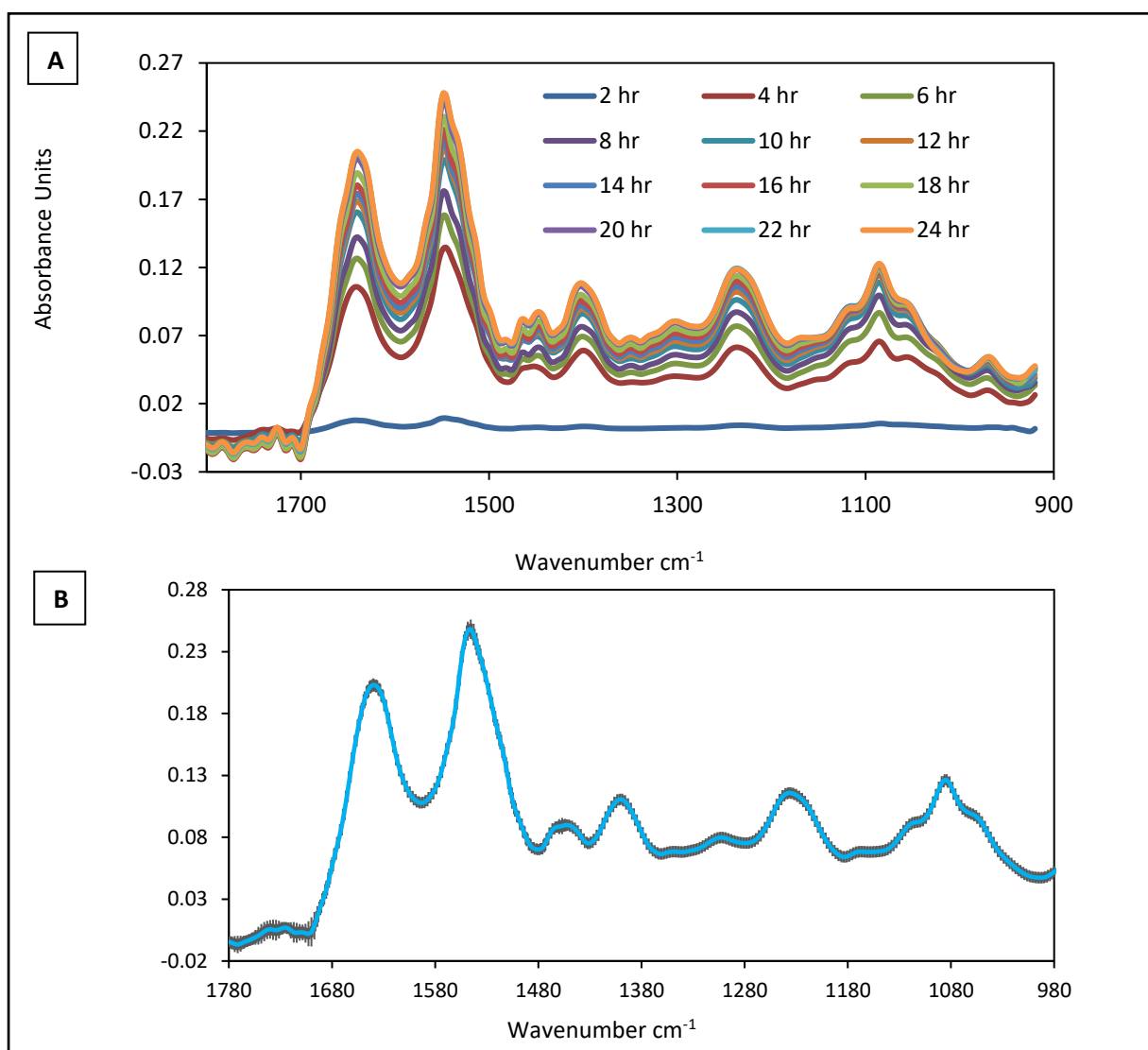


Figure 10. HepG2 FTIR live-cell spectra every 2hr of seeding time (A) and the error bars of 24th hour (B)

2.3.3 Cell Viability assay

The MTT (3-(4,5-dimethylthiazol-2-yl)-2,5-diphenyltetrazolium bromide) tetrazolium colorimetric reduction assay was carried out to assess cell viability. The colorimetric assay principle is that the viable cells with active mitochondrial activity (dinucleotide phosphate (NADPH)-dependent cellular oxidoreductase) will reduce the tetrazolium dye MTT to formazan, which produce a purple product that generates an absorbance maximum near 570 nm. Dead cells cannot convert MTT into formazan; the color formation is a convenient marker of viable cells[89, 90]. The general protocol is as follows: HepG2 cells (2.0×10^4 /200 μ L) in DMEM high glucose CO₂ independent medium were cultured in 96-well plates for 24 hours and treated with the different concentrations of the studied solutions or drugs. Cells were cultured in each concentration of the studied solution for 24, 48, or 72 hours (relevant to live-cell FTIR experiment), then 100 μ L of the MTT reagent (0.5mg/mL) (VWR International) in DMEM medium was added to each well. After 2 hours of incubation, the supernatant was removed, and 100 μ L of DMSO was added to each well for the detection of the presence of formazan. The absorbance value at 570 nm was taken using a spectrophotometer (SpectraMAX™ software). The absorbance values measured from each well plate were plotted, and the percentage of cell viability was calculated over each concentration compared with the control by the Microsoft Excel program. The IC₅₀ was represented as mean \pm SD.

2.3.4 Solutions/drugs treatment preparation

The studied solutions or drugs' concentrations used in the live cell FTIR experiment were guided by the IC₅₀ obtained from MTT assay results. The drugs were prepared in DMSO to make a stock solution and kept in a -20 °C freezer. For the live-cell FTIR study of drugs, the concentration was diluted to reach 0.1% v/v DMSO, which cells can tolerate well and remain viable during the FTIR experiment. For the solution treatment, the suspension of cells was

seeded on the ATR plate for 24 hours. The tested solution, e.g., 25 mM glucose in DMEM CO₂ independent medium, was prepared in 2% FBS before refreshing on the ATR plate.

2.3.4.1 FTIR Spectra of Compounds/Drugs

The live-cell FTIR approach explores the interaction between cells and compounds/drugs inside the cells. The spectra of all compounds/drugs have been measured, as shown in [figure 11](#). The compounds/drugs spectra will be further subtracted or compared to the cell and drug/compounds treatment in the FTIR data processing to avoid misinterpreting drug accumulation in cells as cellular changes.

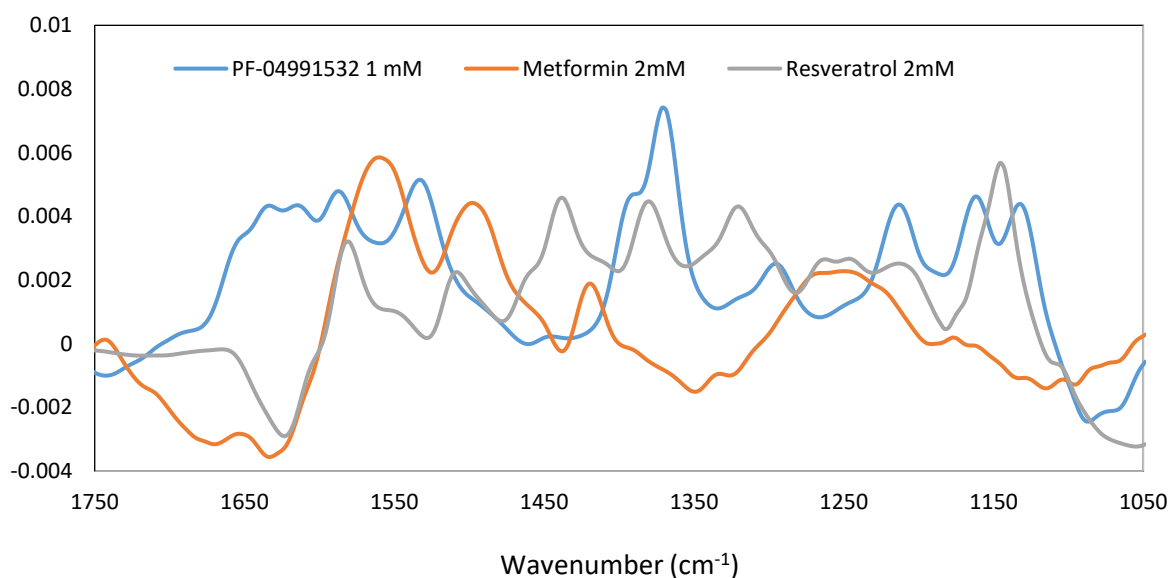


Figure 11. The FTIR spectra of PF-04991532 (blue), metformin (orange), and Resveratrol (grey)

2.3.4.2 Considering using 2% FBS in HepG2 compound treatment

To minimize spectral changes due to cell growth, after the cell was seeded for 24 hours in a 10% FBS DMEM CO₂ independent medium, the medium was changed to 2% FBS. Cells were viable at this level of FBS and can respond to the treatment without significant cell growth.

After 6 hours of a refreshing medium, the higher absorbance value of cell spectrum treatment with 10% FBS has shown in [figure 12](#) compared to the lower value of 2% FBS treatment.

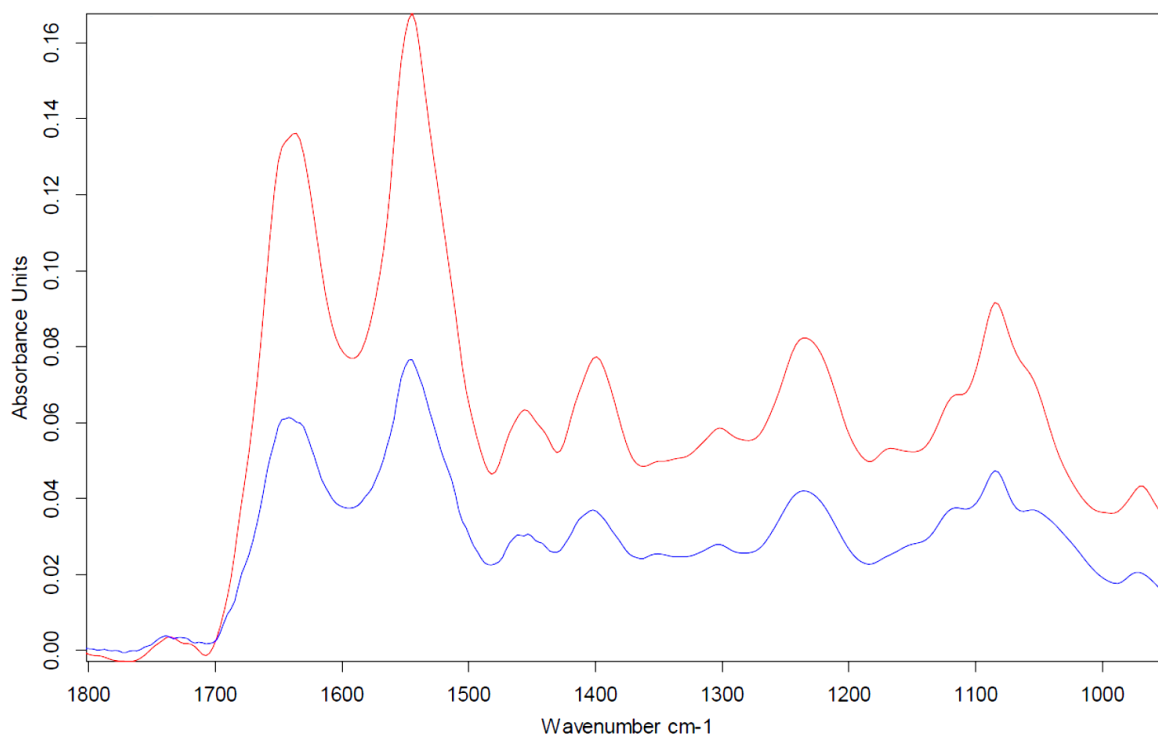


Figure 12. The absorbance value of HepG2 cell in 10% FBS (Red color) and 2% FBS DMEM CO₂ independent medium (blue color) after 6 hours of refreshing medium

2.3.5 FTIR data analysis

For the live-cell FTIR approach, the treated cell spectra were acquired by using the first spectrum measured after exchanging the medium to the medium containing the compounds/drugs as a background to underline the alteration occurring inside the cells resulting from that medium change. Five steps of data pre-processing were carried out before the PCA analysis. The five steps include water vapor correction, truncation, spectra subtraction, baseline correction, and vector normalization, as described in more detail in the following sections.

2.3.6.1 Water Vapour Correction

Water vapor can decline the quality of FTIR spectra and affect the analysis outcome. This is the first significant step before data processing. The desiccant is routinely changed every two weeks before the experiment. The water compensation was also selected in the OPUS software to avoid the contribution of water vapor. Despite this, we found that there is still some water vapor absorbance in the spectra. For the unsmooth drug-treated cell spectra, the OPUS atmospheric compensation step was applied, and the improvement from this operation is shown in [figure 13](#).

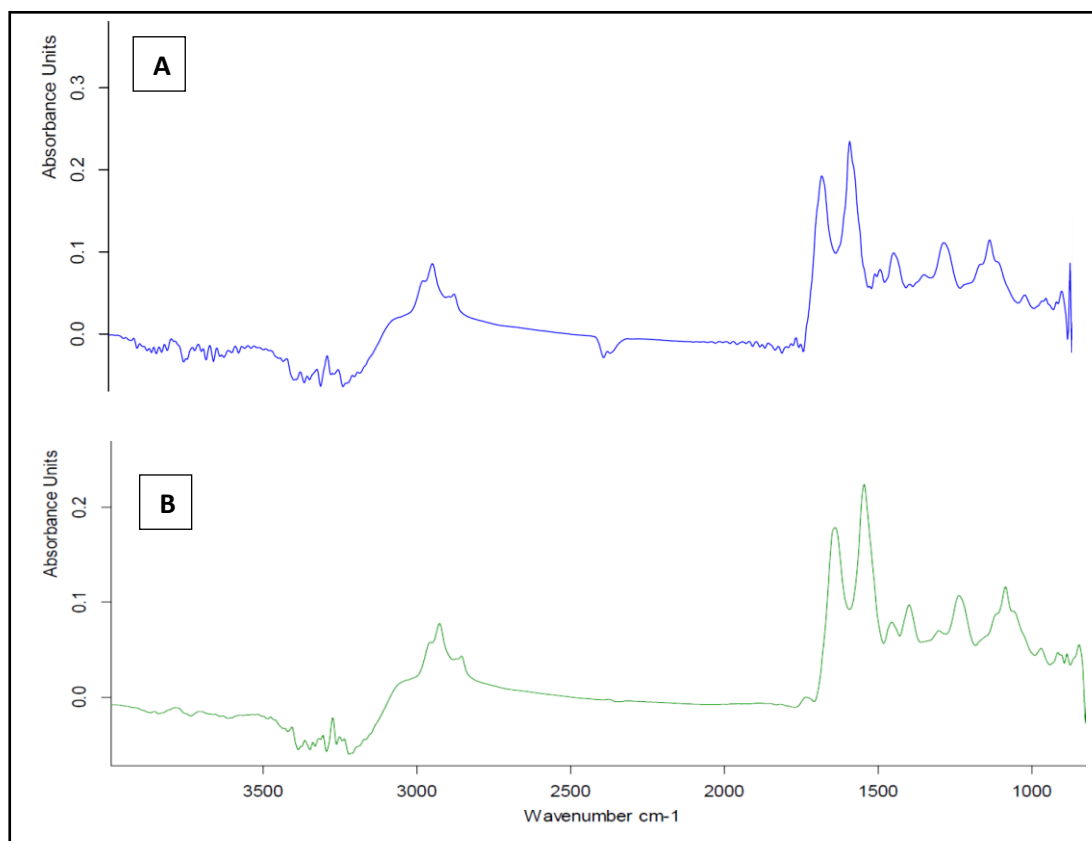


Figure 13. An ATR FTIR different spectrum o HepG2 cells (blue) and after (green) water vapor compensation

2.3.6.2 Spectra truncation

The spectra were obtained using the first measurement after the change of medium as the background to highlight the spectral changes resulting from the medium change. High spectral noise in the 3600-3000 and 900-800 cm^{-1} regions are due to the aqueous water absorbance peaks and excluded in the analysis. The three representative spectra (after drug treatment) have shown significant changes in the fingerprint region between 1700-900 cm^{-1} , as highlighted in [Figure 14](#).

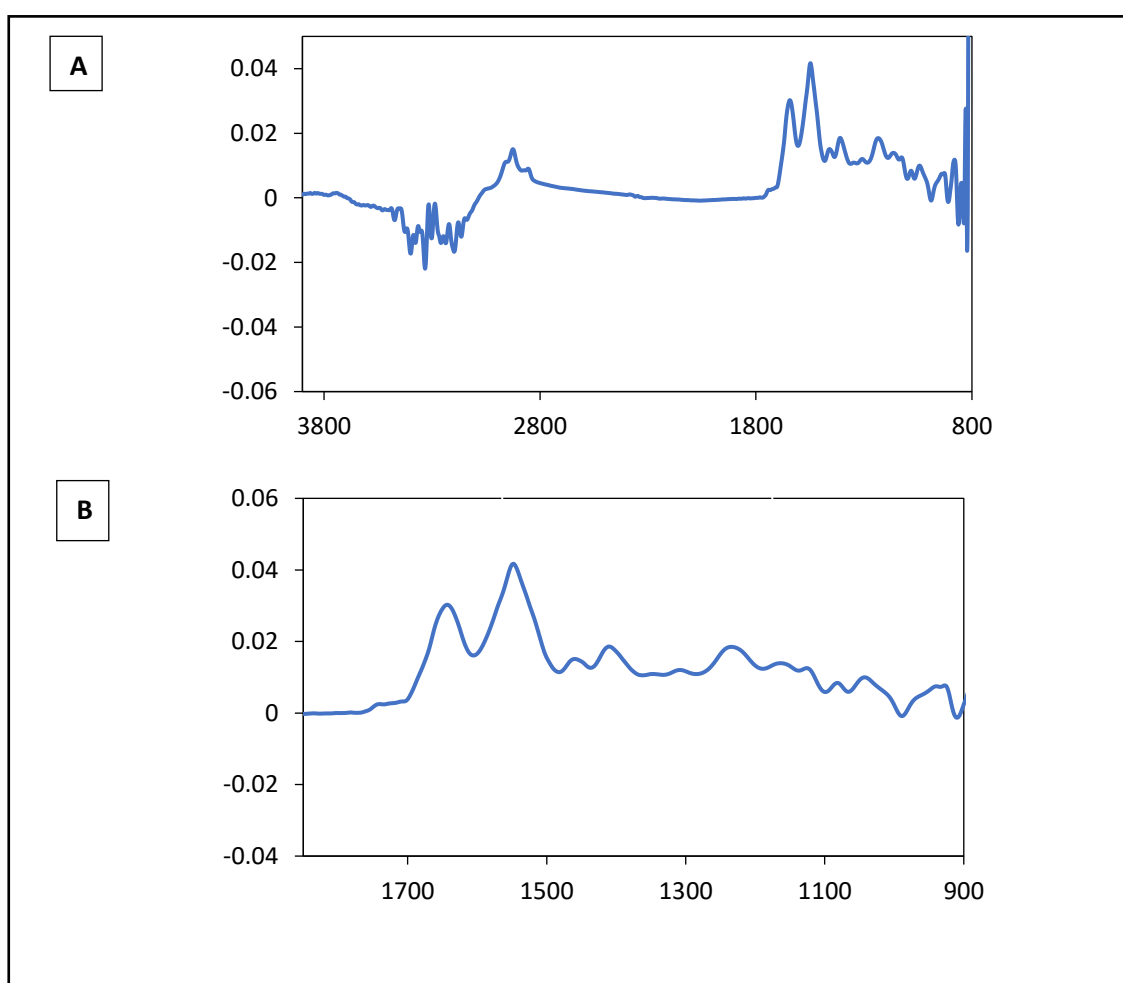


Figure 14. An ATR FTIR different spectrum of HepG2 cells before (A) and after truncation (B)

2.3.6.3 Baseline correction

The different spectra were baseline-corrected using concave rubber band baseline correction (1 iteration with 16 baseline points was sufficient) from the OPUS software. An example of the result of this step is shown in [figure 15](#)

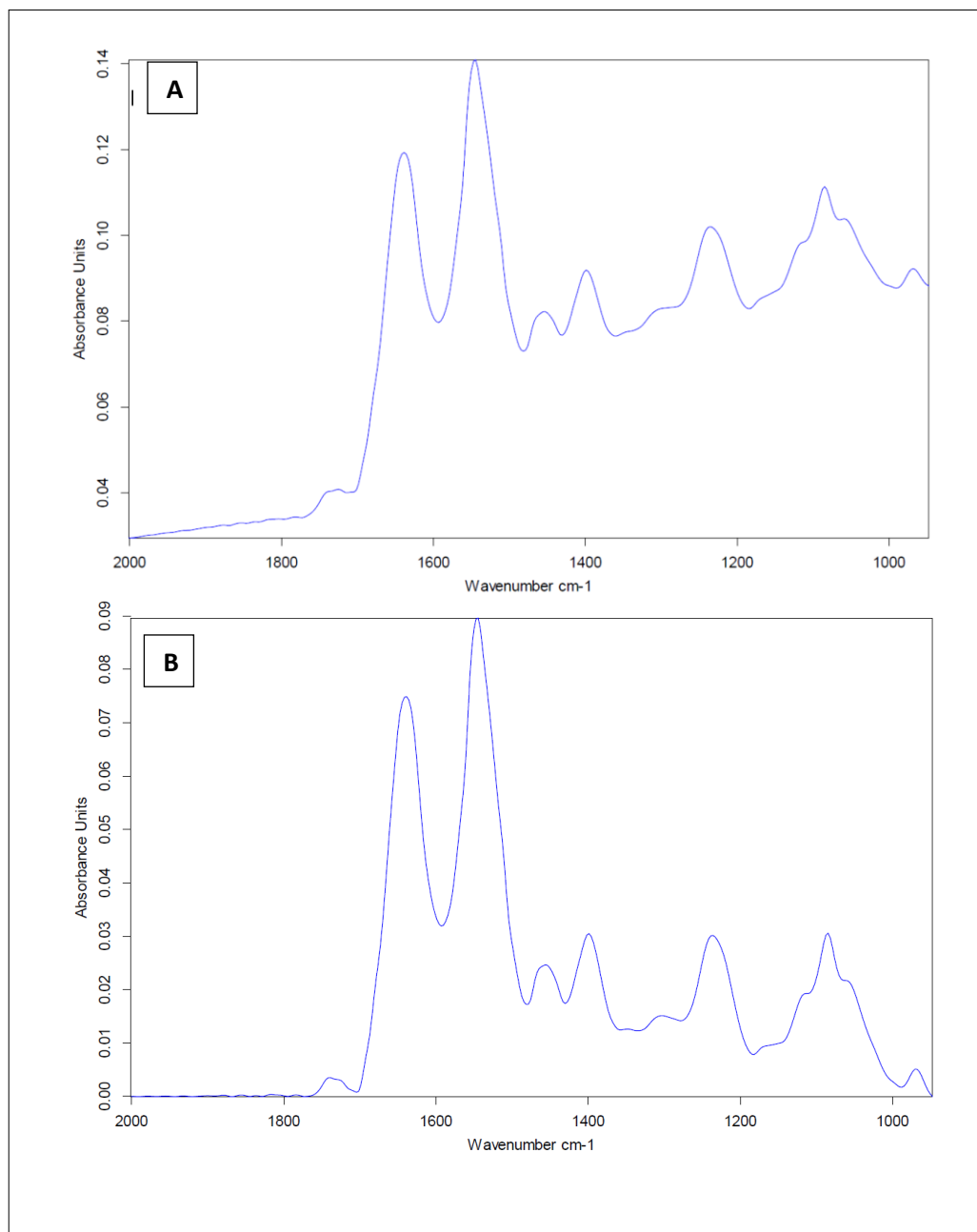


Figure 15. The FTIR spectrum before baseline correction (A) and B represents the spectrum after baseline correction

2.3.6.5 Vector normalization

FTIR spectra normalization is essential to account for confounding factors such as the varying thickness of the sample. Standard normalization methods are min-max amide I/II peak normalization and vector normalization. Amide I/II normalization is often used after baseline correction. In contrast, vector normalization is often used after spectra differentiation (after modification by spectrum subtraction, there is no longer a consistent amide I/II peak in the spectra to allow for amide I/II peak normalization[91]. Altharawi A[92] found that vector normalization can help discriminate the effect on cells from the different anti-cancer treatments.

2.3.7 PCA analysis of Live-cell FTIR spectra

The live-cell ATR-FTIR experiment can monitor cell/compound/drug over time. The combination of live cells FTIR experiment with PCA analysis can enhance relationships and agreements between main spectral change and compound/drug treatment. In the PCA of the data represented in Chapters 3 and 4, we compared cells treated in two compound conditions over time. Chapter 5 shows that PCA can distinguish between compounds and drug cell treatments. PCA was carried out using PyChem 3.5 beta version software (<http://pychem.sourceforge.net/>). This analysis was applied to reduce the dimension of the spectroscopic data. Correlation matrix and nonlinear iterative partial least squares (NIPALS) were selected for the PCA.

Chapter 3 Live-cell ATR-FTIR spectroscopy as a novel bioanalytical tool for cell glucose metabolism research

Published in *Biochimica et Biophysica Acta (BBA) - Molecular Cell Research* Poonprasartporn A, Chan KLA. Volume 1868, Issue 7, June 2021.

3.1 Abstract

Current novel drug developments for the treatment of diabetes require multiple bioanalytical assays to interrogate the cellular metabolism, which are costly, laborious and time-consuming. Fourier-transform infrared (FTIR) spectroscopy is a non-destructive, label-free, sensitive, and low-cost technique that was recently found to study living cells. This study aims to demonstrate that live-cell FTIR can be applied to study the differences in glucose metabolism in cells in normal culturing medium and cells treated in high glucose (a diabetes model) to highlight the potential of the technique in diabetes research. Live HepG2 cells were treated in normal glucose (3.8 mM; control) or high glucose (25 mM) medium and were measured directly using the FTIR approach. Principal component analysis was used to highlight any possible correlated changes 24, 48 and 72 h after treatments. FTIR spectra of live cell treated in normal and high glucose medium have shown significant differences ($p < 0.05$) for all treatment times. The control cells have seen an increased absorbance at 1088, 1240, and 1400 cm^{-1} , which are associated with phosphate stretching mode vibrations from phosphorylated proteins and DNA back bone, and symmetric stretching mode vibration of COO^- from fatty acids, amino acids, lipids, and carbohydrate metabolites. However, the high glucose treated cells have shown a different change in the 1000-1200 cm^{-1} region, which is linked to the glycogen and ATP: ADP ratio. In conclusion, live-cell FTIR can be a low-cost method for studying metabolic changes in cells.

3.2 Introduction

Powerful analytical methods for developing highly effective and safe medications for diabetic treatment is essential. Cell-based biochemistry with metabolite measurement is a key platform for diabetes and metabolism research. Metabolomics is currently a promising method that can identify and quantify metabolites from biological samples. Low molecular weight molecules such as lipids, amino acids, peptides, nucleic acids, and carbohydrates have important roles in disease/metabolism studies, and therefore rich metabolome data are highly valuable. However, dynamics in biological rhythm and interference from non-specific substances are some challenges that can affect the analysis outcome [93, 94]. Non-destructive methods for metabolomics measurement of a live cell, which is often preferred over measuring dead, lysed cell, for drug/cell metabolism is still lacking. Techniques reported for studying metabolites in live cells include colorimetric assays, fluorometric assays, and immunoassays. However, due to the complex metabolic changes in cells, multiple assays are often needed to increase the specificity, making these approaches expensive, laborious and time-consuming.

Fourier-Transform Infrared (FTIR) spectroscopy is a non-destructive, non-invasive, label-free, chemically specific, and high-throughput technique. FTIR analysis of cells has been shown to be able to distinguish the different stages of the cell cycle [95] , cell death [96], drug-cell sensitivity and resistance [97, 98], diseases [99], and biomedical changes from the clinical biomarkers in various type of cancers [100-103]. FTIR has been introduced in diabetes and metabolism research since 2007 as a diagnostic tool for analyzing chemical deposition in hair samples with different blood sugar levels [75]. In 2013, FTIR has been shown to be able to clearly differentiate healthy and type I diabetic rats [69] and diagnose diabetes in human from the measurement of blood, urine, lip and saliva [70-73]. FTIR also represents a promising

blood-glucose monitoring tool during insulin and metformin treatment [74, 75]. FTIR spectroscopy can be used to diagnose diabetes with and without retinopathy complications from patients' blood samples with 90% sensitivity, 92.7% specificity, and 90.5% overall accuracy [104]. However, metabolism in live cells, which has the potential to improve the understanding of diabetes, has not yet been demonstrated. We hypothesize that live-cell FTIR can produce useful biomolecular information to aid diabetes research. The aim of this work is to demonstrate that live-cell FTIR can be used to study the chemical transformation of hepatocyte from the healthy state (cultivated in normal glucose level) to diabetic state (after exposed in hyperglycaemia condition for 24 hr) [105-107] to relate and confirm the metabolism change in cells.

3.3 Materials and Methods:

Human hepatocyte carcinoma cell (HepG2) were kindly provided by Professor Khuloud Al-Jamal (School of Cancer and pharmaceutical science, King's College London). Cells were maintained in Dulbecco's Modified Eagle's Medium (DMEM from Sigma Aldrich, UK) high glucose containing 10% fetal bovine serum (FBS from Sigma Aldrich, UK), 50 U/mL penicillin and 100 µg/mL streptomycin, 1% non-essential amino acid and 1% L-glutamine. Cells were maintained in T25 culture flask and incubated in a humid atmosphere containing 5% CO₂ at 37°C.

3.3.1 Cell viability assay

Cells concentration of $2.0 \times 10^4/200 \mu\text{L}$ were cultured in 96-well plates for 24 hours and treated with the different concentrations of glucose (5, 10, 25, 35, 50, 75, and 100 mM). Cells were cultured with each concentration for 24, 48, and 72 hours, and then 100 μL of the MTT reagent (0.5mg/mL) (VWR International) was added to each well. After 2 hours of incubation, 100 μL of DMSO was added to each well to detect the presence of formazan. The absorbance value at 570 nm was taken using a spectrophotometer (SpectraMAX™ software). The importance of absorbance of each well plate were plotted, and the percentage cell viability was calculated over each individual concentration compared with the Microsoft Excel program.

3.3.2 Live-cell FTIR measurement

HepG2 cells in the T25 flask were trypsinised at ~80% confluence and suspended with $2 \times 10^6/2$ mL in DMEM CO₂-independent medium. The cells were seeded on the temperature-controlled ZnS attenuated total reflectance (ATR) plate with 10 reflections on the sampling side (HATR, Pike Technologies, USA; ZnS ATR crystal was purchased from Crystran Ltd., UK). The plate was sealed with a warmed lid to avoid evaporation. This condition also let the attached cell to reach high confluence on the ATR element's measuring surface as shown in [Figure 8](#). According to the small penetration depth of measurement, around 2-3 μm from the ATR element's surface (smaller than the thickness of the living cell (~5-10 μm), absorbances are contributed mainly from the attached live cells with negligible contribution from the medium [97, 108-110].

Visible images of cells on the ZnS ATR plate and in T25 flask were respectively captured in reflection and transmission mode after 24 hours of incubation using a 10x objective. The

seeded HepG2 cell spectra were monitored for 24, 48 and 72 hours using a FTIR spectrometer (Tensor II, Bruker Optics). Normal glucose (3.8 mM; control) or high glucose (25 mM) concentrations in DMEM CO₂ independent medium was applied for the cell-glucose metabolism study. After seeding the cells in the live-cell ATR plate, a measurement was taken every 10 minutes at 8 cm⁻¹ spectral resolution with 9 minutes scanning time (1024 scans) for a total duration of 24 hours. DMEM CO₂ independent medium was used to avoid the requirement of 5% CO₂ at the spectrometer.

The cell suspension was incubated for 24 hours to allow cell attachment. Once cells were attached, which is indicated by a slow but steady growth in the amide II band (around 24 hour), the medium was changed to fresh normal glucose (3.8 mM in 2% FBS DMEM CO₂ independent medium; control) or high glucose (25 mM in 2% FBS DMEM CO₂ independent medium; diabetic) medium. A background was measured at this point. The change of spectrum was then monitored for a further 72 hours with a measurement taken at every 10 minutes. Each experiment was repeated for 3 times based on 3 independent cultures with a similar passage number range 24-34 and on a different day.

2.3 Data processing and analysis

Spectra were water vapor compensated and cut to the wavenumber range of 1780-900 cm⁻¹, followed by concave rubber band baseline correction (1 iteration with 16 baseline points was found to be sufficient) and vector normalisation. Principal component analysis (PCA) from PyChem[®] software (available from [:http://pychem.sourceforge.net/](http://pychem.sourceforge.net/)) was used as the statistical tool for possibly correlated changes observation from the experiment setting [91]. T-test was applied to find the significant difference among the treatment groups compared

to control. Significance difference was defined as $P.value < 0.05$ calculated using Microsoft Excel.

3.4 Results

3.4.1 Cell culturing

To establish that the HepG2 cell behaviour is similar between cells cultured under standard protocols and under experimental conditions, i.e. on the ZnS ATR plate, visible images of HepG2 cells captured 24 hours after seeding on the ATR plate in the DMEM CO₂ independent medium have shown that cells were fully attached (Figure 16A). Comparing to cells cultured in T25 tissue culture flask incubated with standard DMEM medium in 5% CO₂ environment, the cells have shown a similar morphology (Figure 16B). Selected spectra of a typical experiment of the living cells, with culture medium as the background, are shown in Figure 17A. The cells have shown a small absorbance 2 hours after seeding, which rapidly increased at the 4th hour. The seeded cells had further grown on the ATR plate for another 20 hours until the increase in absorbance had clearly plateaued, indicating a full attachment of cell layer on the ATR plate [82, 111, 112]. The spectra of HepG2 cell have shown clear peaks of amide I at 1645 cm⁻¹, amide II at 1550 cm⁻¹, $\nu_{sym}(\text{COO}^-)$ at 1400 cm⁻¹, amide III at 1235 cm⁻¹, the asymmetric and symmetric stretching mode of phosphate bands between at ~1240 and 1080 cm⁻¹ and the carbohydrates bands between 1150-1000 cm⁻¹ (Figure 17A.). Figure 17B shows the averaged spectra measured from the three separate repeated experiments of live HepG2 cells at the 24th hour after seeding, the very small standard deviations (grey colour) represented the high reproducibility of the ATR FTIR experiments.

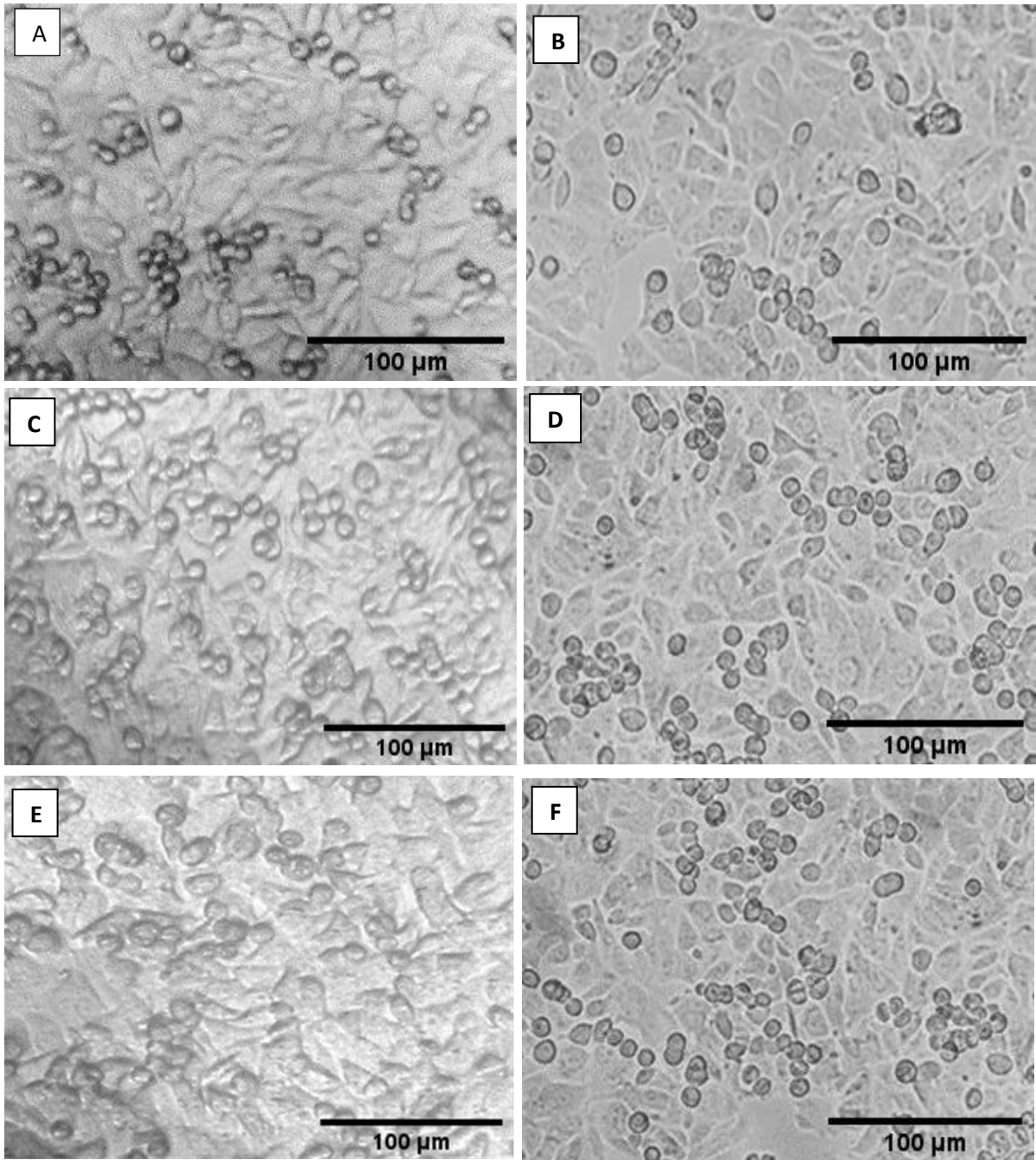


Figure 16. Image of HepG2 cells at different time of seeding on the ATR element and T25 flask, respectively; 24 hour A and B, 48 hour C and D, 72 hour E and F

When the cells reached the plateau phase, around 24 hours after seeding, the medium was replaced by the test medium for the attached cells to study the reaction between cells and the testing conditions.

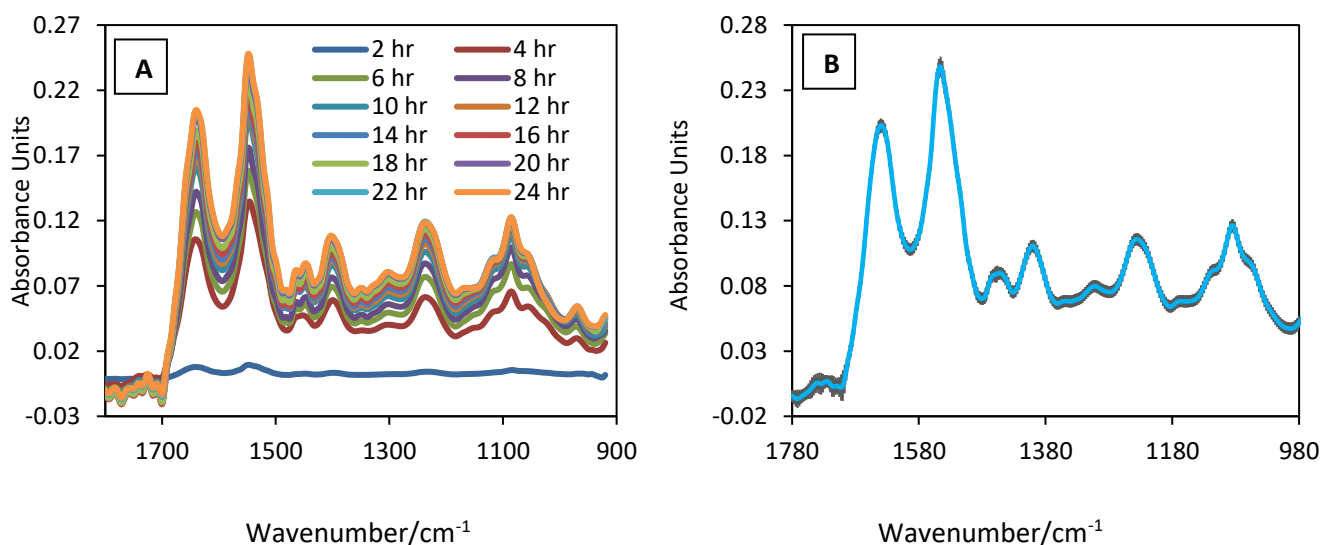


Figure 17. HepG2 live-cell FTIR spectra every 2 hr. of seeding time (A) and the error bar of 24th hour (B)

To further confirm that the ATR substrate and the CO₂ independent medium produces a cell behaviour that is comparable to other diabetic studies in the literature using the HepG2 cell model, we have compared the viability of cells according to the published IC₅₀ of glucose for HepG2 cells, which was ~50 mM at 72 h in diabetes studies [113]. The results have shown that >80% of the HepG2 cell had survived in 5 and 10mM with insignificant differences compared to control. At 50 mM and 72-hour incubation, the cell viability has dropped to 50% (Figure 18), which is similar to the results from the literature ($p < 0.05$ compared to normal glucose treatment) [114].

In this experiment, 25 mM was selected for the high glucose concentration because it is commonly used to create diabetic cell models [105, 113-115]. Figure 4 shows an insignificant effect on the viability of cells at the 25 mM glucose treatment compared to control for all duration of treatments. Our previous studies [82, 111, 112] on anticancer agent has shown that cell-death can produce significant changes to the cellular molecular composition, the results in Figure 18 shows that cells remain largely viable at 25 mM and therefore confirming that cell death is not a significant contributor to the differences

between high glucose (25 mM) and control (normal glucose) treatments. This ensures that the difference observed between high and normal glucose-treated cells are due to a change in the metabolism of cells rather than cell death.

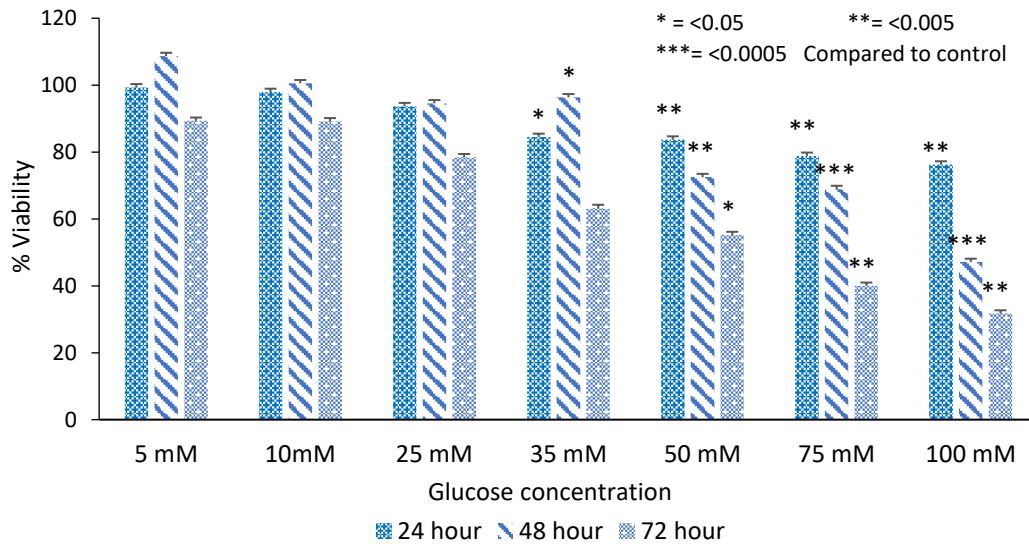


Figure 18. HepG2 cell viability compared to control (3.8mM) for 24, 48 and 72 hours with error bars representing the standard deviation between the three independent repeated experiments

3.4.2 Live-cell FTIR experiment

Figure 19A shows the representative spectra of HepG2 cells treated in a medium with 25mM glucose (hyperglycemia model) measured at 3 different time points (24, 48, and 72 hours) with the spectral range between 3800-800 cm^{-1} . The spectra were obtained using the first measurement after the change of medium as the background to highlight the spectral changes resulting from the change of the medium. High spectral noise occurred in the 3600-3000 and 900-800 cm^{-1} regions due to the strong aqueous water absorption and are excluded in the analysis. The three representative spectral have shown major changes in the fingerprint region between 1700-900 cm^{-1} as highlighted in Figure 19B. Cells appeared to have continued to grow slowly 24 hours after the medium change with an increase in the amide II band (a key

marker for protein) but slightly reduced towards the 72nd hour, which is in agreement with the MTT assay results. Clear changes in the phosphate and carbohydrate bands in the 1350-950 cm^{-1} are apparent and consistent across the three repeated experiments. Figures 20 shows all spectra from the repeated measurements after 24- 48- and 72-hour treatments with a marked difference can be observed between the normal and 25 mM glucose treatment groups. Pair-wised PCA of the normal glucose versus 25 mM glucose treatment in this range has reviewed a clear grouping with PC1 showing the statistical difference of <0.025 , <0.01 , and <0.03 for 24th, 48th and 72nd hour, respectively. The normal glucose-treated cells have seen an increase in absorbance at 1088, 1240, and 1400 cm^{-1} (Figure. 20B). These spectral peaks are associated with nucleic phosphate acid stretching mode PO_2^- and symmetric stretching of COO^- which is from fatty acids, amino acids, and carboxylate metabolites vibration. Whereas the high glucose treated cells at 24th hour have shown an apparent reduction of the PO_2^- stretching mode band. At time 48th and 72nd, an increasing band at $\sim 1200 \text{ cm}^{-1}$ is shown.

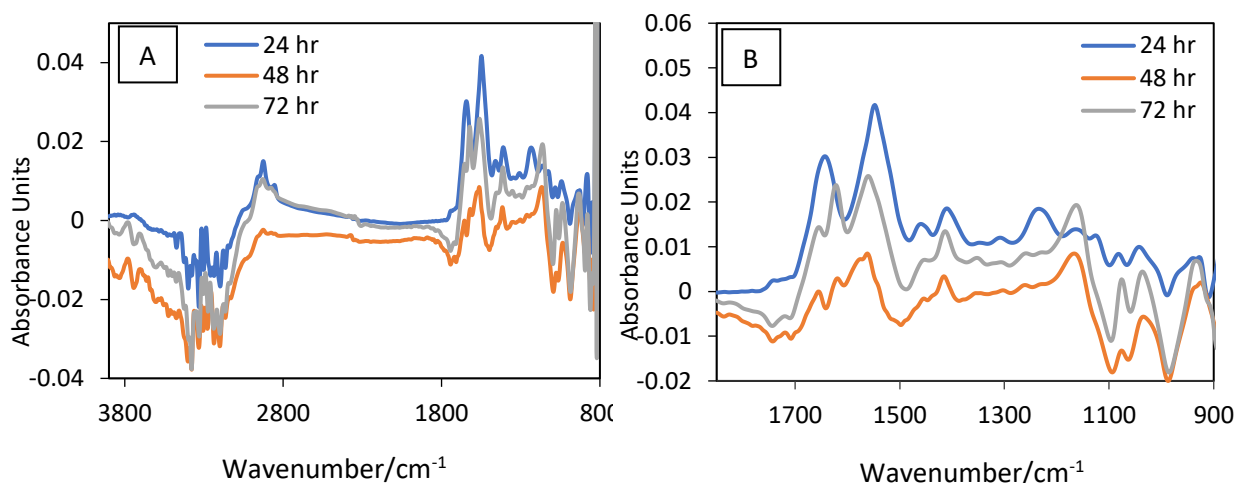


Figure 19. Spectra of HepG2 treated with 25mM glucose in 3 different time points (24, 48 and 72 hour) with spectra range between 3800-800 cm^{-1} (A) and spectra range between 1780-900 cm^{-1} (B)

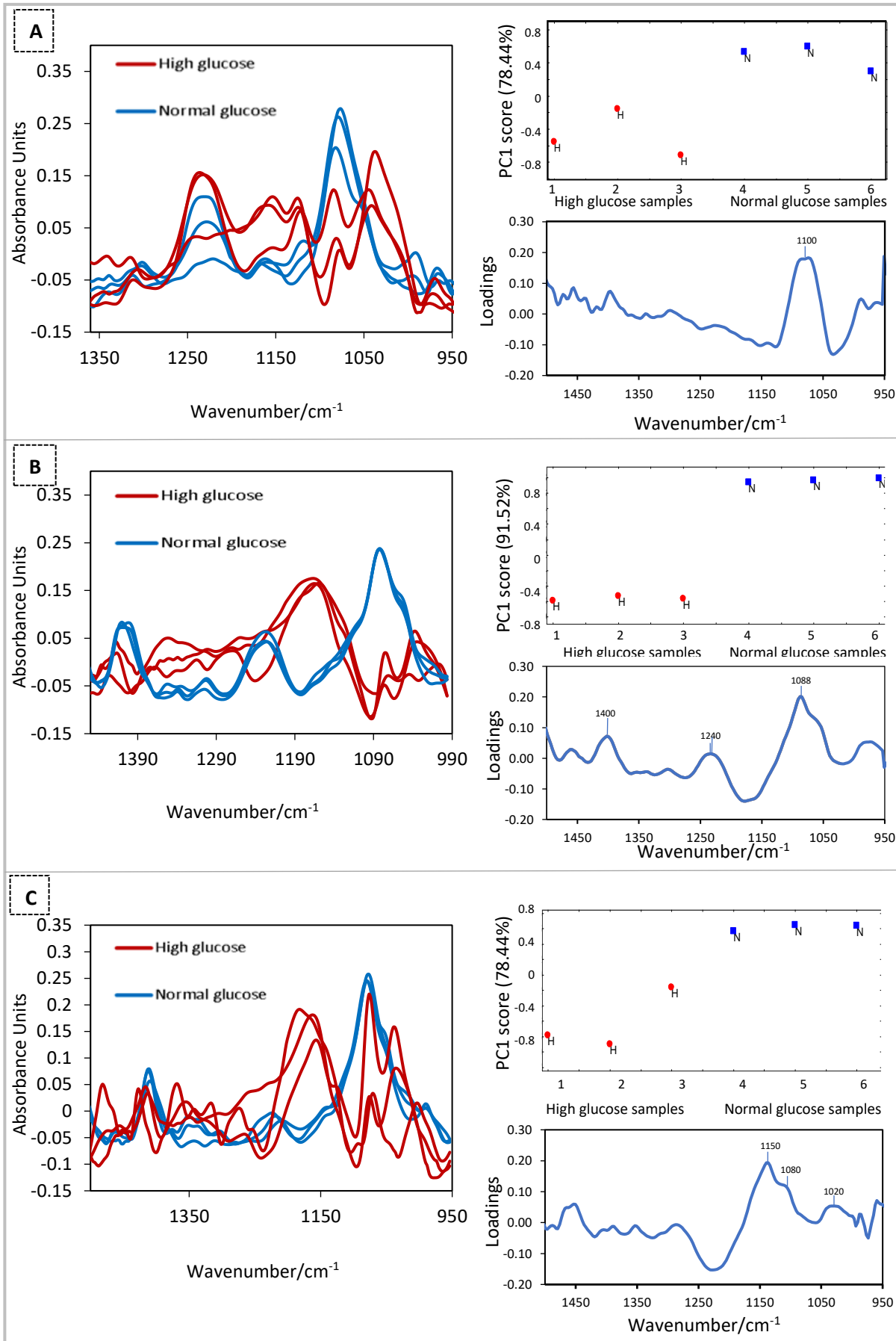


Figure 20. The spectral changes as a function of time (left panel) between HepG2 treated in high (Red) and normal (Blue) glucose solution and the corresponding PCA1 score and loading plots (right panel) at (A) 24th, (B) 48th and (C) 72nd hour.

3.5 Discussion

An adequate energy supply for the vital organs in the body is regulated by glucose homeostasis. Liver has an essential role in controlling several pathways of glucose metabolism including glycolysis, gluconeogenesis, glycogenesis, and glycogenolysis [116, 117].

During the feeding stage, glucose molecules from the carbohydrate digestion process enter the hepatocytes, phosphorylated to glucose 6-phosphate, followed by several metabolic pathways to generate adenosine triphosphate or ATP. The catabolism of glucose into pyruvate, in terms of glycolysis, is conserved as a crucial pathway to produce ATP. Pyruvate is carried into the mitochondrial matrix where it is transformed to acetyl-CoA by pyruvate dehydrogenase cascading enzyme and integrated into the tricarboxylic acid cycle (TCA) in concurrence with oxaloacetate. The TCA cycle generates the electron carriers for electron transport chain-oxidative phosphorylation to produce ATP in the final process. The extra amount of carbohydrates in the liver are converted into glycogen and stored as the energy reserve in the liver and muscle cells (glycogenesis).

Moreover, in a high carbohydrate diet, the excess amount of dietary glucose is also converted into lipid (lipogenesis) and stored in the adipose tissue. Therefore, liver glucose homeostasis during fasting stage is also crucial. When blood sugar level drops, liver releases glucose to the bloodstream either from the stored glycogen(glycogenolysis) or by breaking down triglyceride to glycerol and combined with alanine and lactate to produce glucose(gluconeogenesis)[117, 118].

Glucose-cell metabolism imbalance can induce metabolic syndromes such as insulin resistance, type 2 diabetes, obesity, non-alcoholic fatty liver disease (NAFLD), and cardiovascular conditions. Several *in vivo* studies have demonstrated that oxidative stress,

inflammation, and disease progression are due to glucotoxicity [119-123]. However, complex alterations such as endocrines, hormones, and environmental factors may influence the physiological metabolite change in the energy metabolism and organ responses [124, 125]. Thus, *in vitro* study may be an ideal platform to understand glucose metabolic change inside cells better.

Immortal hepatocyte cell lines are widely used to explain the regulation of hepatic metabolism. The primary hepatocyte cells are better than the cancerous cell line because they mimic the *in vivo* situation more. But the primary hepatocyte availability and accessibility are limited. Moreover, the phenotype is unsteady, and this cell type can only be cultured for a short period [126, 127]. Sefried et al. [108] have demonstrated and compared the gluconeogenesis gene expression and protein regulated hepatic metabolism or hepatokine among primary hepatocyte and immortalized cell lines; AML12, THLE-2, and HepG2. The results showed that HepG2 cells appear to be closer to the *in vivo* situation than AML12, THLE-2 despite its tumorigenic origin. Thus, we concluded that regarding the similarity of HepG2 cell line hepatic gene expression, this cancerous cell line can be used in *in vitro* of the diabetes-related research.

Live-cell FTIR measurements show cellular changes over time in normal glucose treatment mainly from the seeded cells' growth. The symmetric and asymmetric phosphate stretching mode at 1078 cm^{-1} and 1220 cm^{-1} regions, originating from DNA backbone and phospholipids products from cell expansion, have continued to rise as a function of incubation time. Another two major regions that indicate cell expansion are Amide III (1220 cm^{-1}), which is overlapped with the asymmetric phosphate band, and the amide II band at 1550 cm^{-1} . These two bands have shown simultaneously increasing with the phosphate peaks. Increases in

these spectral regions have confirmed the cells were growing in the normal glucose treatment (Figure 21).

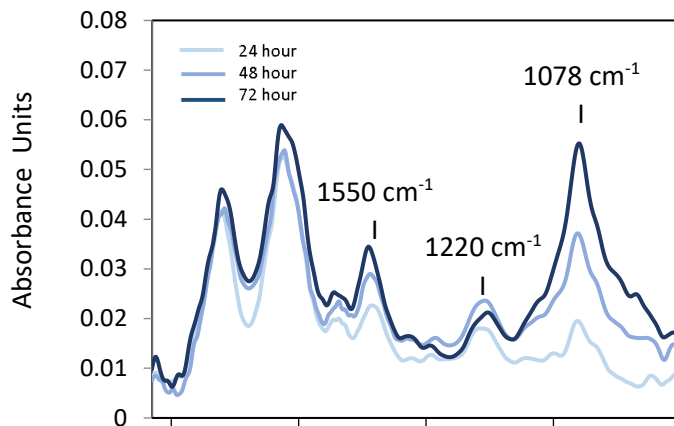


Figure 21. Comparison of normal glucose treated HepG2 FTIR spectra for time 24th 48th and 72nd hour

On the other hand, normalized FTIR cells spectra treated in high (25 mM) glucose have revealed a different pattern of cellular component changes compared to the normal treatment. Apparent different changes are found in the phosphate stretching and carbohydrate spectral band regions, which has shown an overall decrease in absorbance overtime (Figure.22) relative to the protein amide II peak, suggesting large changes in the phosphate and carbohydrates metabolites in the cells upon high glucose treatment.

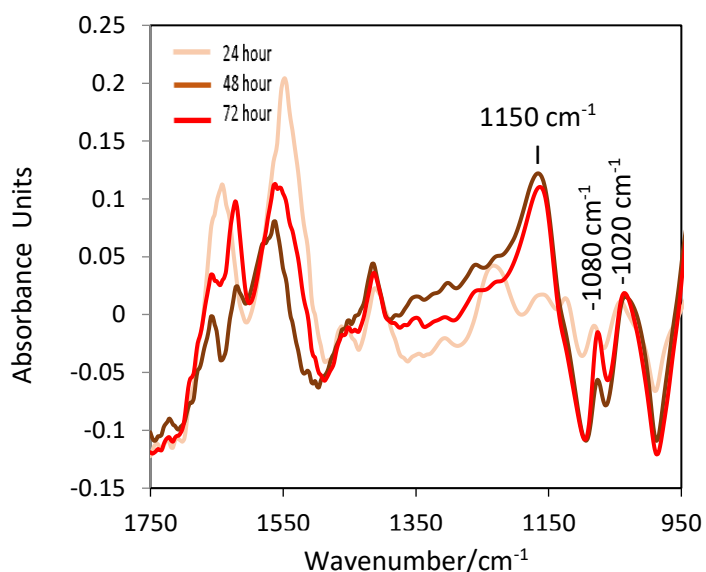


Figure 22. Comparison of high glucose treated HepG2 normalized FTIR spectra for time 24th 48th and 72nd hour

According to the literature of hepatic glucose utilization, hepatocytes consume glucose as a fuel to produce ATP from ADP through oxidative phosphorylation. Excess glucose would be converted into glycogen and stored in the liver. Comparison of the spectral changes of the HepG2 cells exposed in high glucose for 24 h to the difference spectra of ATP-ADP has shown a remarkable similarity as shown in [Figure 23](#), suggesting the production of ATP from the phosphorylation of ADP can be observed using live cell FTIR measurement. Furthermore, a closer look at the spectral change at 48th and 72nd hour exposure, a rise in the characteristic glycogen peaks at ~ 1020 , 1080 , and 1150 cm^{-1} [128]([Figure 22](#)) can be observed, indicating that FTIR can detect the glucose metabolism changes in the treated cells.

Energy metabolism in the normal cell culture condition depends mainly on oxidative phosphorylation (OXPHOS) for ATP production because ATP, which is the key energy unit, is more efficiently produced from this process (36 ATP) than glycolysis (2 ATP)[126]. However, many cancer cells prefer using the glycolytic pathway due to a permanent impairment of mitochondrial OXPHOS, as founded by Otto Warburg [127]. However, this view is altered by

recent publications, which found that the function of mitochondrial OXPHOS in most cancers is still intact. Cancerous cells have different metabolic phenotypes of energy metabolism even in the same type of origin. Due to the common trait of rapid growth, they adapt and reprogram to the environmental change to overcome disturbance of growth conditions. Therefore, the ratio between glycolysis and OXPHOS to yield total ATP is flexible for cancer cells, which results in a selective advantage over a non-cancerous cells in unfavorable environments [126].

ATP is the determinant of cellular mitochondrial respiration. The amount of intracellular ATP is subtly changed by metabolic inhibitor to test mitochondrial toxicity. The level of ATP is generally sustained in a normal living cell. When cells become injured, the intracellular ATP amount can be lowered rapidly. Thus, an advanced technique for ATP extraction, which is normally analyzed from lysed/fixed cell, that avoids cell degradation from both physical and nonphysical procedures is essential [129]. Rita et al. [130] have developed and verified a one-step extraction and bioluminescence assay for quantifying glucose and ATP levels in cultured HepG2 cells in high glucose conditions for testing drug-induced mitochondrial toxicity. The advantage of this method over traditional biochemical assay is that it requires only one extraction step that disintegrates cellular proteins with concomitants and steadily releases cellular glucose and ATP from HepG2 cells. The method allows the measurement of considerable changes in ATP levels with no detectable cell loss (no protein content disruption), suggesting that the proposed assays could be a precise multiparameter-based measurement of cytoprotective/cytotoxic compounds. However, compared to the parallel cytometry assay, the limitation of this method is that it cannot distinguish between

live and dead cells, where the glucose contents and ATP are not comparable. Whilst the conversion of ADP to ATP and glycogen in cells can be measured using

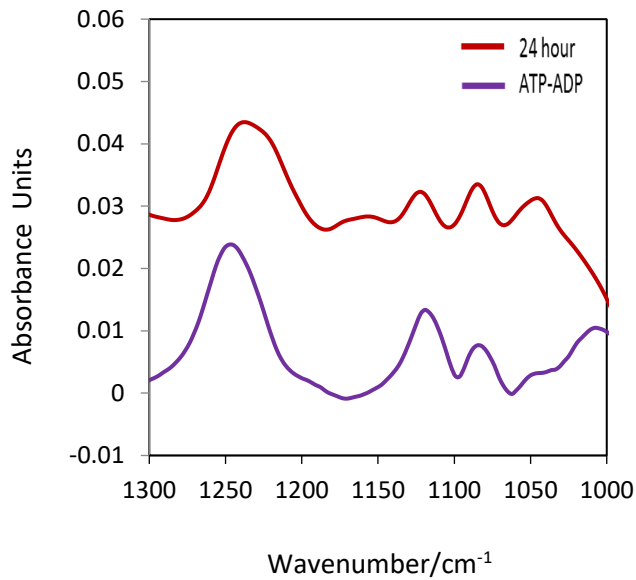


Figure 23. Comparison between ATP-ADP FTIR spectrum and high glucose treated HepG2 at time 24th

conventional biochemical essays or LC/MS metabolomics approach, we would like to highlight the outstanding benefits of the live-cell FTIR method, such as it can continuously automatically measure the cells throughout the experiment, the method does not require any labeling and there is no need to destroy or extract the metabolites from the cell samples. No expensive chemical reagents are needed, and the measurement is relatively quick. Although the measurement was set to scan for 9 min per spectrum in this experiment, as the timescale for the cellular changes was relatively slow, high-quality spectra can typically be obtained in less than a minute.

3.6 Conclusions

In conclusion, live-cell FTIR helps to understand cell metabolism and can be an additional tool for providing some information that can assist in studying energy metabolism or diabetes. In the future, live-cell FTIR can be applied to study glucose-cell metabolism related to other organs, e.g., pancreas, muscle, and adipose cell, or potentially be an alternative tool for drug-cell metabolism study.

3.7 Acknowledgements

We thank Prof Khuloud Al-Jamal's research group for help and advice on cell culture. We thank Dr Andrei Tarasov from Oxford for the stimulating discussion. We thank Dr Ali Altharawi for his general support. We also thank the Thai Government for providing a Ph.D. studentship for Anchisa Poonprasartporn to carry out this research. We also thank EPSRC (EP/L013045/1) for the funding that started this research theme in the group.

Chapter 4 Label-free study of intracellular glycogen level in Metformin and Resveratrol-treated insulin-resistant HepG2 by live-cell FTIR spectroscopy

4.1 Introduction

Insulin resistance is a complex pathological condition with impaired cellular response to insulin in insulin-related cells such as hepatocytes, myocytes, adipocytes, and cardiomyocytes[131]. This condition is considered a significant risk factor of metabolic syndrome, one of the most dangerous factors for increasing heart attack risks[132, 133]. It is estimated that a quarter of the world's adult population has metabolic syndrome, which can increase the risk of developing type 2 diabetes by 5-fold [134]. This can lead to an increase of up to 460 million people with diabetes, exacerbating the most common worldwide chronic disease - one of the four leading causes of non-communicable disease mortality in 2021[135]. The accumulation of cardiovascular disease (CVD) risk factors that classify metabolic syndrome is now appraised to be the root of a new CVD epidemic.

Regarding metabolic syndrome contributing to the global epidemic of type 2 diabetes and CVD, current drug treatments remain sub-optimum; therefore, early diagnosis and better-targeted therapies are urgently needed. This can be achieved through innovative research approaches at pre-clinical and clinical stages. In addition, advances in understanding the molecular dynamic inside cell systems are essential for novel or targeted drug development.

Current *in vitro* diabetes assays typically focus on using metabolic profiling technologies, e.g., metabolomics (for example, by liquid chromatography-mass spectrometry), multi-target immunoassay and/or biochemical assay to obtain information

about treatment response, especially during the drug development stage. In addition, a particular biomarker produced from the drug-cell interaction can also monitor the drug efficacy. However, these techniques are costly, and laborious, and the biomarker needs to be identified first, which could also involve the time-consuming task of designing a suitable dye. Recently, non-invasive, label-free, high-throughput screening techniques that can provide molecular information and detect cell-produced metabolites in pre-clinical research have attracted much attention[136].

Fourier-Transform Infrared (FTIR) spectroscopy is a non-destructive, non-invasive, label-free, high sensitivity, high accuracy, and rapid technique. However, it has yet to be applied in the study of diabetes treatments. Our preliminary work has shown that studying living cell culture *in situ* using FTIR (so called “live-cell FTIR”) can detect changes in glycogen and ATP: ADP levels in a label-free manner when living HepG2 cells were exposed in a medium containing high glucose concentration[137]. In that simple study, we demonstrated the potential of live-cell FTIR for studying cell metabolic changes at the molecular level. The advantages of live-cell FTIR over FTIR study of dead cells are the reduced artifacts associated with the fixative procedure and the opportunity to measure dynamic events[138]. Moreover, FTIR is a quantitative method whereby the absorbance of peaks is linearly related to sample concentration following the Beer-Lambert’s law [139]. We had recently shown that the live-cell FTIR method could quantify drug within living respiratory cells at a micromolar level *in situ* when drug solution was added to the culture medium[140].

The study of diabetes is, however, more complex. First, it requires the development of a diabetic model by pre-treating the HepG2 cells in high glucose and/or insulin environment to develop insulin resistance. Then glucose assay or fluorescence glucose dye are typically

used to measure glucose uptake inside cells to confirm insulin resistance. The diabetic model can then be used to study the drug's effect on metabolic changes. We hypothesize that live-cell FTIR can directly monitor the changes in intracellular composition and glycogen level due to glucose uptake to reveal the effect of anti-diabetic drugs, which can reinstate the insulin sensitivity and metabolic profile of cells. We aim to illustrate that the live-cell FTIR approach can discriminate the biochemical alteration of HepG2 cells in four different culture conditions; normal glucose and high glucose conditions with/without insulin for 24 hours[118, 141-143]. We will be demonstrating the approach by studying the effect of metformin (a first line insulin sensitizer [144]) and Resveratrol (a plant-derived polyphenol compound that has been reported for insulin sensitizer in diabetic HepG2 model[145]). This is the first time that the efficacy of anti-diabetic drugs is directly studied by the label-free live-cell FTIR method.

4.2 Materials and Methods

4.2.1 FTIR measurement of treatment samples

For the insulin response study, the attached HepG2 cells on the ATR element were first incubated in the high glucose (25mM, Gibco, UK) or normal glucose (4 mM) medium for 24 h, respectively, to generate the diabetic model and the normal model. To avoid the interference from cell proliferation and the risk of bacterial infection, a reduced FBS supplement (2% v/v instead of 10% v/v) and 50 U/mL penicillin, and 100 µg/mL streptomycin in the DMEM CO₂ independent medium was used in all treatments[91, 137]. After the incubation, 100 nM insulin (Sigma, UK) or 67µL PBS 1X (pH 7.4) (the control) were added in the cultured medium, and the cells were measured for another 24 hours. For the anti-diabetic drug study, 2 mM of metformin (Sigma, UK) or 50 µM of Resveratrol (Fluorochem, UK, 98% purity) in high glucose

with 100 nM insulin[146] were added, and the cells were measured for 24 hours where the results were compared to the same treatment but without the drug (control) using an FTIR spectrometer (Tensor II, Bruker Optics). In all cases, measurements were taken at every 10 minutes at 8 cm⁻¹ spectral resolution with 9 minutes of scanning time (1024 scans) and a spectral range of 4000 to 900 cm⁻¹. The OPUS software (Bruker vers.7.8, UK) was used for all data processing. All experiments were performed in triplicate based on 3 independent cultures with a passage number range between 33-43. Full spectra of the cells were acquired using the plain medium as the background. However, in the insulin response and anti-diabetic drug studies, difference spectra were analyzed with the attached cell spectrum (immediately after the treatment was applied, i.e., time 0 hour) being used as the background. The same strategies were successfully used in previous live-cell FTIR studies on drug-cell interactions[112, 137].

4.2.4 Cell viability assay

Cells concentration of 2.0x10⁴/200 µL were cultured in 96-well plates with 3 replicates for 24 hours and treated with high glucose concentration (25 mM) with/without insulin mentioned previously for 24 hours compared with 2% FBS normal glucose (control). Then, 100 µL of the MTT reagent (0.5mg/mL) (VWR International) was added to each well. After 4 hours of incubation, 100 µL of DMSO was added to detect the formazan.

4.2.5 Glycogen assay

Cellular glycogen content was determined using the glycogen assay kit (MAK-016, Sigma, UK). The experiment was repeated 3 times on 3 separate cell culture flasks. 1 million HepG2 cells were seeded in 6 well plates using 10% FBS supplemented DMEM high glucose medium. After

incubating overnight, all treatments; high glucose (25mM) and insulin 100 nM (diabetic model) with or without 2mM metformin/50µM Resveratrol in 2% DMEM CO₂ independent medium were introduced for 18 hours. The medium was then removed and then washed by cold 1X PBS, followed by 5 min of 1X trypsin, counted to 1 million, and centrifuged at 1000 rpm to a cell pellet. The packed cells were added with 100 µL of water for homogenization, where the intracellular glycogen can be extracted. A triplicate measurement was performed following the assay kit protocol, using the calorimetric method, with the absorbance value measured at 570 nm. The glycogen concentration in the treated cells was subtracted from the glycogen content of the blank to obtain the amount of glycogen production.

4.2.6 Data processing and Statistical analysis

The water vapor compensation algorithm (OPUS 7.8, Bruker Optics Ltd) was applied to all FTIR spectra, followed by normalization against the amide II peak to account for the difference in cell proliferation of the HepG2 between experiments. The normalized spectra were cut to the wavelength range between 1500-950 cm⁻¹ followed by concave rubber band baseline correction (1 iteration with 16 baseline points), second-order derivative (13 smoothing points, selected from a 9 to 25 points range) (41, 42) and vector normalization (38). The spectral range between 1500-950 cm⁻¹ was selected to focus the analysis on the carbohydrate and phosphate absorbance bands and to avoid noise from the residual water vapor absorbance, especially around the Amide I band at 1650 cm⁻¹(43). Pairwise principal component analysis (PCA) was performed using the PyChem[®] software (available from <http://pychem.sourceforge.net/>) for correlating changes from the different treatment settings (38). T-test was applied to determine the statistical significance between the

treatment groups and the control. The difference was considered significant for p.value < 0.05, calculated using Microsoft® Excel 2010.

4.3 Results

4.3.1 Viability assay

The MTT assay was used to verify that HepG2 cells remain viable in the insulin-resistant model in the live-cell FTIR experiment conducted without a 5% CO₂ supplement. The results showed that both high glucose (25mM) + high insulin (100 nM) and normal glucose (4 mM) + high insulin (100nM), were well tolerated by cells with up to 100% viability compared to the control (Figure 24). These results were also in agreement to the other studies that created the insulin-resistant model in HepG2 cells (25, 28, 37,38). Although diabetic HepG2 cells containing either 2mM metformin or 50 µM Resveratrol have shown lower viability to 80 and 78 %, respectively, the viability is still high, and cells showed healthy morphology (figures 25,26 and 27). The results demonstrated that the conditions used (based on anti-diabetic study literature (32, 41, 42)) were suitable.

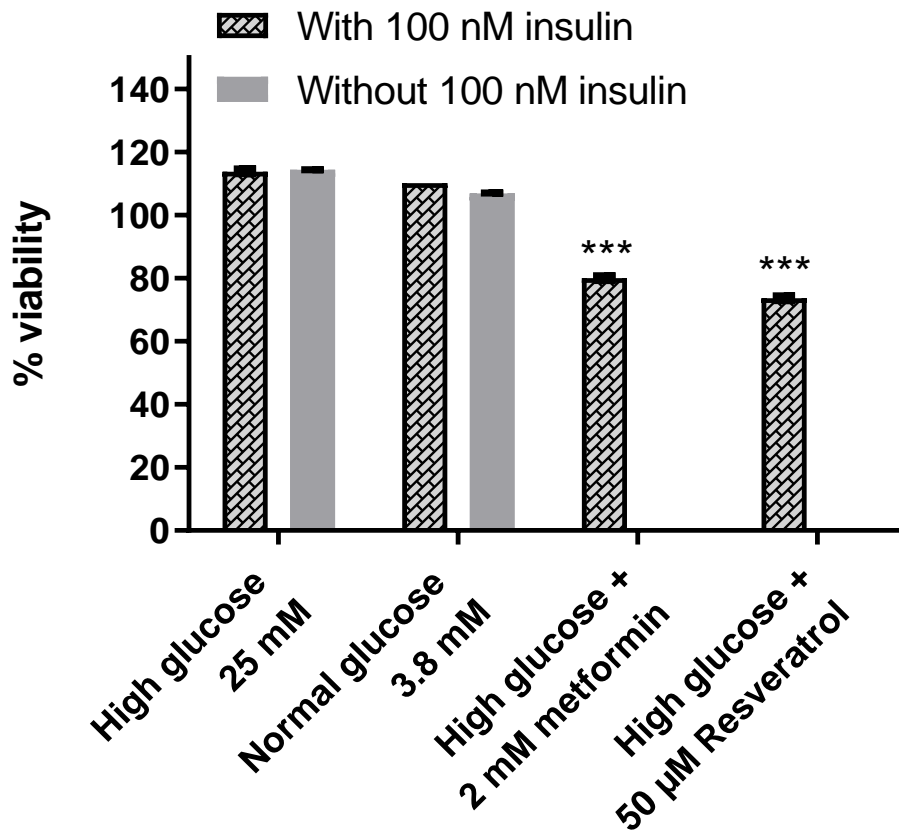


Figure 24. HepG2 cell viability in high (25mM) and normal glucose (4 mM) medium with 100nM insulin (brick plot) and without insulin (plain plot) of 24 h seeding with the error bar represents standard deviation

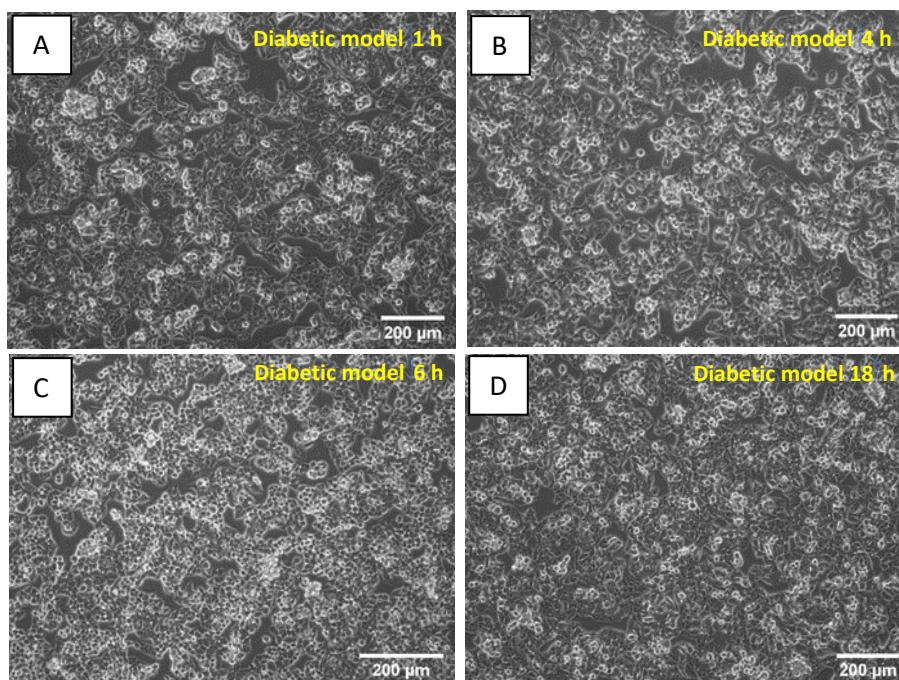


Figure 25. HepG2 morphology in diabetic model or control (high glucose 25 mM and 100 nM insulin) in different time points

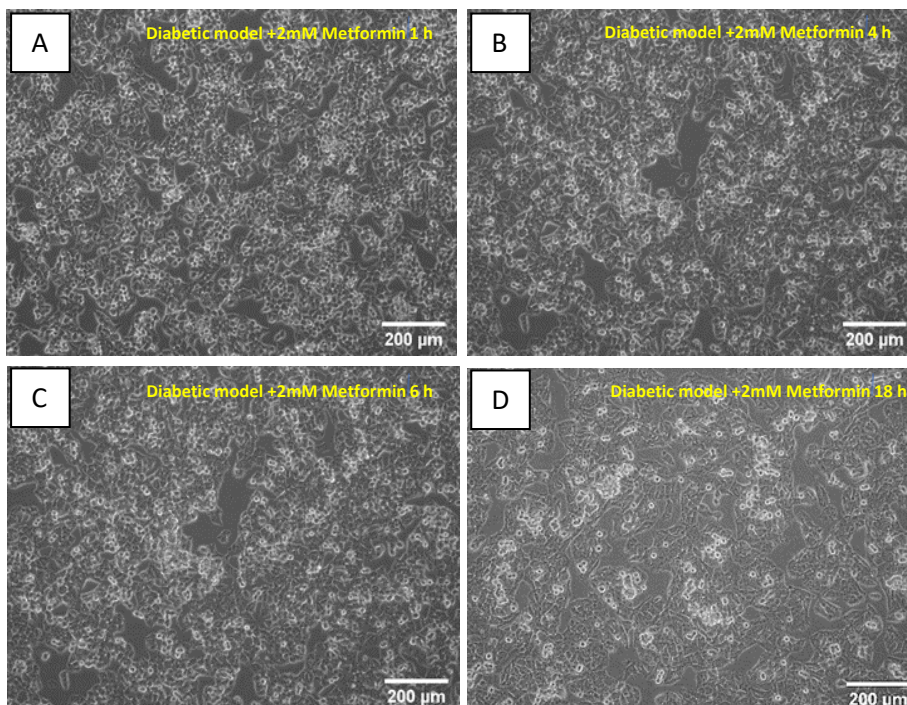


Figure 26. HepG2 morphology in diabetic hepG2 model and 2mM metformin treatment in different time points

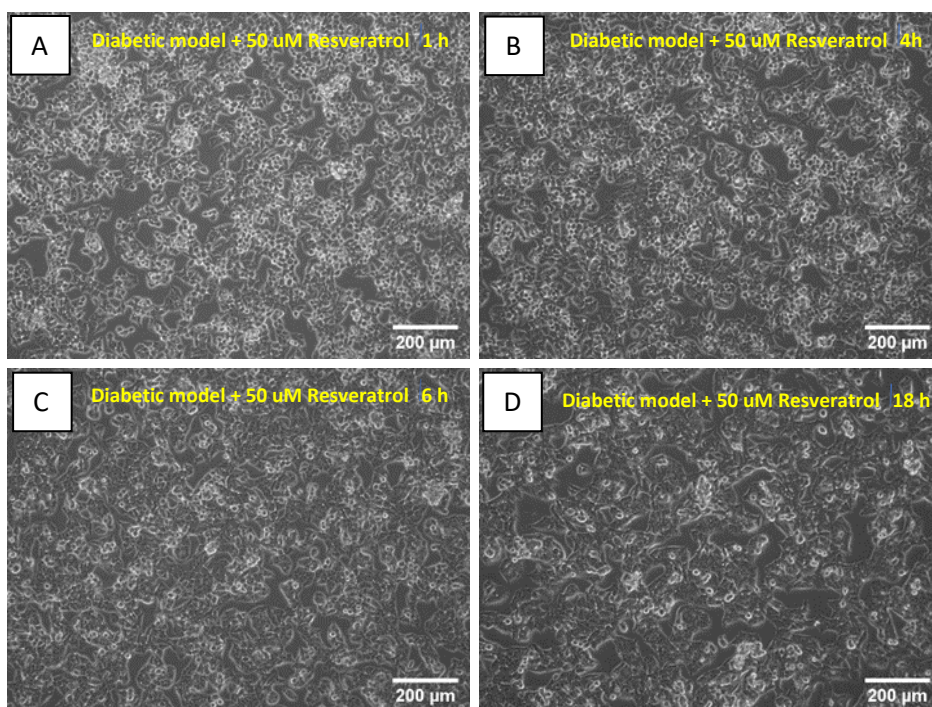


Figure 27. HepG2 morphology in diabetic hepG2 model and 50 μM Resveratrol treatment in different time points

4.3.3 Live-cell ATR FTIR experiment

The HepG2 cell layer on the ATR trough plate was then pretreated in high glucose medium (25 mM) for 24 h to develop the insulin-resistant model[125, 141, 143, 147]. An insulin response study was carried out to demonstrate the lack of insulin response from these insulin-resistant cells. The cells were treated with 100 nM of insulin and compared to the control group. (Figure 28, A and B) The results of the control insulin-resistant HepG2 cells (no insulin added, blue lines) and the 100 nM insulin-treated cells (red lines), including all three replicates, at 1st and 18th h after treatment. The analysis was focused in the spectral range of 1500-950 cm⁻¹, where the influence from the background water absorbance is minimal while many spectral features of metabolites are found.

The control and the insulin-treated group have shown similar spectral changes with a decrease in the absorbance at around 1000-1150 cm^{-1} and an increase in the 1150-1200 cm^{-1} regions at all analysed time points (Figure 28, A and B). These peaks are assigned to the cellular nucleic acid, phosphodiester linkage DNA, and carbohydrate component[148], reflecting the dynamic fluctuation of biochemical composition inside the living cell. However, the score plots in the pairwise PCA have not shown a significant difference between the treated and the control group ($p>0.05$). These results have confirmed the lack of response of the insulin-resistant cells to insulin.

To demonstrate that HepG2 cell, if not pretreated in 25 mM glucose for 24 h, will respond to insulin, a separate experiment with cells that have not been pretreated (labeled as “normal glucose”) was tested. The spectra of the normal glucose cells with and without 100 nM insulin exposure (magenta and light green, respectively) have shown clear differences in the spectra. The loadings plot from the pairwise PCA have shown an increase in the absorbance between 1000-1150 and 1150-1200 cm^{-1} regions for the insulin-treated group for all time points after the treatment. Interestingly this resembles the spectral changes observed when cells were treated in high glucose (25 mM) condition. The score plot has also shown that PC1 has shown a significant difference between with and without insulin ($p < 0.001$) for all time points (Figure 28, C and D) .

Next, we explored if the live-cell FTIR approach can be used to study the effect of anti-diabetic drugs. Metformin (2 mM), an insulin sensitizer, and 100 nM insulin were added to the insulin-resistant cell. The spectral changes were compared to the same experiment but without adding metformin. The pairwise PCA results have shown a significant difference between with

and without metformin treatments for both time points ($p < 0.05$) (figure 29, A and B) . Likewise, in the Resveratrol treatment study, the PCA of the FTIR spectra showed significant differences at both time points ($p < 0.05$) (Figure 29, C and D) . Notably, the PCA loadings plot for the 1st h metformin treatment has shown three characteristic peaks of glycogen at 1150, 1080, and 1020 cm^{-1} [128] (Figures 29, 3A), suggesting an increase in glycogen level in the cells while no peaks associated with metformin were found. At the 18th h of the treatment, the loading plots (Figure 3B) show peaks at around 1080, 1235, 1400, and 1450, resembling the peaks observed when the cells were treated in normal glucose conditions (Figures 28C, 2D).

The increase of intracellular glycogen indicates an increased glucose uptake when an insulin sensitizer was added. The mean integrated characteristic glycogen absorbance peak between 1060 -1000 cm^{-1} of the treatment and control has been plotted and compared over 24 h. The results show that both metformin and Resveratrol treated cells have more glycogen than the control as presented in Figure 29A. This integrated glycogen absorbance supports the PCA results that glycogen is being generated after the insulin sensitizer treatment (Figures 29, 3A).

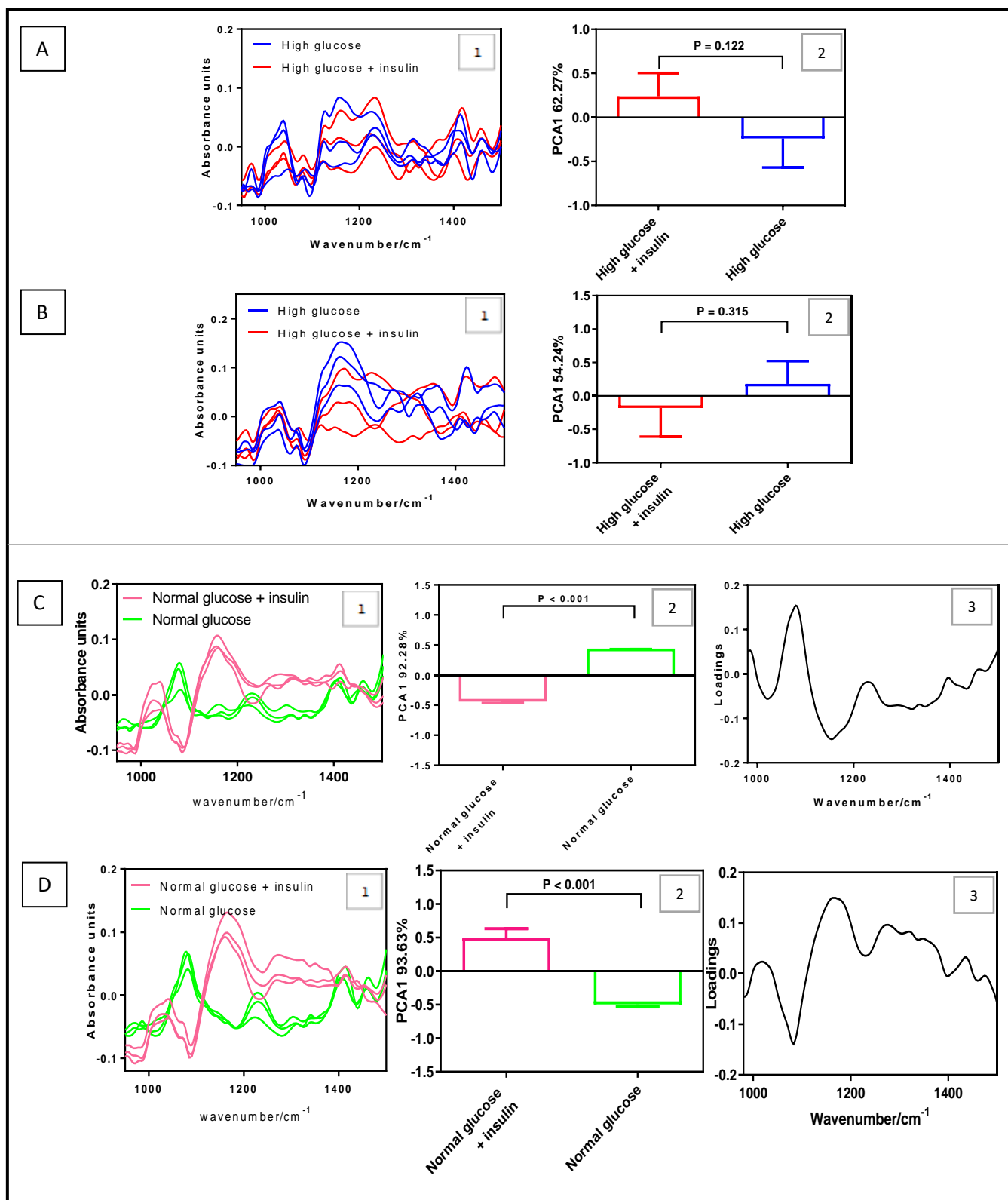


Figure 28. The comparison of three replicate HepG2 FTIR spectra between high glucose (blue) and high glucose + insulin (red) with PCA score at time 1 h(A) and 18 h (B) and the comparison of three replicate HepG2 FTIR spectra between normal glucose (light green) and normal glucose + insulin (magenta) with PCA score and loadings at time 1 h(C), and 18 h (D) with error bars representing the standard deviation

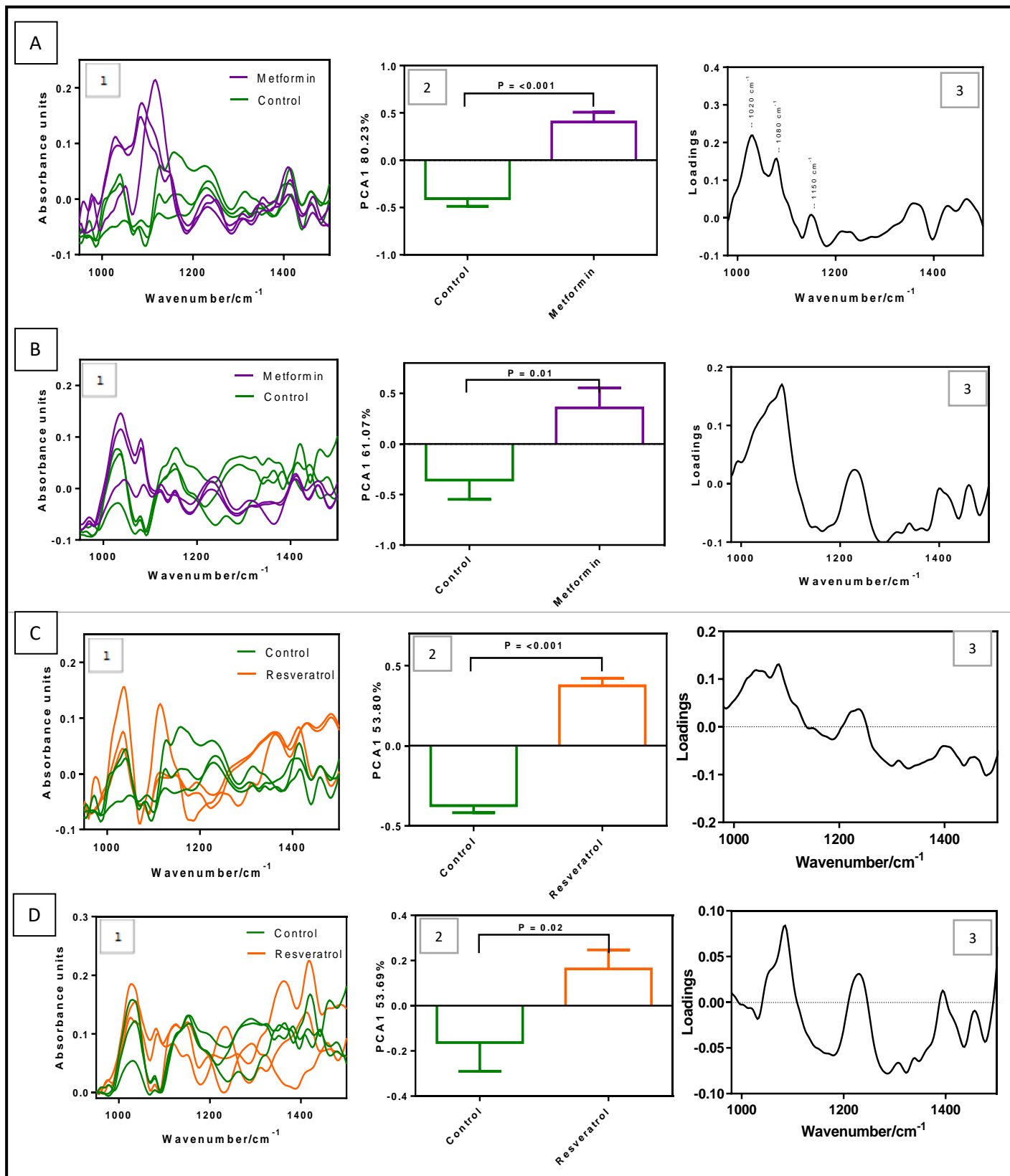


Figure 29. The comparison of three replicate HepG2 FTIR spectra between high glucose+ insulin: control (green) and high glucose+ insulin + 2mM metformin; treatment (purple) with PCA score at time 1 h(A) and 18 h (B) and the comparison of three replicate HepG2 FTIR spectra between high glucose+ insulin: control (green) and high glucose+ insulin + 50 μ M Resveratrol; treatment

(orange) with PCA score and loadings at time 1 h(C), and 18 h (D) with error bars representing the standard deviation

4.3.4 Glycogen assay

To confirm the live-cell FTIR findings, the same experiment was repeated with the intracellular glycogen level measured using the glycogen enzymatic assay kit. The results (Figure 30B) have shown that after the introduction of metformin and Resveratrol, cells have produced significantly higher intracellular glycogen at time 1st and 18th h compared to diabetic cells without treatment (Control), which are in good agreement with the FTIR results that shown an accumulation of glycogen after adding insulin sensitizer overtime. It is important to highlight that live-cell FTIR measurement does not require expensive reagents. It provides an opportunity to obtain a time profile of glycogen level of the same batch of living cells, which is impossible with the glycogen biochemical assay. (Figure 30B)

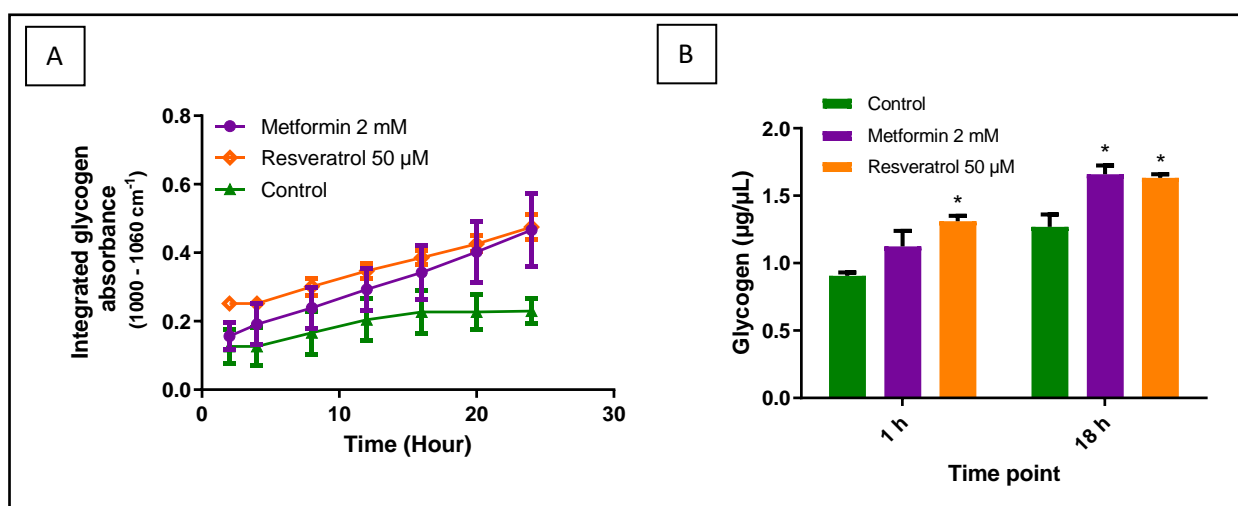


Figure 30. The comparison of the integrated absorbance of glycogen peak by FTIR approach among metformin (purple), Resveratrol(orange), and control(green) over 24 hours treatment (A) and the comparison of glycogen amount in diabetic HepG2 model by glycogen assay among diabetic HepG2 (control) with metformin or resveratrol treatment at time 1, and 18 h (B) with error bars representing the standard deviation

4.4 Discussion

In diabetes studies and the development of a new drug for diabetic treatments, *in vitro* models are often used to understand cellular metabolism. Current *in vitro* insulin-resistance analytical methods include glucose uptake assay, glycogen assay, Western blot, and qPCR analysis[149, 150]. These conventional biochemical assays provide precision and accuracy in both quantitative and qualitative studies. However, multiple biochemical assays are often required, which is time-consuming, expensive, and laborious[151]. The live-cell FTIR approach combined with PCA is a promising tool for studying the cellular response to drug treatments because it is label-free, low-cost, high throughput, highly reproducible, and non-destructive. This is the first time that live-cell FTIR is applied to test two anti-diabetic compounds' effect on a diabetic HepG2 model.

The cells pre-treated with 25 mM of glucose for 24 h did not respond to the 100 nM insulin treatment is expected because the cells were diabetic. The insulin-treated and non-treated diabetic cells have shown similar spectral bands at 1100 and 1250 cm^{-1} , which could be used as the marker for diabetic cells. When healthy cells (cultured in normal glucose) were treated in 100 nM of insulin, a similar spectral profile to the diabetic cells showing both the 1100 and the 1250 cm^{-1} bands emerged (Figure 28C and D). This is in contrast to the non-treated healthy cells, showing a different spectral profile with peaks at 1080, 1235, 1400, and 1450 cm^{-1} . The high insulin treatment can induce diabetes in HepG2 cells [125, 143, 152, 153], and the results have demonstrated that FTIR can capture this change.

Moreover, when cells were simultaneously treated in 25 mM glucose and 100 nM insulin, which is another method to generate diabetic models[142, 146, 154, 155] , the characteristic diabetic cells spectral profile was again observed as shown in Figure 28 A-D. The results show

that live-cell FTIR can provide information regarding insulin sensitivity and resistance. The introduction of metformin to the diabetes HepG2 model has produced a significant biochemical response and is clearly shown by the spectral changes. Concurrent with an apparent increase in glycogen peaks at ~ 1020 , 1080 , and 1150 cm^{-1} [128] 1 h after the introduction of metformin (Figures 29, 3A) provided a clear evidence of the increased glycogen level in the living HepG2 cell. At longer drug treatment time (18 h), the loading plot, which highlights the differences between the spectrum of cells with and without the presence of drug, has shown a return of a spectral profile closer to the cells treated in normal glucose condition. These findings suggested that metformin has improved insulin sensitivity and restored the cells' metabolic profile [143, 156].

Resveratrol is a plant-derived polyphenol reported for insulin resistance improvement in diabetic animals and humans, and there is much evidence of being effective in treating diabetic Hepg2 cells[145, 157, 158]. Teng W. et al. [159] have demonstrated the mechanism of Resveratrol metabolite action in insulin resistance HepG2 cells; the results have shown that Resveratrol, similar to metformin, can enhance cellular glucose uptake and glycogen synthesis and restore the metabolic profile of the cells. Furthermore, the live-cell FTIR study have demonstrated that both drugs have produced similar results, which is expected as Resveratrol also regulates insulin signaling and ameliorates insulin resistance by modulating the IRS-1/AMPK signaling pathway, similar to metformin[145].

Traditional glycogen assays typically require extracting the intracellular glycogen from the sample and removing insoluble materials. Through this process, intracellular glycogen is significantly diluted and some glycogen could be lost, even when samples were protected in cold environment [160]. In contrast to the method presented in this study, glycogen level

inside cells was measured directly without requiring extraction. The plot of the glycogen absorbance peak shown in [Figure 30A](#) indicates the relative increase in glycogen level in cells as a function of treatment time. The increasing trend agrees with the results obtained from the standard glycogen assay kit. Although the exact amount of glycogen produced was not calculated from the FTIR result, a multivariate calibration method, such as partial least square, could be applied to determine this, should the glycogen level in cells be of interest. To illustrate that this is possible, the spectra of 2 and 4 mg/mL glycogen standard solution are shown in [Figure 31](#) highlighting the absorbance of the 4 mg/mL glycogen solution is approximately double of the 2 mg/mL solution. When comparing the glycogen spectra to Resveratrol treated cell spectra at the 6th h time point, the glycogen peaks can be clearly observed, confirming that the method can detect and quantify the increase in glycogen level in cells.

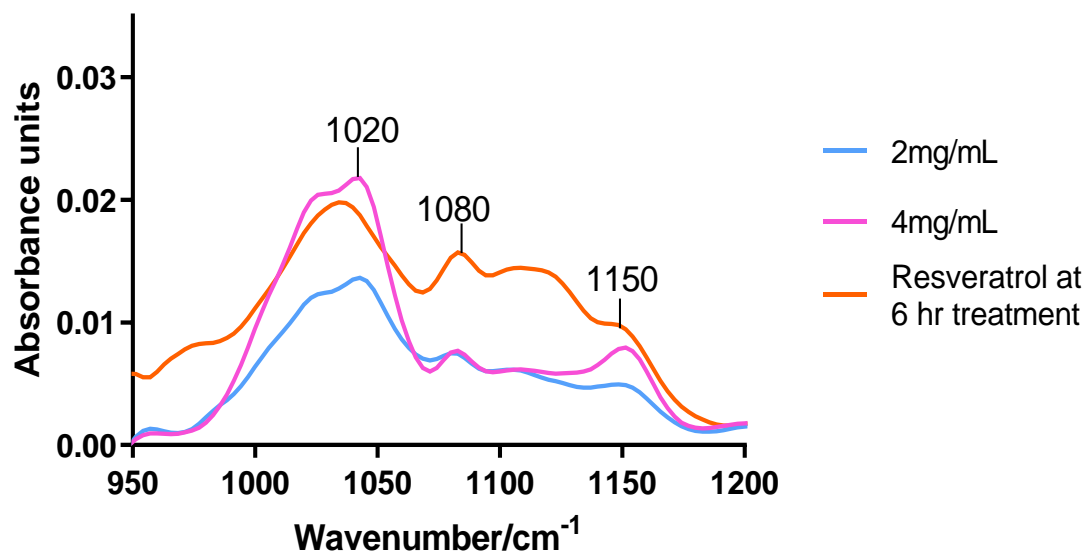


Figure 31. A characteristic of glycogen peak from 4 mg/mL (pink), 2mg/mL(blue) glycogen solution and at 6th h of resveratrol treatment

4.5 Conclusions

Live-cell FTIR spectroscopy was demonstrated to be suitable for studying the effect of the drug on insulin-resistance HepG2 diabetes model. Metformin and Resveratrol were shown to produce an improvement in insulin sensitivity by the direct FTIR measurement of changes in intracellular glycogen level and the restoration of the spectral profile, which represent the molecular composition of the cell, with no extraction and dilution requirements, highlighting the advantages of the label-free method to detect the changes in intracellular metabolic profile and glycogen level. It can be a complementary tool for drug efficacy screening, especially for insulin sensitizers. Live-cell FTIR is a relatively low-cost, sensitive, reliable, and high throughput method that can be used as a promising tool to accelerate the anti-diabetes drug discovery process.

Chapter 5 Live-cell FTIR approach to investigate the mechanism of action from liver selective glucokinase activator

5.1 Introduction

Glucokinase activators (GKAs) are the new class of potential antidiabetic agents that have recently paid a greater interest to many researchers with various publications *in vitro*, *in vivo*, and clinical trials. Glucokinase (GK) or human hexokinase IV, hexokinase D, and ATP: D-hexose 6-phosphotransferase is an enzyme that facilitates the phosphorylation of glucose to glucose6-phosphate, where glucose molecules from cytosol enter into the cells. This enzyme plays an essential role in glucose homeostasis regulation[161]. GK is expressed in various organs, e.g., pancreatic alpha and beta cells, pituitary cells, central nervous system, and gastrointestinal system; these organs comprise 0.1% of the body's total GK activates (Fig 5.0). The rest of the 99.9% comes from the liver. Thus, the liver and pancreatic islet cells are the primary organ of controlling the GK- regulatory system maintaining glucose homeostasis[162].

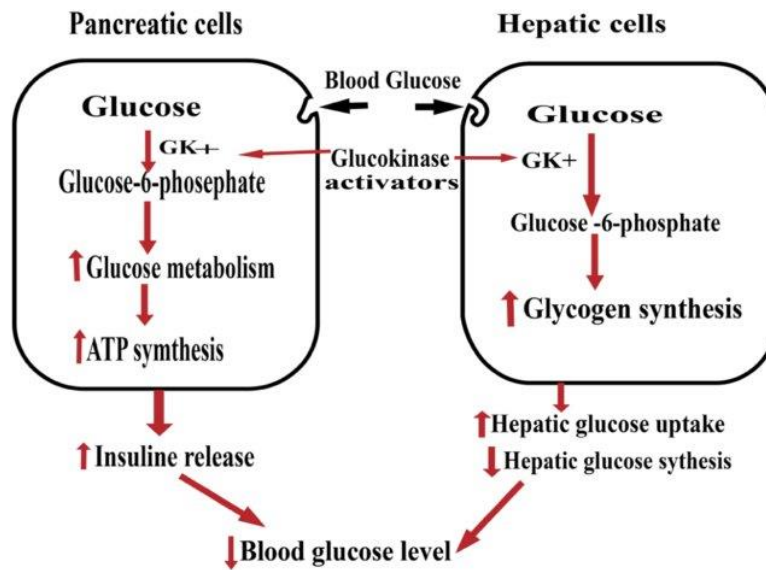


Figure 33. The role of Glucokinase activators in pancreatic and hepatic cells[104]

GK is the rate-limiting enzyme in the glucose-stimulated insulin secretion in pancreatic β -cells or serves as a “glucose-sensor”. GK regulates glucose utilization, glycogen synthesis, and hepatic glucose production in the liver, or called a “gate-keeper”. GKAs lower blood glucose level by increasing the ability of pancreatic β -cells in respond to increasing blood glucose concentration and enhance insulin secretion in a glucose-dependent manner [163](Figure 33). Concurrently, GKAs increase hepatic glucose uptake and glycogen synthesis while decreasing the amount of glucose production (gluconeogenesis). GKAs also have anti- apoptotic effect on β -cells. Moreover, an increased hepatic glucose output, considered the major liver dysregulation related to T2DM, is not effective by the current medication except for metformin. Therefore, GKAs may have the potential to resolve this unmet need in Type 2 diabetes treatment.

The liver GK is a sustained inactive complex with the glucokinase regulatory protein (GKRP), an endogenous inhibitor when blood glucose is less than ~ 10 mM. The GK will be activated only during postprandial or high glucose to increase hepatic glucose uptake (Figure. 34). Thus,

GKRP acts as a competitive inhibitor response to hepatic glucose concentration, preserving GK low concentration of glucose and releasing it in the presence of raised glucose concentrations.

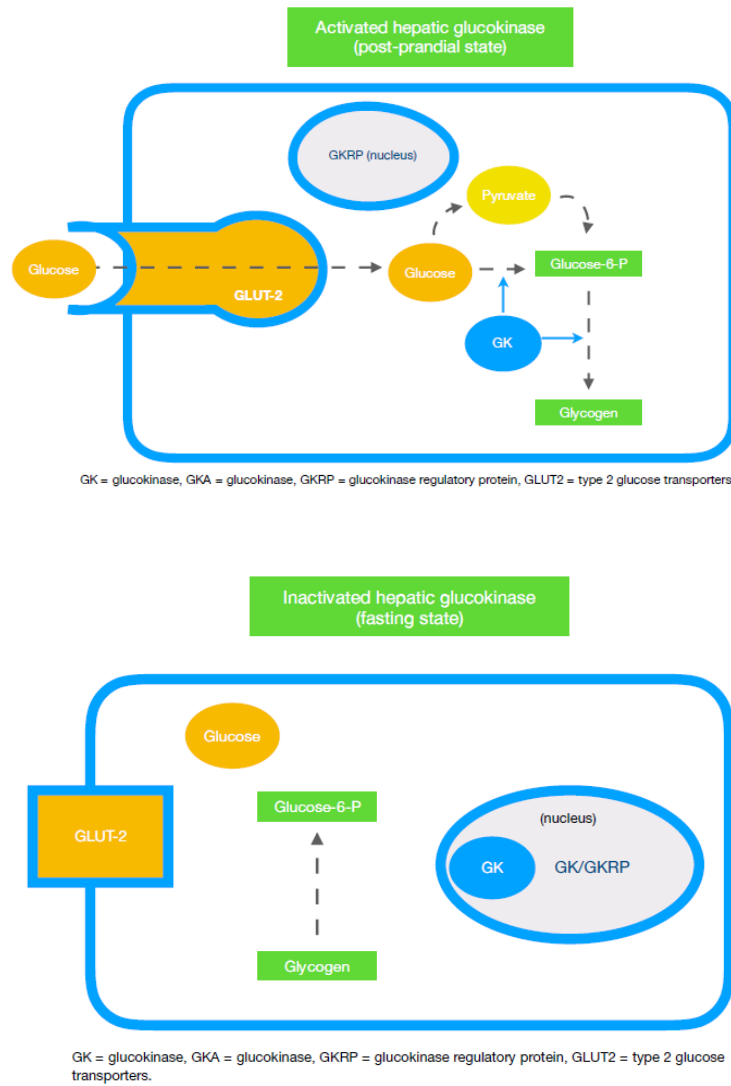


Figure 34. Glucokinase activity in hepatocyte[105]

GKAs can be classified based on the chemical structure or site of action; full GKA agonist, partial agonist, hepato-selective GKAs. However, only a small number of GKAs have reached the clinical trial phase described below.

5.1.1 Present status of glucokinase activators in clinical development

Since 2008, various clinical trials have reported the effect of GKAs in lowering blood glucose levels in diabetic patients. Some of the significant glucokinase activator studies are described below.

A systematic study of Piragliatin

Banadona *et al.*[166, 167] carried out a phase Ib, randomized, double-blinded, crossover trial to investigate the mechanism of blood glucose-lowering effect from Piragliatin in mild type 2 diabetic patients (HbA1C 6.1 ± 0.2 %). The result demonstrated that this agent caused an immediate effect on glucose-lowering effect via increased β -cell function. However, Piragliatin was found to incur hypoglycemia incidence in the higher dose of 100 mg that patients needed to be rescued by glucose infusion. This non-desirable side effect was the main reason to terminate of Piragliatin study.

Long term efficacy and tolerability of MK-0941

Meininger *et al.*[168] assessed the efficacy and safety of MK-0941 in type 2 diabetes patients receiving insulin glargine (\pm metformin $\geq 1,500$ mg/day). Patients were randomly receiving a ranging dose of MK-0941 versus placebo. Initially, blood glucose profiles in the receiving group were improved significantly compared to the placebo groups. However, in week 30 of treatment, the effects of blood glucose reduction were not sustained. Moreover, hypoglycemia and hypertriglyceridemia were observed, and the trial was terminated due to a lack of efficacy and increasing side effects.

It was suggested that the genetic of the β -cell glucokinase activation had caused an immediate and dramatic reduction of blood glucose levels. However, this reduction was not sustained over time, and the blood glucose returned to a high level because of the toxicity of GKAs on the beta cells. GKAs could be combined with beta-cell proliferators such as incretin drugs to eradicate this significant drawback, which may worsen drug adherence in patients. The authors suggested that the solution to minimize hypoglycemia's risk is to use a partial GK activator or liver or hepatoselective GKAs[168].

PF- 04937319, A partial glucokinase activator

N.B Amin et al.[169] evaluated the efficacy and safety of a once-daily dose ranging of PF-04937319 as an add-on therapy to metformin in type 2 diabetic patient(T2DM) patients compared with both placebo and titrated glimepiride. Their results have shown that 50 and 100 mg of PF- 04937319 are the most effective dose for HbA1C reduction compared with placebo (-4.94 or -5.11 mmol/L (-0.45 or -0.47%, sig), but the efficacy was lower than titrated glimepiride(-9.07 mmol/L (-0.83%). On the other hand, hypoglycaemia events were lower with the PF- 04937319 100 mg than the 10 mg glimepiride (5.1% and 34.4%, respectively). However, the clinical trial results yielded a superior glycaemic lowering effect with once-daily PF-04937319 (300 mg), split-dose PF-04937319 (150+100 mg; breakfast+lunch), compared with a once-daily dose of 100 mg sitagliptin (PF-04937319: split-dose, -0.88%; once daily, -0.94%; sitagliptin, -0.63%). Unfortunately, hypoglycaemia occurred in patients received PF-04937319 in both regimen more often than patients received sitagliptin 100 mg[170].

The hepatoselective glucokinase activator- PF-04991532

Previous clinical trials have shown that hepatic glucokinase overexpression such as MK-0491 could repair glucose disequilibrium in diabetic patients. However, this overstimulation has also illustrated unwarranted increases in hepatic glucokinase activity that may have caused hepatosteatosis. Thus, Erion *et al.*[171] assessed whether using a hepatoselective glucokinase activator effectively reduces hyperglycemia without causing hypertriglyceridemia. In that study, they tested the compound PF-04991532 in Goto-Kakizaki rats. The result has shown that PF-04991532 can improve glucose profiles of the rats independent of insulin concentrations in a dose-dependent pattern in both acute and sub-chronic treatment. However, PF-04991532 induced dose-dependent increases in plasma triglyceride concentrations. Furthermore, by investigating both the lipid and lipid gene expression changes in the liver, it was found that there was no relationship between hepatic triglyceride concentrations and serum triglyceride in Goto-Kakizaki rats. However, the researcher suggested that increasing the AMP: ATP ratio in hepatocytes could activate AMP-activated protein kinase (AMPK), preventing hepatic steatosis.

TMG-123, a novel glucokinase activator

Pharmaceutical Development Research Laboratories, Teijin Pharma Limited, Tokyo, Japan, have attempted to produce an effective hepatic glucokinase activator that minimizes side effects, especially hypertriglyceridemia. TMG-123 is a potential anti-diabetes substance that can successfully lower the glucose level in animal models with ongoing clinical trials. TMG-123 improves the impaired glucose tolerance without hypertriglyceridemia in the insulin-deficient and -resistant diabetic mice model. The beneficial effect on glucose tolerance was

better than current antidiabetic drugs such as metformin and glibenclamide. TMG-123 also improves glucose tolerance when used in combination with metformin. Moreover, TMG-123 has a sustained effect on HbA1c levels even after 24 weeks. In summary, TMG-123 has the most significant efficacy on acute and chronic symptoms and no adverse event on triglyceridemia[172].

A novel Glucokinase Activator, HMS5552, on Glucose Metabolism in the T2DM human and Rat Model

Ping Wang et al. [173] explored the possible effects of HMS5552 on T2DM male Sprague-Dawley rats. The rats were divided into four groups: control, diabetic, low-dose (10 mg/kg), and high-dose (30 mg/kg) of HMS5552. The glucose and lipid profile change was determined by oral glucose tolerance test and total cholesterol triglyceride, respectively. There was no increase in insulin level during the administration of this drug. After administering both doses of HMS5552, glucose levels were reduced by ~25% and 31% ($P < 0.05$), respectively, compared with the control. Moreover, on the 27th of the chronic study experiment, the glucose-lowering effect was still sustained and significantly reduced plasma glucose levels by ~18% ($P < 0.05$). The total cholesterol and triglyceride were not changed after taking the compound compared to the diabetic groups.

Recently, a study of the pharmacokinetics of HMS5552, conducted with a dose-ranging of 5–50 mg in healthy subjects, was also investigated. The results show that HMS5552 at doses of up to 50 mg in healthy volunteers was safe and tolerable [174].

To summarize, GKAs are classified into 3 categories: non-specific GKAs, liver-specific GKA, and optimum GK receptor stimulation. Due to the accessibility and availability of glucokinase activators, we initially selected PF-04991532, a liver-specific test for cellular change using the live-cell FTIR approach. Based on the mechanism of action of liver-specific glucokinase activators that facilitate glucose from cytosol or medium into the cell. We hypothesized that the cellular change regarding the increase in glucose uptake might represent an increase in carbohydrates in FTIR spectra.

Aims: to illustrate that the live-cell FTIR approach can discriminate the biochemical alteration of HepG2 cells high glucose with PF-04991532 culture conditions and confirm the change to the literature

5.2 Material and methods

5.2.1 MTT assay: HepG2 cells were tested with a range of PF-04991532 concentration (1 -100 μ M) to ensure the cell remains viable at the concentration used in the live-cell FTIR experiment. Cells concentration of 2.0×10^4 /200 μ L were cultured in 96-well plates for 24 hours and treated with the different concentrations of glucokinase activator (PF04991532). Cells were cultured with each reagent for 24 hours, and then 100 μ L of the MTT reagent (0.5mg/mL) (VWR International) was added to each well. After 2-hour of incubation, 100 μ L of DMSO was added to each well to detect formazan. The absorbance value at 570 nm and 630 was taken using a spectrophotometer (SpectraMAX). The values of absorbance of each well plate were plotted, and the percentage cell viability was calculated over each concentration

5.2.2 Live-cell FTIR experiment:

2 million HepG2 cells were seeded on the attenuated total reflectance (ATR) plate. The attached living cells were treated in either high glucose concentration (25 mM) with or without 10 μ M PF-04991532 in DMEM CO₂ medium with spectra of the cells measured every 10 min. Spectra were examined 24 hours after treatment by subtracting the spectrum at treatment time 0. Spectra were truncated to 1780-900 cm^{-1} , followed by baseline correction and vector normalization. Principal component analysis was used as the statistical tool to highlight any possible correlated changes observed in the experiment.

5.3 Results and Discussions

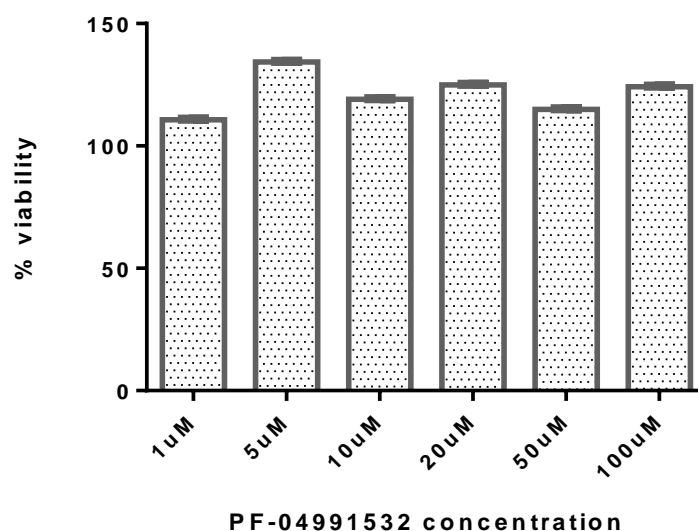
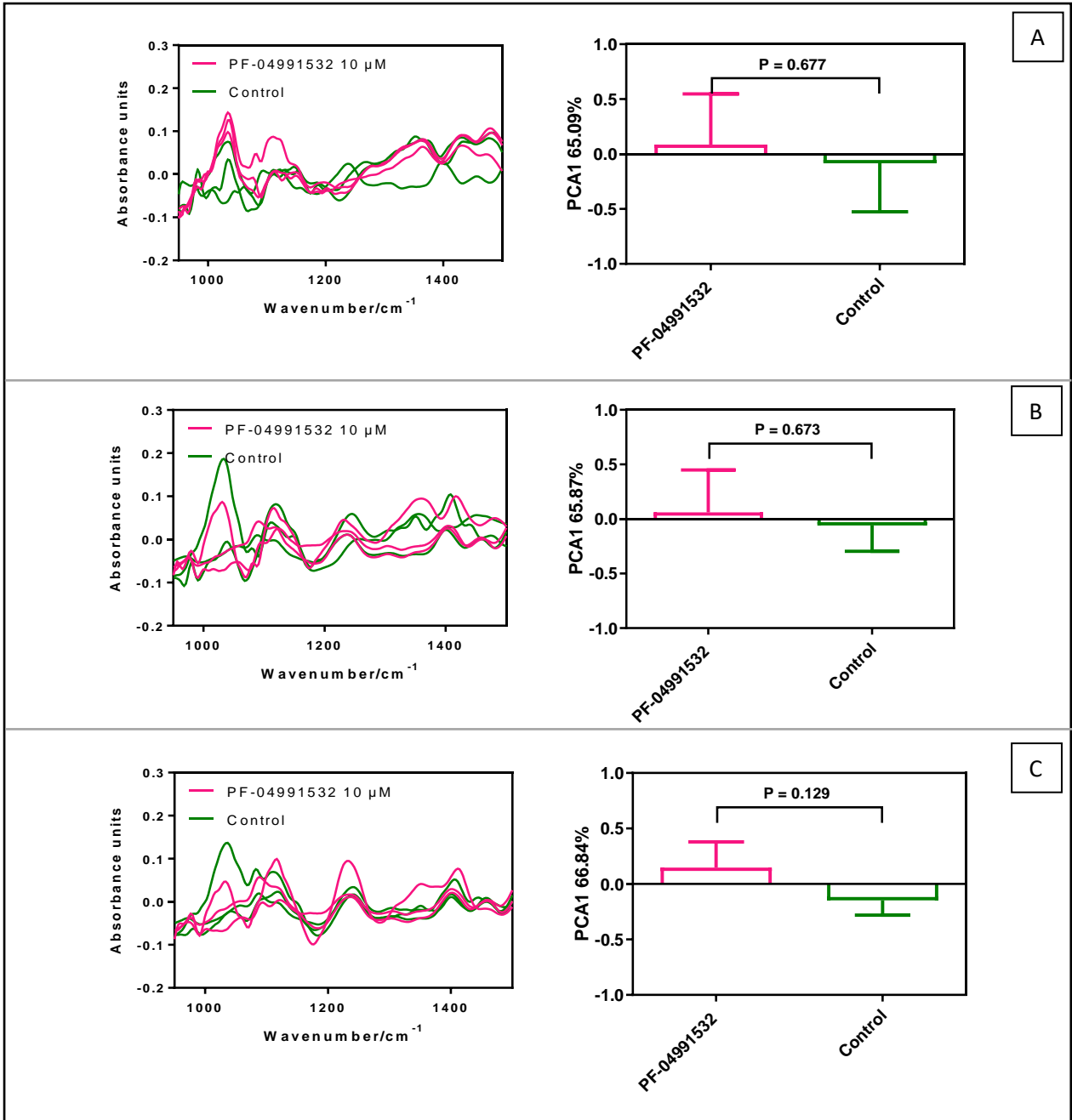
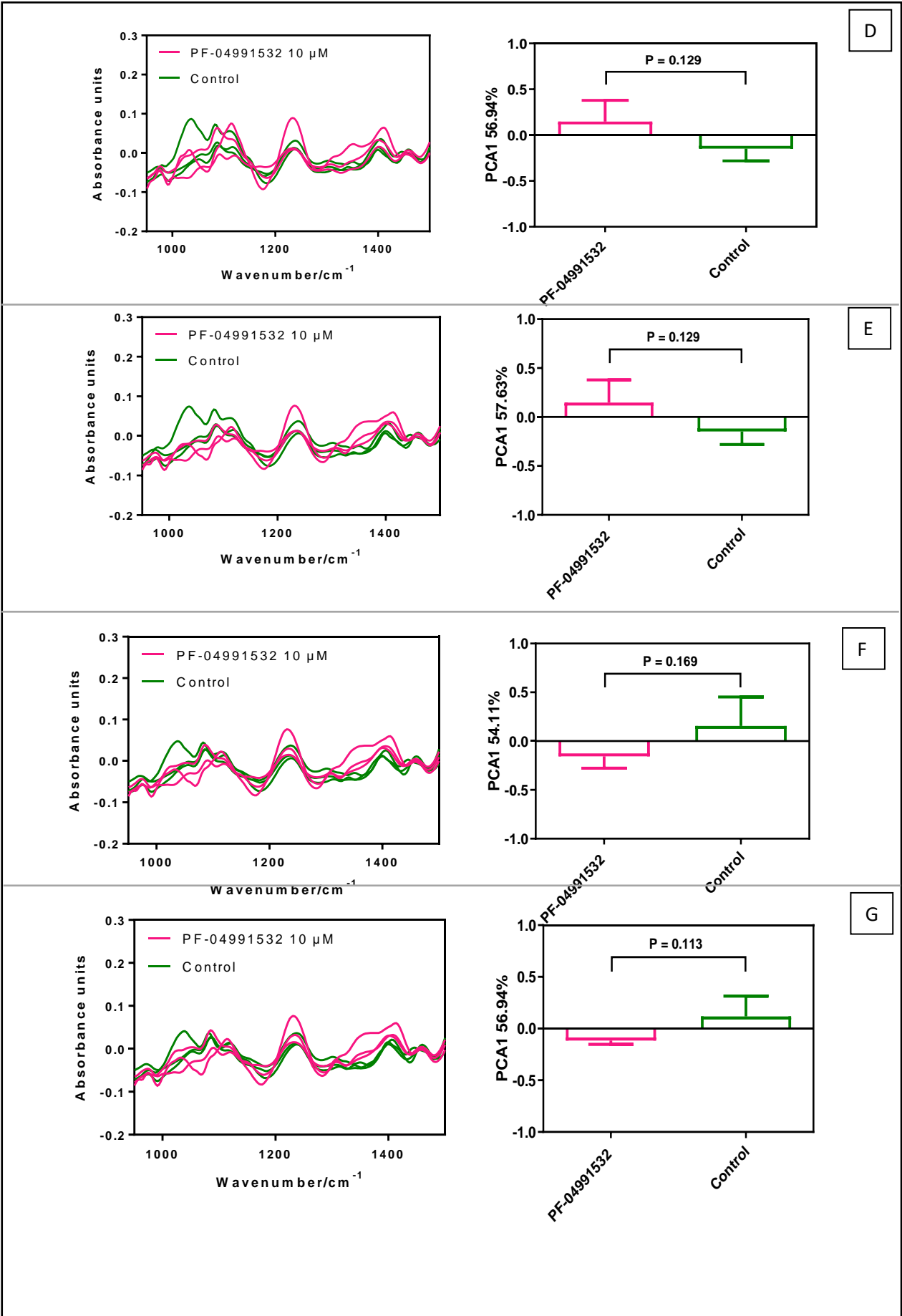


Figure 35. The viability of HepG2 cells after PF-04991532 for the 24-hour treatment with error bars representing the standard deviation between the three independent repeated experiments





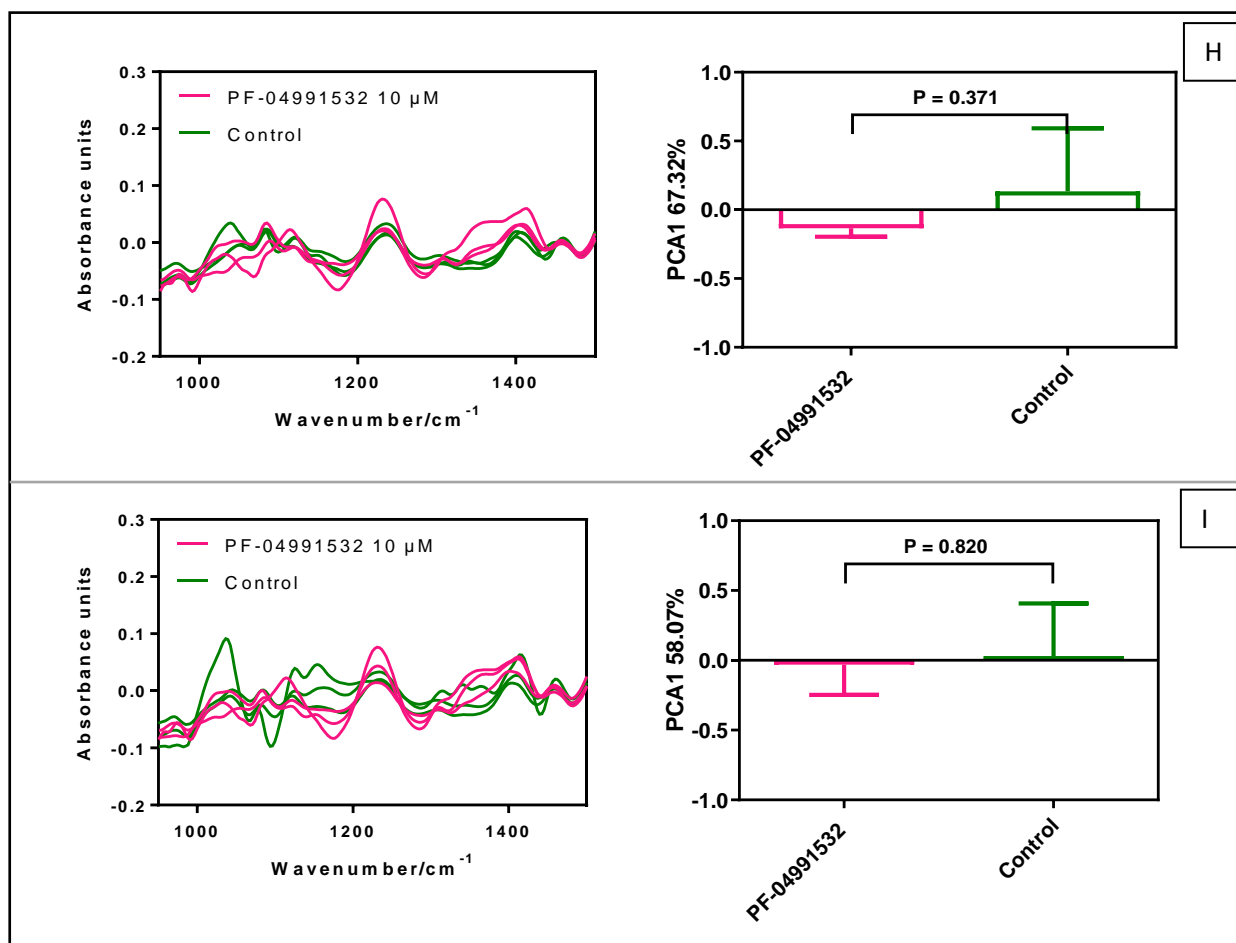


Figure 36. The comparison of live-cell FTIR spectra between control (green color) and PF-04991532 (pink color) and box plot for time 10 (A), 10 min(B), 1h (C), 2 h(D),3 h (E) 4h(F), 6(G), 12(H), and 24 h (I) with error bars representing the standard deviation between the three independent repeated experiments

The cell viability of PF-04991532 ranging from 1 -100 μM shows more than 80% viability for all concentrations up to 24 hours of treatment, which means that HepG2 can tolerate well in each FITR experiment (Figure.35). The concentration we used in our experiment was similar to in vitro efficacy study of PF-04995132[171].

Based on the liver glucokinase activator mechanism of action, we expected an increase of spectrum in carbohydrate region and/or glycogen after treatment. However, FTIR results of

PF-04991532 treated HepG2 showed a rise of spectra around 1100, 1200, and 1400 cm^{-1} associated with carbohydrate, phosphodiester linkage in DNA, and a group of fatty acid and amino acids acid, respectively. These changes indicated cell growth generally after treatment with a glucokinase activator. However, there were no significant differences between control and treatment for all time points ($P>0.05$) (Figure 36).

Liver glucokinase action highly depends on the GKR protein GK mRNA gene expression. Typically, GCK is dominant in hepatocyte nucleus. The GCK location depends on the cellular metabolic status. Normal physiology forms a complex with GCKR, while with high glucose concentration (since 10mM), the complex of GK-GKR will be broken down and let GK release to the cytosol[175]. Our study was conducted in high glucose (25mM) diabetic mode to mimic the physiologically disease pathogenesis and test for the effect of treatment. Moreover, the author suggested that liver GK gene expression depends on primary cells' fasting and refeeding stage. Insulin is a primary upregulation, while glucagon acts as the opposite effect[175].

The studies of hepato-selective glucokinase activators have been demonstrated in 2 drugs, PF-04991532 and TTP-399[171]. These two studies were conducted in rat hepatocytes (in vitro) and mice (in vivo), which significantly increased glucose uptake in hepatocytes after treatment. In addition, PF-04991532 has shown increased hepatic glucose uptake and reduced hepatic glucose uptake in a dose-dependent manner. Similarly, TTP-399 stimulates glucose utilization in the liver during a small amount of insulin secretion and no dyslipidemia; these results lead to TTP-399 to achieve the Phase II clinical trials[176-178]. One thing in common, these two studies had used the primary cell in the studies, not the cancerous cell

line. And also lack data on a cancerous cell line that directly studies glucokinase activators, especially in HepG2 cells.

Min Q. et al. [179]. have demonstrated the activity of natural compounds name mangiferin as a potential liver glucokinase activator in HepG2 cells and diabetic mice. Before cell-based assay and *in vivo*, they have tested the binding conformation between mangiferin and glucokinase enzyme. The results showed that mangiferin has the best score binding, meaning it is a good fit for the GK enzyme. Furthermore, mangiferin-treated HepG2 significantly increased glucose consumption detected by glucose uptake assay; this result was also related to the significant lowering of blood glucose in diabetic mice. However, I believe there was no confirmation that the increase of glucose uptake in HepG2 *and in vivo* came from the glucokinase activation mechanism. Since diabetes is complex and the mechanism of anti-diabetes is varied. For example, Wang C. et al. [180] found that mangiferin salt has potent activities in reducing intracellular lipid accumulation, enhancing glucose consumption in HepG2 cells by stimulating AMPK. Niu C. et al. also supported this mechanism of action that the AMPK pathway is associated with this therapeutic effect of mangiferin[181]. Thus, the mechanism of mangiferin on glucokinase activation in HepG2 cells cannot be confirmed by structure-based virtual ligand screening and enzyme assay outside the HepG2 cell system.

The possibility of insignificant differences in glucokinase activator in HepG2 cells may be because the cancerous cell line lacks GK mRNA gene expression like a primary cell. This can be proved by the study of Zheng HT et al. [182] that carried the retroviral vector containing the glucokinase (GK) gene to infect HepG2 cells to study the dose-response effect of glucose on insulin secretion that mimics the Beta-cell action. The results showed that the artificial

beta cell obtained a glucose-stimulated insulin secretion with maximal insulin secretion at 1.75-2.00 mmol/L glucose concentrations. However, these results still show the sensitivity of Live-cell FTIR in detecting the negative control from non-transfected GK HepG2 treated with GKAs by providing non-significant results. The future work for this experiment will be use the transfected glucokinase HepG2 cell line or primary hepatocyte for testing with current glucokinase inhibitors candidates.

Chapter 6 Conclusions and Future work

6.1 Conclusions

This thesis proposes to use live-cell FTIR spectroscopy as a screening tool in diabetes metabolism study and the preclinical stage of anti-diabetes drug development.

FTIR spectroscopy is a non-destructive, sensitive, label-free, and low-cost technique that can integrate drug-cell interaction. This approach can detect the chemical bonds represented in the samples, which is a suitable tool for studying complex biological systems like drug-cell interactions. The introduction of anti-diabetic drugs into the cells induces various cellular changes or biomarkers directly reflected in the IR spectrum of cells. It provides the chance of acquiring the signature spectrum of the biochemical pathways objected by these drugs. The biomarker from drug-cell interaction usually is needed to extract from the cells or design a suitable dye to probe the biomarker of interest, which requires lots of chemical assays, is time-consuming, and expensive. Moreover, many studies were carried out on fixed cells with a specific time point that may have some artifact of the fixing process interfere with the results. The live cellular study using ATR FTIR spectroscopy in response to an anti-diabetes drug can monitor the real-time cellular change at many time points and diminish the artifacts that originated from the chemical fixation.

We have established that FTIR spectroscopy can be used in the live-cell glucose metabolism measurement by exhibiting the suitability of its approach in obtaining the spectral variations of IR spectra in living cancer cells after exposure to a glucose-containing medium. For this purpose, the hepatocellular carcinoma cell line or HepG2 that has been widely used in *in vitro*

diabetes metabolism was examined. We demonstrated that FTIR could monitor glucose metabolism in living HepG2 cells in situ. This technique could detect the cellular change regarding the medium's different glucose concentrations and establish the diabetes model using high glucose treatment. FTIR spectra of live cells treated in normal and high glucose medium have shown significant differences ($p < 0.05$) for all treatment times. The control cells have seen an increase in absorbance at 1088, 1240, and 1400 cm^{-1} , which are associated with phosphate stretching mode vibrations from phosphorylated proteins and DNA backbone; and symmetric stretching mode vibration COO^- from fatty acids, amino acids, lipids, and carbohydrate metabolites. Moreover, the high glucose treated cells have shown different changes in the 1000–1200 cm^{-1} region, which is linked to the glycogen and ATP: ADP ratio.

Secondly, we investigated the potential use of this technique as an analytical tool in the diabetes treatment study. In this study, HepG2 cells were introduced to insulin in both normal and high glucose medium to detect insulin sensitivity and establish the insulin resistance diabetic model. And also to study the reinstatement of insulin resistance by insulin sensitizer drugs and natural compounds. The spectra of the normal glucose cells with insulin have shown an increase in the absorbance between 1060-1350 cm^{-1} for the insulin-treated group for both 1st and 2nd h after the treatment. PC1 has shown the difference is significant with $p=0.005$ and $p=0.009$ for 1st, and 2nd h, compared without insulin treatment. Whereas the spectra of high glucose with and without high insulin-treated HepG2 showed similar changes with a decrease in the absorbance around 1000-1150 cm^{-1} and an increase in the 1150-1200 cm^{-1} regions at 1st h and 2nd h. These are allocated to the cellular nucleic acid, phosphodiester linkage DNA, and carbohydrate component. However, the pair-wise PCA comparison between the insulin-treated HepG2 cells spectra has not presented a clear difference from non-treated

insulin, with $p=0.123$ and $p=0.144$ for 1st and 2nd h after introducing insulin. Thus, we can summarise and establish an insulin resistance diabetic model using insulin and high glucose treated HepG2 due to the lack of insulin sensitivity. Furthermore, adding metformin and Resveratrol into the insulin-resistant cell has shown significant spectral changes compared to control both 1st and 2nd h after adding the drug, with P-value <0.01 . Notably, the PCA loadings plot for 1st h after metformin addition has shown three characteristic peaks belonging to glycogen at 1150, 1080, and 1020 cm^{-1} .

Lastly, we attempted to apply this method to detect the spectral change induced by other anti-diabetes drugs. PF-04991532, a liver selective glucokinase activator, has been introduced to high glucose treated HepG2 cells; the experiment was observed for 24 hours. According to its mechanism of action that increases hepatic glucose uptake, we expected that glucose increase in the cell is related to increasing glycogen spectra in the FTIR approach. The results have shown that both control and PF-04991532 treated cells spectra around 1100, 1200, and 1400 cm^{-1} are associated with carbohydrate, phosphodiester linkage in DNA, and a group of fatty acids and amino acids, respectively. These changes indicated cell growth generally after treatment with a glucokinase activator. However, there were no significant differences between control and treatment for all time points ($P>0.05$). We have discussed these insignificant results derived from the malfunction of a cancerous cell line that lacks the GKR gene expression.

6.2 Future Work

The first prospect is to expand the applications of this technique to detect other anti-diabetic compounds that shown the *in vitro* anti-diabetic effect, e.g., glucose transporter inhibitor, enzyme blocker, enzyme activators, etc. The new target of pre-clinical drugs will be included to determine the action of live-cell FTIR to establish a platform for compound action prediction. The ability to detect the mechanism of drug action will be helpful in the pharmacological field that can accelerate the drug screening process.

Secondly, This approach will be examined in other diabetic-related cells, e.g., pancreas, kidney, muscle, and intestine. Due to diabetes being involved in many organs, FTIR would help better understand the whole diabetic metabolism. In addition, this examination of the diabetic cell cluster combined with machine learning can be a tool to predict the responses of the FTIR-diabetic live-cell system.

The final aim would like to enhance the ability of label-free glycogen detection that can be an alternative assay compared to the conventional glycogen assay in a quantitative way. This can be demonstrated by testing live cells with the anti-diabetic drug with a glycogen biochemical pathway, glycogen phosphorylase inhibitors, glucose transporter blockers, and detecting the drug's efficacy in a dose-dependent manner. Furthermore, the throughput of this method can be increased by the development of multi-well ATR plates for measuring live cells exposed to different conditions at the same time

References

1. Moneta, G.L., *Diabetes mellitus, fasting blood glucose concentration, and risk of vascular disease: a collaborative meta-analysis of 102 prospective studies*. Yearbook of Vascular Surgery, 2011. **2011**: p. 49-51.
2. Bourne, R., et al., *Causes of vision loss worldwide, 1990-2010: A systematic analysis*. The Lancet Global Health, 2013. **1**.
3. Saeedi, P., et al., *Global and regional diabetes prevalence estimates for 2019 and projections for 2030 and 2045: Results from the International Diabetes Federation Diabetes Atlas, 9th edition*. Diabetes Research and Clinical Practice, 2019. **157**: p. 107843.
4. Zhou, B., et al., *Worldwide trends in diabetes since 1980: a pooled analysis of 751 population-based studies with 4.4 million participants*. The Lancet, 2016. **387**(10027): p. 1513-1530.
5. Mayer-Davis, E.J., et al., *Incidence Trends of Type 1 and Type 2 Diabetes among Youths, 2002–2012*. New England Journal of Medicine, 2017. **376**(15): p. 1419-1429.
6. American Diabetes, A., *Standards of Medical Care in Diabetes-2019 Abridged for Primary Care Providers*. Clinical diabetes : a publication of the American Diabetes Association, 2019. **37**(1): p. 11-34.
7. American Diabetes, A., *Standards of Medical Care in Diabetes—2013*. Diabetes Care, 2013. **36**(Supplement 1): p. S11.
8. Chi, G.Y.H., *Some issues with composite endpoints in clinical trials*. Fundamental & Clinical Pharmacology, 2005. **19**(6): p. 609-619.
9. Cannon, C.P., *Clinical perspectives on the use of composite endpoints*. Controlled Clinical Trials, 1997. **18**(6): p. 517-529.
10. Ferreira-González, I., et al., *Methodologic discussions for using and interpreting composite endpoints are limited, but still identify major concerns*. Journal of Clinical Epidemiology, 2007. **60**(7): p. 651-657.
11. *9. Pharmacologic Approaches to Glycemic Treatment: &em>Standards of Medical Care in Diabetes—2020*. Diabetes Care, 2020. **43**(Supplement 1): p. S98.
12. Han, Y., et al., *Effect of metformin on all-cause and cardiovascular mortality in patients with coronary artery diseases: a systematic review and an updated meta-analysis*. Cardiovascular Diabetology, 2019. **18**(1): p. 96.
13. Hu, Y., et al., *Metformin Use and Risk of All-Cause Mortality and Cardiovascular Events in Patients With Chronic Kidney Disease—A Systematic Review and Meta-Analysis*. Frontiers in Endocrinology, 2020. **11**(789).
14. Gangji, A.S., et al., *A Systematic Review and Meta-Analysis of Hypoglycemia and Cardiovascular Events*. Diabetes Care, 2007. **30**(2): p. 389.
15. Simpson, S.H., et al., *Mortality risk among sulfonylureas: a systematic review and network meta-analysis*. The Lancet Diabetes & Endocrinology, 2015. **3**(1): p. 43-51.
16. Ling, J., et al., *The efficacy and safety of dipeptidyl peptidase-4 inhibitors for type 2 diabetes: a Bayesian network meta-analysis of 58 randomized controlled trials*. Acta Diabetologica, 2019. **56**(3): p. 249-272.
17. Kaneko, M. and M. Narukawa, *Meta-analysis of dipeptidyl peptidase-4 inhibitors use and cardiovascular risk in patients with type 2 diabetes mellitus*. Diabetes Research and Clinical Practice, 2016. **116**: p. 171-182.
18. Hsia, D.S., O. Grove, and W.T. Cefalu, *An update on sodium-glucose co-transporter-2 inhibitors for the treatment of diabetes mellitus*. Current opinion in endocrinology, diabetes, and obesity, 2017. **24**(1): p. 73-79.
19. Tentolouris, A., et al., *SGLT2 Inhibitors: A Review of Their Antidiabetic and Cardioprotective Effects*. International journal of environmental research and public health, 2019. **16**(16): p. 2965.

20. Nissen, S.E. and K. Wolski, *Effect of Rosiglitazone on the Risk of Myocardial Infarction and Death from Cardiovascular Causes*. New England Journal of Medicine, 2007. **356**(24): p. 2457-2471.
21. Singh, S., Y.K. Loke, and C.D. Furberg, *Long-term Risk of Cardiovascular Events With Rosiglitazone A Meta-analysis*. JAMA, 2007. **298**(10): p. 1189-1195.
22. Nissen, S.E. and K. Wolski, *Rosiglitazone Revisited: An Updated Meta-analysis of Risk for Myocardial Infarction and Cardiovascular Mortality*. Archives of Internal Medicine, 2010. **170**(14): p. 1191-1201.
23. Holman, R.R., et al., *Effects of Once-Weekly Exenatide on Cardiovascular Outcomes in Type 2 Diabetes*. New England Journal of Medicine, 2017. **377**(13): p. 1228-1239.
24. Zinman, B., et al., *Liraglutide and Glycaemic Outcomes in the LEADER Trial*. Diabetes therapy : research, treatment and education of diabetes and related disorders, 2018. **9**(6): p. 2383-2392.
25. Marso, S.P., et al., *Semaglutide and Cardiovascular Outcomes in Patients with Type 2 Diabetes*. New England Journal of Medicine, 2016. **375**(19): p. 1834-1844.
26. Miller, B.R., et al., *New and emerging drugs and targets for type 2 diabetes: reviewing the evidence*. American health & drug benefits, 2014. **7**(8): p. 452-463.
27. Timmis, A.D., B.R. Chaitman, and M. Crager, *Effects of ranolazine on exercise tolerance and HbA1c in patients with chronic angina and diabetes*. European Heart Journal, 2006. **27**(1): p. 42-48.
28. Chisholm, J.W., et al., *Effect of ranolazine on A1C and glucose levels in hyperglycemic patients with non-ST elevation acute coronary syndrome*. Diabetes care, 2010. **33**(6): p. 1163-1168.
29. Vlassara, H., et al., *Effects of Sevelamer on HbA1c, Inflammation, and Advanced Glycation End Products in Diabetic Kidney Disease*. Clinical Journal of the American Society of Nephrology, 2012. **7**(6): p. 934.
30. Bays, H.E., et al., *Colesevelam Hydrochloride Therapy in Patients With Type 2 Diabetes Mellitus Treated With Metformin: Glucose and Lipid Effects*. Archives of Internal Medicine, 2008. **168**(18): p. 1975-1983.
31. Brønden, A., et al., *Sevelamer in a diabetologist's perspective: a phosphate-binding resin with glucose-lowering potential*. Diabetes, Obesity and Metabolism, 2015. **17**(2): p. 116-120.
32. Adeva-Andany, M.M., et al., *Liver glucose metabolism in humans*. Bioscience reports, 2016. **36**(6): p. e00416.
33. Llano, A., M. Fisher, and G. McKay, *Drug development and licensing in diabetes*. Practical Diabetes, 2016. **33**(2): p. 60-64.
34. Dhandapani, M. and A. Goldman, *Preclinical Cancer Models and Biomarkers for Drug Development: New Technologies and Emerging Tools*. Journal of Molecular Biomarkers & Diagnosis, 2017. **08**.
35. Srinivasan, K. and R. Poduri, *Animal models in type 2 diabetes research: An overview*. The Indian journal of medical research, 2007. **125**: p. 451-72.
36. Wagner, J.A., *Early Clinical Development of Pharmaceuticals for Type 2 Diabetes Mellitus: From Preclinical Models to Human Investigation*. The Journal of Clinical Endocrinology & Metabolism, 2002. **87**(12): p. 5362-5366.
37. Institute of, M., *Countering the Problem of Falsified and Substandard Drugs*, ed. O.G. Lawrence and J.B. Gillian. 2013, Washington, DC: The National Academies Press.
38. Kaur, H., et al., *Antimalarial drug quality: Methods to detect suspect drugs*. Therapy, 2010. **7**: p. 49-57.
39. Malet-Martino, M., V. Gilard, and S. Balayssac, *Counterfeit drugs: Analytical techniques for their identification*. Analytical and bioanalytical chemistry, 2010. **398**: p. 77-92.
40. Rajawat, J. and G. Jhingan, *Chapter 1 - Mass spectroscopy*, in *Data Processing Handbook for Complex Biological Data Sources*, G. Misra, Editor. 2019, Academic Press. p. 1-20.

41. van Breemen, R., A. Newsome, and J. Dahl, *Mass Spectrometry and Drug Discovery*. 2010.
42. Aretz, I. and D. Meierhofer, *Advantages and Pitfalls of Mass Spectrometry Based Metabolome Profiling in Systems Biology*. International journal of molecular sciences, 2016. **17**(5): p. 632.
43. R, S.K., et al., *Nuclear Magnetic Resonance (NMR) Spectroscopy*. 2017. p. 69-79.
44. Zloh, M., *NMR spectroscopy in drug discovery and development: Evaluation of physico-chemical properties*. ADMET and DMPK, 2019. **7**: p. 242.
45. Roggo, Y., K. Degardin, and M. Ulmschneider, *Near Infrared Spectroscopy in Drug Discovery and Development Processes*. 2012.
46. Orlando, A., et al., *A Comprehensive Review on Raman Spectroscopy Applications*. Chemosensors, 2021. **9**.
47. Paudel, A., D. Raijada, and J. Rantanen, *Raman spectroscopy in pharmaceutical product design*. Advanced Drug Delivery Reviews, 2015. **89**: p. 3-20.
48. Wang, W.-t., et al., *Research Progress of Raman Spectroscopy in Drug Analysis*. AAPS PharmSciTech, 2018. **19**(7): p. 2921-2928.
49. Gala, U. and H. Chauhan, *Principles and applications of Raman spectroscopy in pharmaceutical drug discovery and development*. Expert Opinion on Drug Discovery, 2015. **10**(2): p. 187-206.
50. Guerrero-Pérez, M.O. and G.S. Patience, *Experimental methods in chemical engineering: Fourier transform infrared spectroscopy—FTIR*. The Canadian Journal of Chemical Engineering, 2020. **98**(1): p. 25-33.
51. Sabbatini, S., et al., *Infrared spectroscopy as a new tool for studying single living cells: Is there a niche?* Biomedical Spectroscopy and Imaging, 2017. **6**: p. 85-99.
52. Whelan, D.R., et al., *Monitoring the reversible B to A-like transition of DNA in eukaryotic cells using Fourier transform infrared spectroscopy*. Nucleic Acids Research, 2011. **39**(13): p. 5439-5448.
53. Huang, H.L., et al., *Trypsin-induced proteome alteration during cell subculture in mammalian cells*. Journal of biomedical science, 2010. **17**(1): p. 36.
54. Chan, K.L.A. and P.L. Fale, *Label-free in situ quantification of drug in living cells at micromolar levels using infrared spectroscopy*. Analytical chemistry, 2014. **86**(23): p. 11673-11679.
55. Fale, P.L., A. Altharawi, and K.L.A. Chan, *In situ Fourier transform infrared analysis of live cells' response to doxorubicin*. Biochimica et Biophysica Acta (BBA) - Molecular Cell Research, 2015. **1853**(10, Part A): p. 2640-2648.
56. Baker, M.J., et al., *Using Fourier transform IR spectroscopy to analyze biological materials*. Nature Protocols, 2014. **9**(8): p. 1771-1791.
57. Tatulian, S.A., *Structural characterization of membrane proteins and peptides by FTIR and ATR-FTIR spectroscopy*, in *Lipid-protein interactions*. 2013, Springer. p. 177-218.
58. Goormaghtigh, E., V. Raussens, and J.M. Ruysschaert, *Attenuated total reflection infrared spectroscopy of proteins and lipids in biological membranes*. Biochimica Et Biophysica Acta-Reviews on Biomembranes, 1999. **1422**(2): p. 105-185.
59. Baker, M., et al., *Using Fourier transform IR spectroscopy to analyze biological materials*. Nature protocols, 2014. **9**: p. 1771-1791.
60. Matthäus, C., et al., *Chapter 10: Infrared and Raman microscopy in cell biology*. Methods in cell biology, 2008. **89**: p. 275-308.
61. Mistek-Morabito, E. and I.K. Lednev, *FT-IR spectroscopy for identification of biological stains for forensic purposes*. Spectroscopy (Santa Monica), 2018. **33**: p. 8-19.
62. Mello, M. and B. Vidal, *Changes in the Infrared Microspectroscopic Characteristics of DNA Caused by Cationic Elements, Different Base Richness and Single-Stranded Form*. PloS one, 2012. **7**: p. e43169.
63. Boydston-White, S., et al., *Microspectroscopy of single proliferating HeLa cells*. Vibrational Spectroscopy, 2005. **38**(1-2): p. 169-177.

64. Gasparri, F. and M. Muzio, *Monitoring of apoptosis of HL60 cells by Fourier-transform infrared spectroscopy*. Biochemical Journal, 2003. **369**: p. 239-248.
65. Liu, K.Z., et al., *Quantitative determination of apoptosis on leukemia cells by infrared spectroscopy*. Apoptosis, 2001. **6**(4): p. 269-278.
66. Verdonck, M., et al., *Breast cancer and melanoma cell line identification by FTIR imaging after formalin-fixation and paraffin-embedding*. Analyst, 2013. **138**(14): p. 4083-4091.
67. Zwielly, A., et al., *Discrimination between drug-resistant and non-resistant human melanoma cell lines by FTIR spectroscopy*. Analyst, 2009. **134**(2): p. 294-300.
68. Zhang, L.E.I. and S. Hassan, *FOURIER TRANSFORM INFRARED (FTIR) IN DIABETES RESEARCH BY ANALYZING HAIR SAMPLES*. Journal of the North Carolina Academy of Science, 2007. **123**(3): p. 163-166.
69. Severcan, F., et al., *FT-IR spectroscopy in diagnosis of diabetes in rat animal model*. Journal of biophotonics, 2010. **3**: p. 621-31.
70. Eikje, N., *Diabetic interstitial glucose in the skin tissue by atr-ftir spectroscopy versus capillary blood glucose*. Journal of Innovative Optical Health Sciences, 2010. **03**.
71. Yang, X., et al., *Pre-diabetes diagnosis based on ATR-FTIR spectroscopy combined with CART and XGBoots*. Optik, 2019. **180**: p. 189-198.
72. Yoshida, S., et al., *Optical screening of diabetes mellitus using non-invasive Fourier-transform infrared spectroscopy technique for human lip*. Journal of Pharmaceutical and Biomedical Analysis, 2013. **76**: p. 169-176.
73. Scott, D.A., et al., *Diabetes-related molecular signatures in infrared spectra of human saliva*. Diabetology & metabolic syndrome, 2010. **2**: p. 48-48.
74. Caixeta, D.C., et al., *Salivary molecular spectroscopy: A sustainable, rapid and non-invasive monitoring tool for diabetes mellitus during insulin treatment*. PLOS ONE, 2020. **15**(3): p. e0223461.
75. Sundaramoorthi, K., et al., *Efficacy of metformin in human single hair fibre by ATR-FTIR spectroscopy coupled with statistical analysis*. Journal of Pharmaceutical and Biomedical Analysis, 2017. **136**: p. 10-13.
76. Simonescu, C.M., *Application of FTIR Spectroscopy in Environmental Studies*. Advanced Aspects of Spectroscopy, Pakistan, 2021: p. 49-84.
77. Chan, K.L.A. and P.L.V. Fale, *Label-Free in Situ Quantification of Drug in Living Cells at Micromolar Levels Using Infrared Spectroscopy*. Analytical Chemistry, 2014. **86**(23): p. 11673-11679.
78. Olkin, I. and A.R. Sampson, *Multivariate Analysis: Overview*, in *International Encyclopedia of the Social & Behavioral Sciences*, N.J. Smelser and P.B. Baltes, Editors. 2001, Pergamon: Oxford. p. 10240-10247.
79. J. Anzanello, M., et al., *Performance of some supervised and unsupervised multivariate techniques for grouping authentic and unauthentic Viagra and Cialis*. Egyptian Journal of Forensic Sciences, 2014. **4**(3): p. 83-89.
80. Budevskaa, B.O., *Minimization of optical non-linearities in Fourier transform-infrared microspectroscopic imaging*. Vibrational Spectroscopy, 2000. **24**(1): p. 37-45.
81. Jolliffe, I. and J. Cadima, *Principal component analysis: A review and recent developments*. Philosophical Transactions of the Royal Society A: Mathematical, Physical and Engineering Sciences, 2016. **374**: p. 20150202.
82. Pedro L Fale, A.A., K L Andrew Chan, *In situ Fourier transform infrared analysis of live cells' response to doxorubicin*. Biochim Biophys Acta., 2015. **Oct;1853**((10 Pt A)): p.:2640-8.
83. Lv, Y., et al., *Metabolic switching in the hypoglycemic and antitumor effects of metformin on high glucose induced HepG2 cells*. Journal of Pharmaceutical and Biomedical Analysis, 2018. **156**: p. 153-162.
84. Sosa-Gutiérrez, J.A., et al., *Effects of Moringa oleifera Leaves Extract on High Glucose-Induced Metabolic Changes in HepG2 Cells*. Biology, 2018. **7**(3).

85. Li, P., et al., *Curcumin metabolites contribute to the effect of curcumin on ameliorating insulin sensitivity in high-glucose-induced insulin-resistant HepG2 cells*. Journal of Ethnopharmacology, 2020. **259**: p. 113015.
86. Jiang, B., et al., *Protective effects of marein on high glucose-induced glucose metabolic disorder in HepG2 cells*. Phytomedicine, 2016. **23**(9): p. 891-900.
87. Chandrasekaran, K., et al., *Apoptosis in HepG2 cells exposed to high glucose*. Toxicology in Vitro, 2010. **24**(2): p. 387-396.
88. Lincoln, C.K. and M.G. Gabridge, *Chapter 4 Cell Culture Contamination: Sources, Consequences, Prevention, and Elimination*, in *Methods in Cell Biology*, J.P. Mather and D. Barnes, Editors. 1998, Academic Press. p. 49-65.
89. Riss, T., et al., *Cell viability assays*. Assay Guid. Man., 2013.
90. Kamiloglu, S., et al., *Guidelines for cell viability assays*. Food Frontiers, 2020. **1**.
91. Baker, M.J., et al., *Using Fourier transform IR spectroscopy to analyze biological materials*. Nature Protocols, 2014. **9**(8): p. 1771-1791.
92. Altharawi, A., K. Rahman, and K.L.A. Chan, *Towards identifying the mode of action of drugs using live-cell FTIR spectroscopy*. The Analyst, 2019. **144**.
93. Gonzalez, F.J., *Challenges and Opportunities of Metabolomics*. Journal of cellular physiology, 2018. **227**(8): p. 2975-81.
94. Zhang A, S.H., Wang P, Han Y, Wang X., *Modern analytical techniques in metabolomics analysis*. Analyst, 2012. **2012 Jan 21**;**137**(2): p. 293-300.
95. Holman HY, M.M., Blakely EA, Bjornstad K, McKinney WR, *IR spectroscopic characteristics of cell cycle and cell death probed by synchrotron radiation-based Fourier transform IR spectromicroscopy*. Biopolymers (Biospectroscopy) 2000. **57**: p. 329-335.
96. Kuimova, M., K.L.A. Chan, and S. Kazarian, *Chemical Imaging of Live Cancer Cells in the Natural Aqueous Environment*. Applied spectroscopy, 2009. **63**: p. 164-71.
97. Falé, P., A. Altharawi, and K.L.A. Chan, *In situ Fourier transform infrared analysis of live cells response to doxorubicin*. Biochimica et biophysica acta, 2015. **1853**.
98. Rutter AV, S.M., Filik J, Sandt C, Dumas P, Cinque G, Sockalingum GD, Yang Y, Sulé-Suso J., *Study of gemcitabine-sensitive/resistant cancer cells by cell cloning and synchrotron FTIR microspectroscopy*. Cytometry A, 2014. **2014 Aug**;**85**(8): p. 688-97.
99. Roy, S., et al., *Simultaneous ATR-FTIR Based Determination of Malaria Parasitemia, Glucose and Urea in Whole Blood Dried onto a Glass Slide*. Analytical Chemistry, 2017. **89**(10): p. 5238-5245.
100. Frederick, W., et al., *Near infrared spectroscopy: the practical chemical imaging solution*, in *Spectroscopy Europe*. 2002. p. 12-19.
101. Liu, K.-Z., et al., *Quantitative determination of apoptosis on leukemia cells by infrared spectroscopy*. Apoptosis, 2001. **6**(4): p. 269-278.
102. Kumar, S., T.S. Shabi, and E. Goormaghtigh, *A FTIR Imaging Characterization of Fibroblasts Stimulated by Various Breast Cancer Cell Lines*. PLOS ONE, 2014. **9**(11): p. e111137.
103. Harvey, T., et al., *Discrimination of prostate cancer cells by reflection mode FTIR photoacoustic spectroscopy*. The Analyst, 2007. **132**: p. 292-5.
104. Singh, A.K., et al., *Raman spectral probe and unique fractal signatures for human serum with diabetes and early stage diabetic retinopathy*. Biomedical Physics & Engineering Express, 2018. **5**(1): p. 015021.
105. Zhang, Q., et al., *Mangiferin Improved Palmitate-Induced-Insulin Resistance by Promoting Free Fatty Acid Metabolism in HepG2 and C2C12 Cells via PPAR α : Mangiferin Improved Insulin Resistance*. Journal of Diabetes Research, 2019. **2019**: p. 2052675.
106. Liang, G., et al., *3-Deoxyglucosone induces insulin resistance by impairing insulin signaling in HepG2 cells*. Mol Med Rep, 2016. **13**(5): p. 4506-4512.
107. Mohammadpour, Z., et al., *Hyperglycemia Induction in HepG2 Cell Line*. International Journal of Health Studies, 2016. **22**: p. 28-29.

108. Gaigneaux, A. and E. Goormaghtigh, *A new dimension for cell identification by FTIR spectroscopy: depth profiling in attenuated total reflection*. *The Analyst*, 2013. **138**(14): p. 4070-4075.
109. Kazarian, S. and K.L.A. Chan, *ATR-FTIR spectroscopic imaging: Recent advances and applications to biological systems*. *The Analyst*, 2013. **138**: p. 1940-51.
110. Wehbe, K., et al., *The effect of optical substrates on micro-FTIR analysis of single mammalian cells*. *Analytical and Bioanalytical Chemistry*, 2013. **405**(4): p. 1311-1324.
111. Altharawi, A., K.M. Rahman, and K.L.A. Chan, *Identifying the Responses from the Estrogen Receptor-Expressed MCF7 Cells Treated in Anticancer Drugs of Different Modes of Action Using Live-Cell FTIR Spectroscopy*. *ACS omega*, 2020. **5**(22): p. 12698-12706.
112. Altharawi, A., K.M. Rahman, and K.L.A. Chan, *Towards identifying the mode of action of drugs using live-cell FTIR spectroscopy*. *Analyst*, 2019. **144**(8): p. 2725-2735.
113. Cho, K. and D.-H. Cho, *Telmisartan increases hepatic glucose production via protein kinase C ζ -dependent insulin receptor substrate-1 phosphorylation in HepG2 cells and mouse liver*. *Yeungnam University Journal of Medicine*, 2018. **36**.
114. Li, Y., et al., *Resveratrol suppresses the STAT3 signaling pathway and inhibits proliferation of high glucose-exposed HepG2 cells partly through SIRT1*. *Oncology reports*, 2013. **30**.
115. Chandrasekaran, K., et al., *Apoptosis in HepG2 cells exposed to high glucose*. *Toxicology in vitro : an international journal published in association with BIBRA*, 2009. **24**: p. 387-96.
116. Ferrannini, E., et al., *The Disposal of an Oral Glucose Load in Healthy Subjects: A Quantitative Study*. *Diabetes*, 1985. **34**: p. 580-8.
117. Han, H.-S., et al., *Regulation of glucose metabolism from a liver-centric perspective*. *Experimental & molecular medicine*, 2016. **48**(3): p. e218-e218.
118. Adeva, M., et al., *Liver glucose metabolism in humans*. *Bioscience reports*, 2016. **36**.
119. Poitout, V. and R.P. Robertson, *Glucolipotoxicity: Fuel Excess and β -Cell Dysfunction*. *Endocrine Reviews*, 2008. **29**(3): p. 351-366.
120. Nakamura, S., et al., *Palmitate induces insulin resistance in H4IIEC3 hepatocytes through reactive oxygen species produced by mitochondria*. *The Journal of biological chemistry*, 2009. **284**(22): p. 14809-14818.
121. García-Ruiz, I., et al., *In vitro treatment of HepG2 cells with saturated fatty acids reproduces mitochondrial dysfunction found in nonalcoholic steatohepatitis*. *Disease Models & Mechanisms*, 2015. **8**(2): p. 183.
122. Raza, H., et al., *Elevated Mitochondrial Cytochrome P450 2E1 and Glutathione S-Transferase A4-4 in Streptozotocin-Induced Diabetic Rats Tissue-Specific Variations and Roles in Oxidative Stress*. *Diabetes*, 2004. **53**: p. 185-94.
123. Alnahdi, A., A. John, and H. Raza, *Augmentation of Glucotoxicity, Oxidative Stress, Apoptosis and Mitochondrial Dysfunction in HepG2 Cells by Palmitic Acid*. *Nutrients*, 2019. **11**(9): p. 1979.
124. Iyer, V.V., et al., *Effects of glucose and insulin on HepG2-C3A cell metabolism*. *Biotechnology and Bioengineering*, 2010. **107**(2): p. 347-356.
125. Nagarajan, S., et al., *Lipid and Glucose Metabolism in Hepatocyte Cell Lines and Primary Mouse Hepatocytes: A comprehensive resource for in vitro studies of hepatic metabolism*. *American Journal of Physiology-Endocrinology and Metabolism*, 2019. **316**.
126. Zheng, J., *Energy metabolism of cancer: Glycolysis versus oxidative phosphorylation (Review)*. *Oncol Lett*, 2012. **4**(6): p. 1151-1157.
127. Warburg, O., *On the Origin of Cancer Cells*. *Science*, 1956. **123**(3191): p. 309.
128. Wiercigroch, E., et al., *Raman and infrared spectroscopy of carbohydrates: A review*. *Spectrochimica Acta Part A: Molecular and Biomolecular Spectroscopy*, 2017. **185**: p. 317-335.
129. Geciova, J., D. Bury, and P. Jelen, *Methods for disruption of microbial cells for potential use in the dairy industry--a review*. *International dairy journal*, 2002. **12**(6): p. 541-553.

130. Csepregi, R., et al., *A One-Step Extraction and Luminescence Assay for Quantifying Glucose and ATP Levels in Cultured HepG2 Cells*. International journal of molecular sciences, 2018. **19**(9): p. 2670.
131. Samuel, V. and G. Shulman, *The pathogenesis of insulin resistance: Integrating signaling pathways and substrate flux*. Journal of Clinical Investigation, 2016. **126**: p. 12-22.
132. Hu, G., et al., *Plasma insulin and cardiovascular mortality in non-diabetic European men and women: A meta-analysis of data from eleven prospective studies*. Diabetologia, 2004. **47**.
133. Carr, D.B., et al., *Intra-Abdominal Fat Is a Major Determinant of the National Cholesterol Education Program Adult Treatment Panel III Criteria for the Metabolic Syndrome*. Diabetes, 2004. **53**(8): p. 2087-2094.
134. Stern, M.P., et al., *Does the Metabolic Syndrome Improve Identification of Individuals at Risk of Type 2 Diabetes and/or Cardiovascular Disease?* Diabetes Care, 2004. **27**(11): p. 2676-2681.
135. World Health, O., *World health statistics 2021: monitoring health for the SDGs, sustainable development goals*. 2021, Geneva: World Health Organization.
136. O'Farrell, A., et al., *Non-Invasive Molecular Imaging for Preclinical Cancer Therapeutic Development*. British journal of pharmacology, 2013. **169**.
137. Poonprasartporn, A. and K.L.A. Chan, *Live-cell ATR-FTIR spectroscopy as a novel bioanalytical tool for cell glucose metabolism research*. Biochimica et Biophysica Acta (BBA) - Molecular Cell Research, 2021. **1868**(7): p. 119024.
138. Phelan, J., A. Altharawi, and K.L.A. Chan, *Tracking glycosylation in live cells using FTIR spectroscopy*. Talanta, 2020. **211**: p. 120737.
139. Parker, F.S., *Quantitative Analysis*, in *Applications of Infrared Spectroscopy in Biochemistry, Biology, and Medicine*, F.S. Parker, Editor. 1971, Springer US: Boston, MA. p. 80-83.
140. Terakosolphan, W., et al., *In vitro Fourier transform infrared spectroscopic study of the effect of glycerol on the uptake of beclomethasone dipropionate in living respiratory cells*. International Journal of Pharmaceutics, 2021. **609**: p. 121118.
141. Ding, X., et al., *Ellagic acid ameliorates oxidative stress and insulin resistance in high glucose-treated HepG2 cells via miR-223/keap1-Nrf2 pathway*. Biomedicine & Pharmacotherapy, 2019. **110**: p. 85-94.
142. Cho, K.W. and D.-H. Cho, *Telmisartan increases hepatic glucose production via protein kinase C ζ -dependent insulin receptor substrate-1 phosphorylation in HepG2 cells and mouse liver*. Yeungnam University journal of medicine, 2019. **36**(1): p. 26-35.
143. Huang, Q., et al., *Phenolic compounds ameliorate the glucose uptake in HepG2 cells' insulin resistance via activating AMPK*. Journal of Functional Foods, 2015. **19**: p. 487-494.
144. American Diabetes Association Professional Practice, C., *9. Pharmacologic Approaches to Glycemic Treatment: Standards of Medical Care in Diabetes—2022*. Diabetes Care, 2021. **45**(Supplement_1): p. S125-S143.
145. Teng, W., et al., *Resveratrol metabolites ameliorate insulin resistance in HepG2 hepatocytes by modulating IRS-1/AMPK*. RSC Advances, 2018. **8**: p. 36034-36042.
146. Zhu, X.-P., et al., *Metformin attenuates triglyceride accumulation in HepG2 cells through decreasing stearyl-coenzyme A desaturase 1 expression*. Lipids in Health and Disease, 2018. **17**.
147. Sefried, S., et al., *Suitability of hepatocyte cell lines HepG2, AML12 and THLE-2 for investigation of insulin signalling and hepatokine gene expression*. Open Biology. **8**(10): p. 180147.
148. Malek, K., B. Wood, and K. Bambery, *FTIR Imaging of Tissues: Techniques and Methods of Analysis*. 2014. p. 419-473.
149. Lo, K., et al., *Analysis of In Vitro Insulin-Resistance Models and Their Physiological Relevance to In Vivo Diet-Induced Adipose Insulin Resistance*. Cell reports, 2013. **5**.

150. Zhang, R.X., et al., *The establishment of insulin resistant model in vitro and preliminary application for screening drugs*. Chinese Pharmacological Bulletin, 2008. **24**: p. 971-976.
151. Esber, E.C., *An overview of the strengths and limitations of biological assays in quality control*. J Pharm Biomed Anal, 1989. **7**(2): p. 131-8.
152. Allister, E.M., et al., *Inhibition of apoB secretion from HepG2 cells by insulin is amplified by naringenin, independent of the insulin receptor**. Journal of Lipid Research, 2008. **49**(10): p. 2218-2229.
153. Sefried, S., et al., *Suitability of hepatocyte cell lines HepG2, AML12 and THLE-2 for investigation of insulin signalling and hepatokine gene expression*. Open Biology, 2018. **8**: p. 180147.
154. Hao, J., et al., *Polydatin Improves Glucose and Lipid Metabolisms in Insulin-Resistant HepG2 Cells through the AMPK Pathway*. Biological and Pharmaceutical Bulletin, 2018. **41**(6): p. 891-898.
155. Bricambert, J., et al., *Salt-inducible kinase 2 links transcriptional coactivator p300 phosphorylation to the prevention of ChREBP-dependent hepatic steatosis in mice*. The Journal of Clinical Investigation, 2010. **120**(12): p. 4316-4331.
156. Petersen, M. and G. Shulman, *Mechanisms of Insulin Action and Insulin Resistance*. Physiological reviews, 2018. **98**: p. 2133-2223.
157. Norouzzadeh, M., et al., *Does Resveratrol Improve Insulin Signalling in HepG2 Cells?* Canadian Journal of Diabetes, 2016. **41**.
158. Zhao, H., et al., *Resveratrol reduces liver endoplasmic reticulum stress and improves insulin sensitivity in vivo and in vitro*. Drug design, development and therapy, 2019. **13**: p. 1473-1485.
159. Teng, J.-F., et al., *Potential activities and mechanisms of extracellular polysaccharopeptides from fermented *Trametes versicolor* on regulating glucose homeostasis in insulin-resistant HepG2 cells*. PloS one, 2018. **13**(7): p. e0201131-e0201131.
160. Huijing, F., *A rapid enzymic method for glycogen estimation in very small tissue samples*. Clinica Chimica Acta, 1970. **30**(3): p. 567-572.
161. Matschinsky, F.M., et al., *Glucokinase Activators for Diabetes Therapy*. Diabetes Care, 2011. **34**(Supplement 2): p. S236.
162. Matschinsky, F. and D. Porte, *Glucokinase activators (GKAs) promise a new pharmacotherapy for diabetics*. F1000 medicine reports, 2010. **2**.
163. Aicher, T., et al., *Novel therapeutics and targets for the treatment of diabetes*. Expert review of clinical pharmacology, 2010. **3**: p. 209-29.
164. Belete, T., *A Recent Achievement In the Discovery and Development of Novel Targets for the Treatment of Type-2 Diabetes Mellitus*. Journal of Experimental Pharmacology, 2020. **Volume 12**: p. 1-15.
165. Toulis, K., et al., *Glucokinase Activators for Type 2 Diabetes: Challenges and Future Developments*. Drugs, 2020. **80**.
166. Bonadonna, R., et al., *Piragliatin (RO4389620), a Novel Glucokinase Activator, Lowers Plasma Glucose Both in the Postabsorptive State and after a Glucose Challenge in Patients with Type 2 Diabetes Mellitus: A Mechanistic Study*. The Journal of clinical endocrinology and metabolism, 2010. **95**: p. 5028-36.
167. Nakamura, A. and Y. Terauchi, *Present status of clinical deployment of glucokinase activators*. Journal of Diabetes Investigation, 2014. **6**.
168. Meininger, G., et al., *Effects of MK-0941, a Novel Glucokinase Activator, on Glycemic Control in Insulin-Treated Patients With Type 2 Diabetes*. Diabetes care, 2011. **34**: p. 2560-6.
169. Amin, N., et al., *Two Dose-Ranging Studies with PF-04937319, a systemic partial activator of glucokinase, as add-on therapy to Metformin in Adults with type 2 diabetes*. Diabetes, obesity & metabolism, 2015. **17**.

170. Denney, W., et al., *Glycemic Effect and Safety of a Systemic, Partial, Glucokinase Activator, PF-04937319, in Patients with Type 2 Diabetes Mellitus Inadequately Controlled on Metformin - a Randomized, Crossover, Active-Controlled Study*. *Clinical Pharmacology in Drug Development*, 2016. **5**: p. n/a-n/a.
171. Erion, D., et al., *The Hepatoselective Glucokinase Activator PF-04991532 Ameliorates Hyperglycemia without Causing Hepatic Steatosis in Diabetic Rats*. *PloS one*, 2014. **9**: p. e97139.
172. Tsumura, Y., et al., *TMG-123, a novel glucokinase activator, exerts durable effects on hyperglycemia without increasing triglyceride in diabetic animal models*. *PLOS ONE*, 2017. **12**: p. e0172252.
173. Wang, P., et al., *Effects of a Novel Glucokinase Activator, HMS5552, on Glucose Metabolism in a Rat Model of Type 2 Diabetes Mellitus*. *Journal of Diabetes Research*, 2017. **2017**: p. 1-9.
174. Sheng, L., et al., *Safety, tolerability, pharmacokinetics, and pharmacodynamics of novel glucokinase activator HMS5552: Results from a first-in-human single ascending dose study*. *Drug Design, Development and Therapy*, 2016. **10**: p. 1619.
175. Massa, M., J. Gagliardino, and F. Francini, *Liver Glucokinase: An Overview on the Regulatory Mechanisms of its Activity*. *IUBMB life*, 2011. **63**: p. 1-6.
176. Egan, A. and A. Vella, *TTP399: an investigational liver-selective glucokinase (GK) activator as a potential treatment for type 2 diabetes*. *Expert Opinion on Investigational Drugs*, 2019. **28**.
177. Vella, A., et al., *Targeting hepatic glucokinase to treat diabetes with TTP399, a hepatoselective glucokinase activator*. *Science Translational Medicine*, 2019. **11**: p. eaau3441.
178. Valcarce, C., et al., *TTP399, a Liver-Selective Glucose Kinase Activator (GKA), Lowers Glucose and Does NOT Increase Lipids in Subjects with Type 2 Diabetes Mellitus (T2DM)*. *Diabetes*, 2014. **63**: p. A32-A32.
179. Min, Q., et al., *Identification of mangiferin as a potential Glucokinase activator by structure-based virtual ligand screening*. *Scientific Reports*, 2017. **7**: p. 44681.
180. Wang, C., et al., *The Compound of Mangiferin-Berberine Salt Has Potent Activities in Modulating Lipid and Glucose Metabolisms in HepG2 Cells*. *BioMed Research International*, 2016. **2016**: p. 8753436.
181. Niu, Y., et al., *Mangiferin Decreases Plasma Free Fatty Acids through Promoting Its Catabolism in Liver by Activation of AMPK*. *PloS one*, 2012. **7**: p. e30782.
182. Zheng, H., et al., *Co-transfection of GK and mhPINS genes into HepG2 cells confers glucose-stimulated insulin secretion*. *Cytotherapy*, 2007. **9**: p. 580-6.